

## Advanced UK Instrumentation Training

# Diamond Detectors

Alexander Oh  
University of Manchester

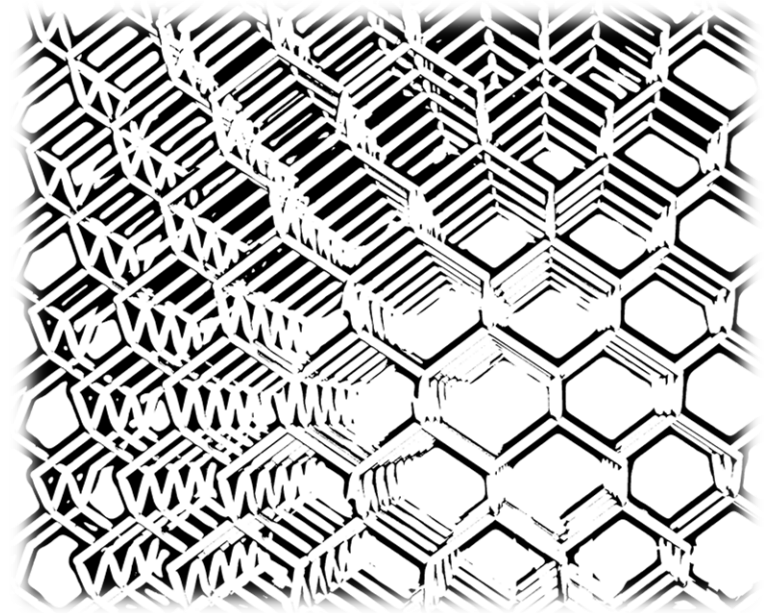
# Outline

## Part 1

- Diamond basics and detector principle
- Diamond strip and pixel detectors
- Radiation Hardness

## Part 2

- 3D Diamond detectors
- Current and future diamond detector installations

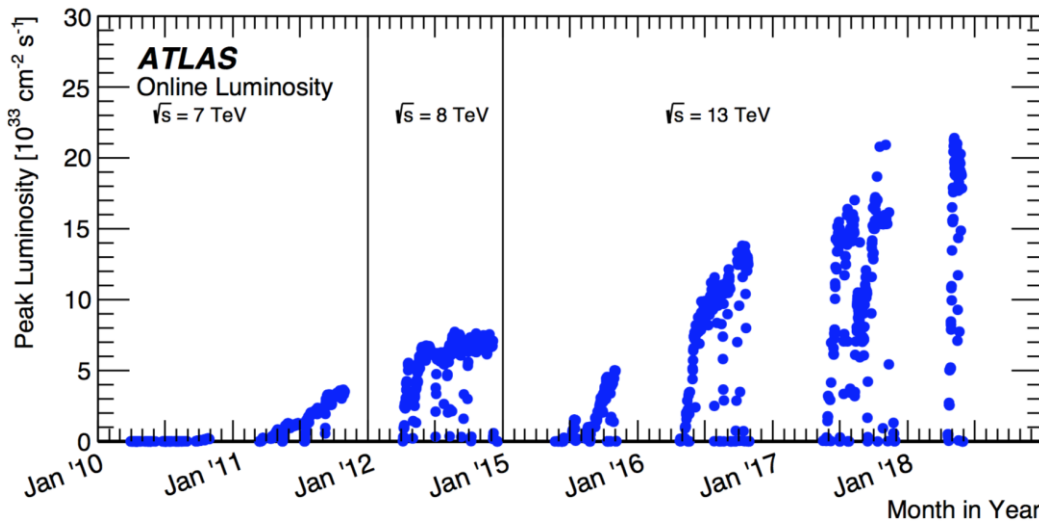
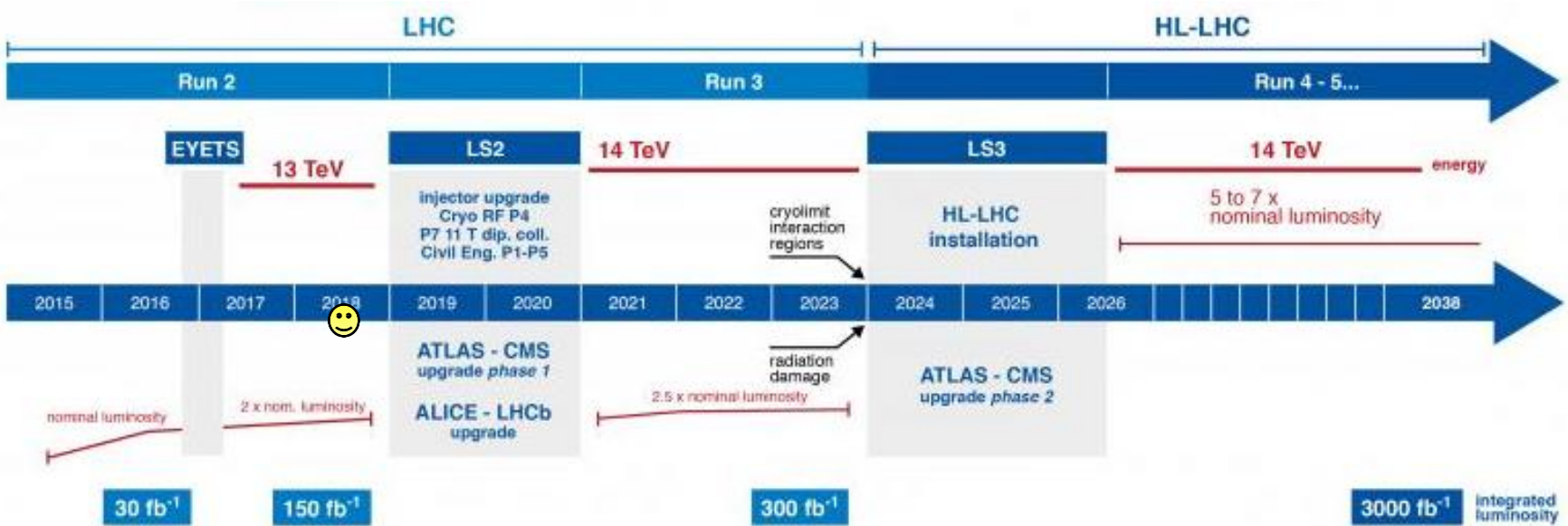


Thanks for the material from the RD42 and ADAMAS collaborations!  
Very soon new working group organisation: **DRD3 WG6**

# PART 1

- Introduction to Diamond detectors
  - properties
  - principle of operation
- Strip and Pixel detectors
- Radiation tolerance
- High rate capability

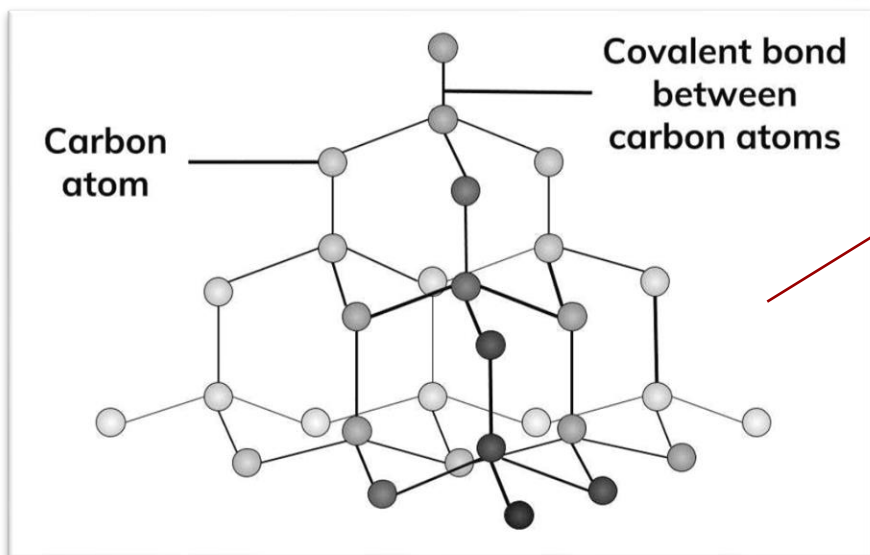
# Challenges Ahead



- Luminosity upgrades of the LHC will increase the luminosity by factor  $\sim 3$ .
- Luminosity  $\sim$  Radiation damage.
- Need new technologies in the innermost layers to survive the radiation levels.

# diamond

- Allotrope of Carbon
- Hardest natural material
- Tetrahedral structure
  - $sp^3$  bonds



	Diamond	Silicon
Band Gap [eV]	5.5	1.1

→ Lower leakage current

	Diamond	Silicon	
Band Gap [eV]	5.5	1.1	→ Lower leakage current
Average Ionisation Density for MIP [eh/μm]	36	81	→ Lower signal

	Diamond	Silicon	
Band Gap [eV]	5.5	1.1	→ Lower leakage current
Average Ionisation Density for MIP [eh/μm]	36	81	→ Lower signal
Displacement Energy [eV]	43	25	→ Radiation Hardness

	Diamond	Silicon	
Band Gap [eV]	5.5	1.1	→ Lower leakage current
Average Ionisation Density for MIP [eh/μm]	36	81	→ Lower signal
Displacement Energy [eV]	43	25	→ Radiation Hardness
Thermal Conductivity [W/cm.K]	10-20	1.5	→ Room temperature operation

	Diamond	Silicon	
Band Gap [eV]	5.5	1.1	→ Lower leakage current
Average Ionisation Density for MIP [eh/μm]	36	81	→ Lower signal
Displacement Energy [eV]	43	25	→ Radiation Hardness
Thermal Conductivity [W/cm.K]	10-20	1.5	→ Room temperature operation
Atomic Number	6	14	→ Tissue equivalence

	Diamond	Silicon	
Band Gap [eV]	5.5	1.1	→ Lower leakage current
Average Ionisation Density for MIP [eh/μm]	36	81	→ Lower signal
Displacement Energy [eV]	43	25	→ Radiation Hardness
Thermal Conductivity [W/cm.K]	10-20	1.5	→ Room temperature operation
Atomic Number	6	14	→ Tissue equivalence
Electron Mobility [cm <sup>2</sup> /V.s]	1900-3800	1350	} → Fast signal
Hole Mobility [cm <sup>2</sup> /V.s]	2300-4500	480	

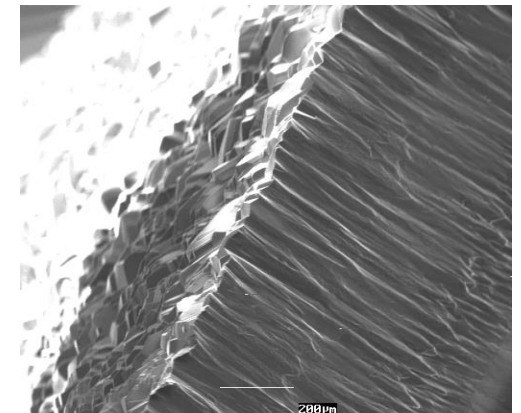
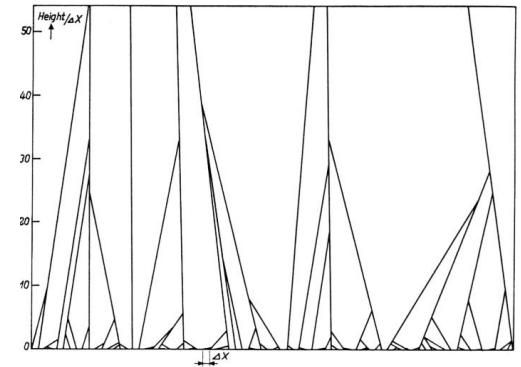
# Natural and synthetic diamond

- Natural diamonds have a **high defect concentration**
  - Grow in different structure to synthetic diamonds
  - Compete with jewellery market
  - There are radiation sensors using natural diamonds



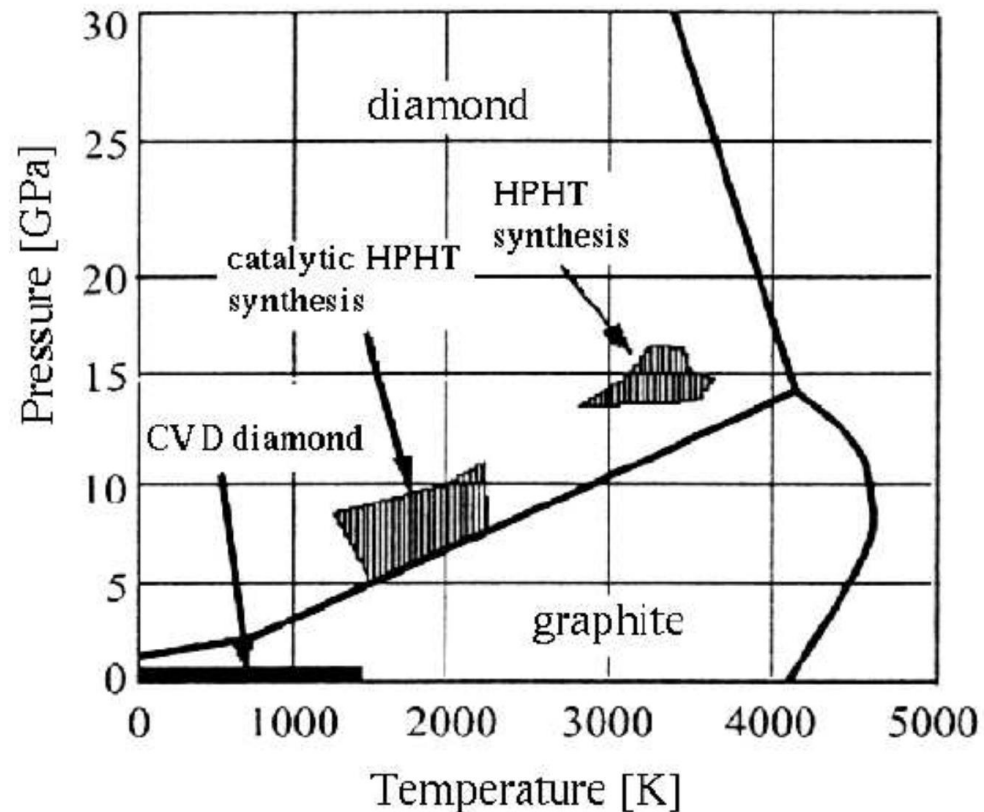
# Diamond

- 1941 – Diamond as particle detector (Stetter)
- 1953- CVD process, synthesis of diamond (Eversole)
- ~1980 – polycrystalline CVD diamond.
- 1994 – first diamond strip detector
- 1996 – first diamond pixel detector
- 2011 – first 3D diamond detector



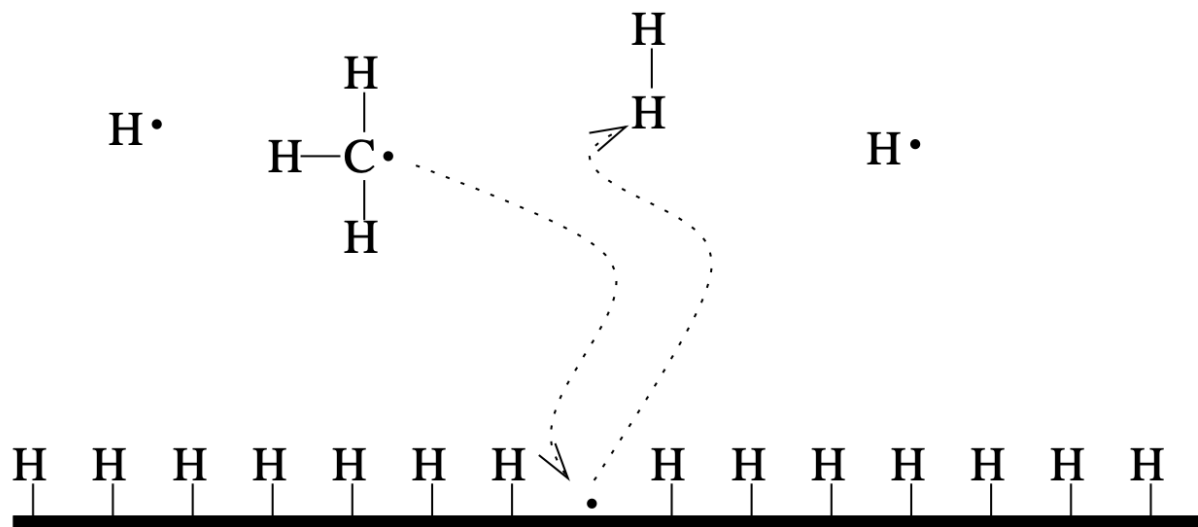
# Synthesis of Diamond

- Chemical Vapour Deposition (CVD) of diamond in the graphite phase space.



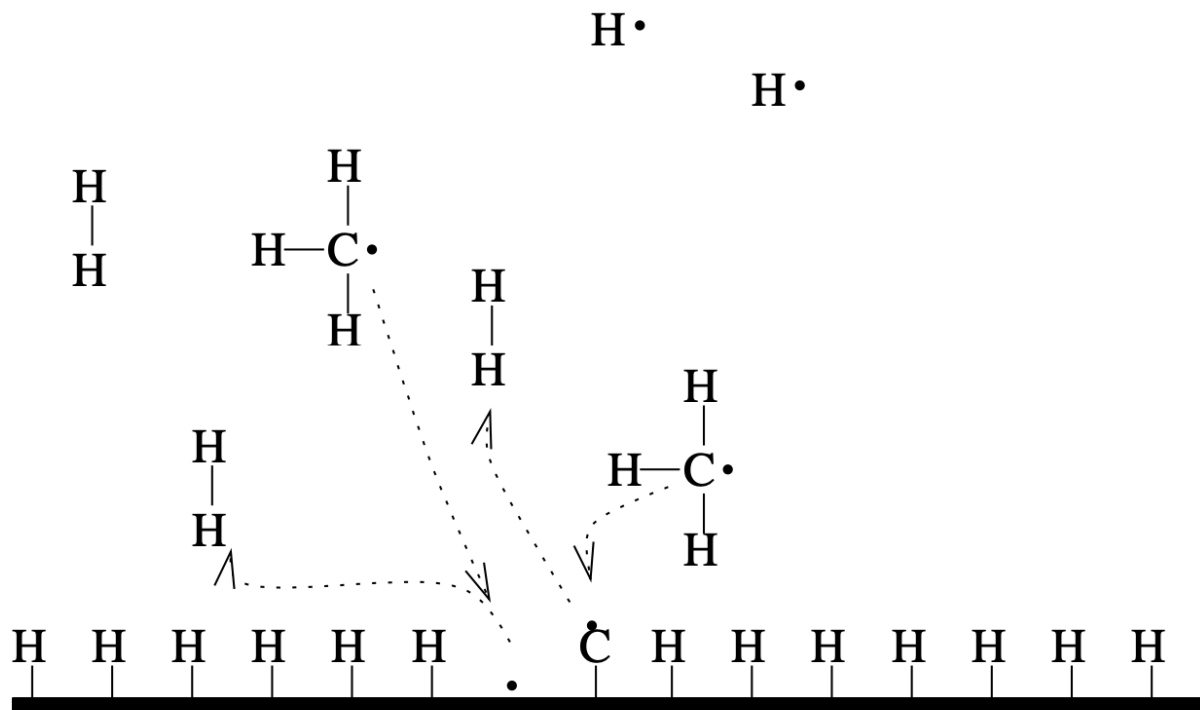
# Synthesis of Diamond

- Hydrogen terminated substrate surface
- Methan and Hydrogen gas are heated with microwaves to form a plasma
- Radicals form



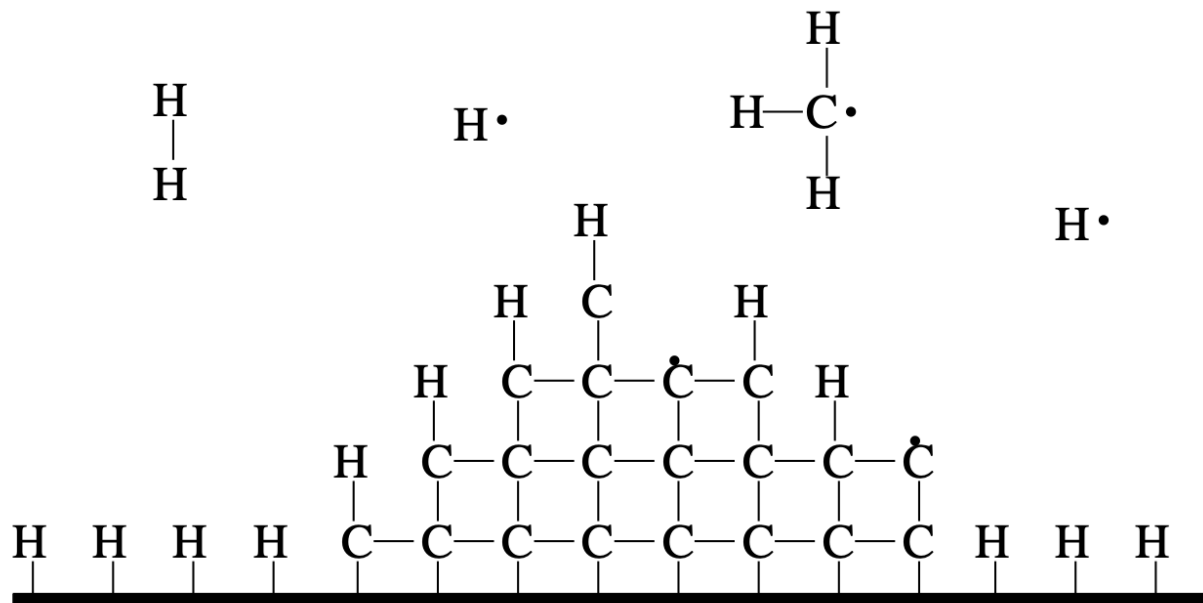
# Synthesis of Diamond

- Hydrogen atoms are replaced with Carbon



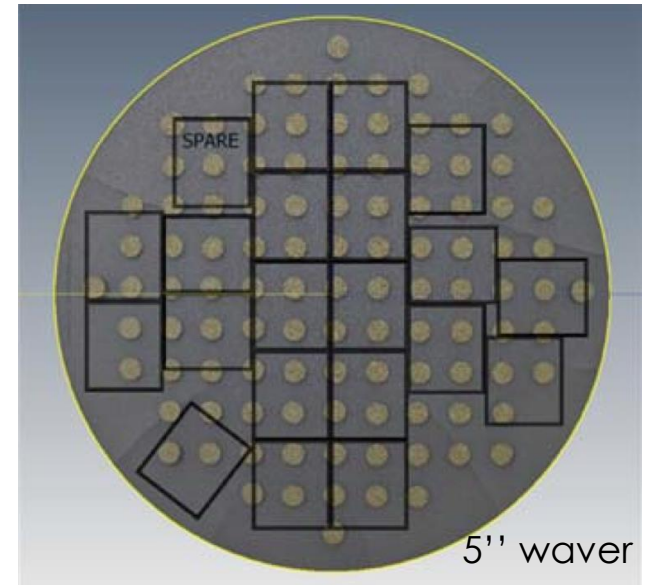
# Synthesis of Diamond

- SP<sup>2</sup> bonds (graphite) are weaker than SP<sup>3</sup> bonds (diamond)
- Hydrogen radicals will etch away graphite, but leave diamond
- A diamond film is grown

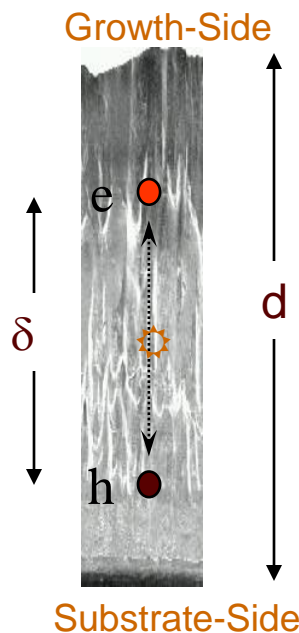


# Development of CVD Diamond for detector applications

- Today two main manufacturers of detector grade diamond
  - **ElementSix Ltd**
    - large **polycrystalline** wafers
    - **single crystal** diamonds
  - **II-VI Semiconductors**
    - large **polycrystalline** wafers
    - relatively recent entry
- Alternative sources
  - Diamond on Iridium (DoI) (Audiatec, Germany)
  - Hetero-epitaxially grown -> **large area**
  - **Highly oriented crystallites.**



■ Principle of detector operation



$$Q = \frac{d}{t} Q_0$$

collected charge

$$\delta = \mu E \tau$$

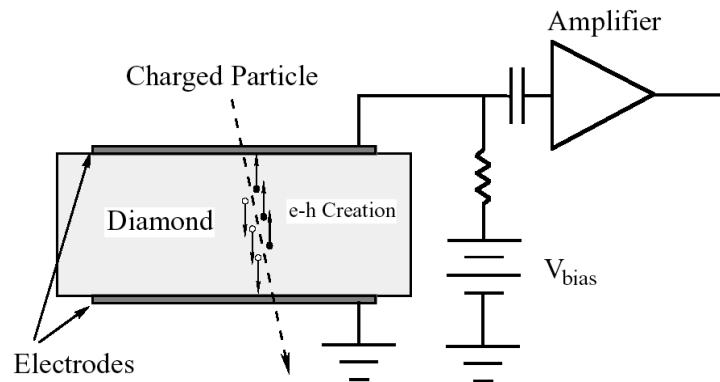
“collection distance”

$$\epsilon = Q / Q_0$$

collection efficiency

$$\mu = \mu_e + \mu_h$$

$$\tau = \frac{\mu_e \tau_e + \mu_h \tau_h}{\mu_e + \mu_h}$$



- MIP signal is measured, expressed in charge collection distance defined as  $\delta [\mu\text{m}] = Q_m [\text{e}] / 36 [\text{e}/\mu\text{m}]$

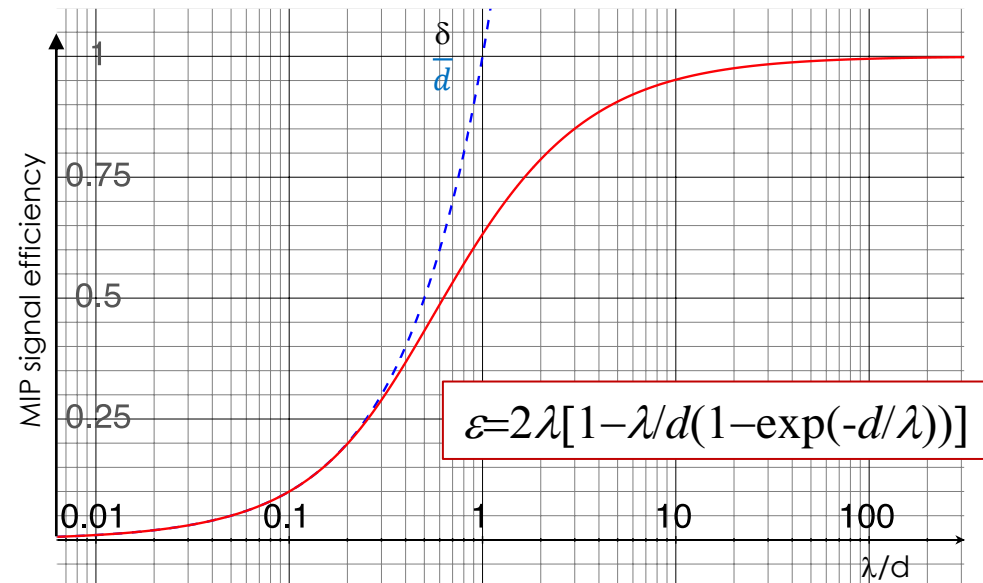
- More accurately the “Schubweg” ( $\lambda$ ).

$$\epsilon = \frac{Q_m}{Q_0}$$

- Relation between MIP signal efficiency  $\epsilon$ , “collection distance”  $\delta$ , and “Schubweg”  $\lambda$ :

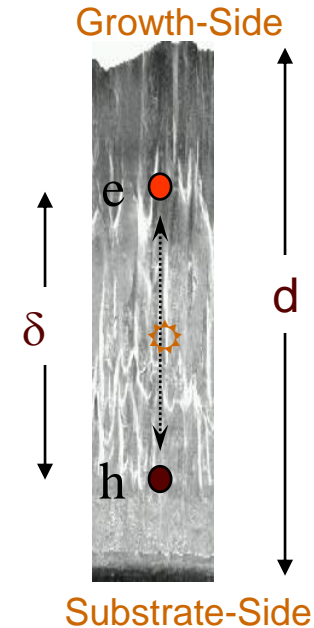
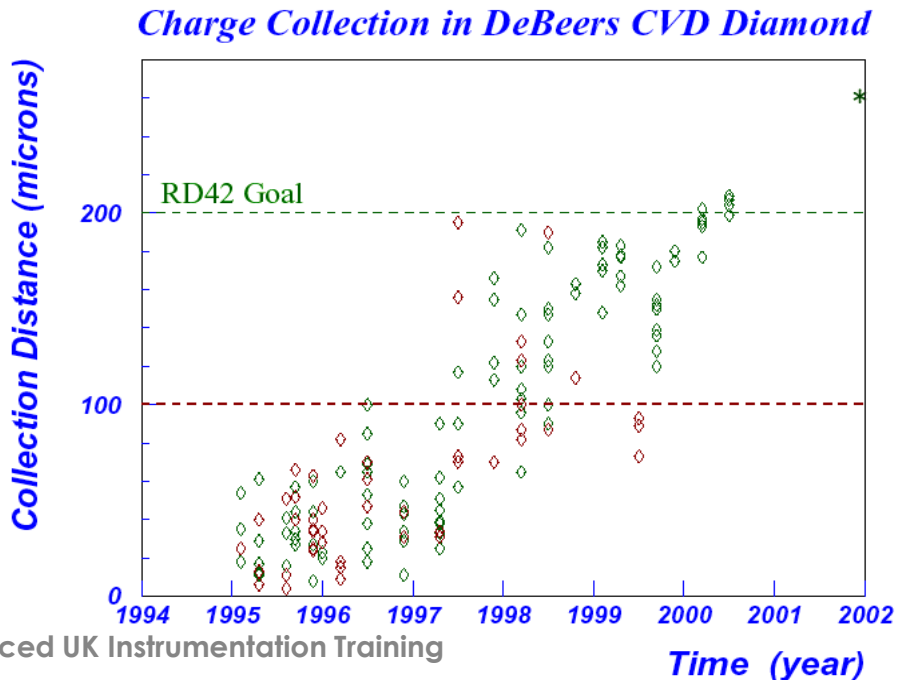
$$\delta = Q_m / 36 [e\mu\text{m}^{-1}]$$

$$\epsilon = 2\lambda [1 - \lambda/d \cdot (1 - \exp(-d/\lambda))]$$



# Development of CVD Diamond for detector applications

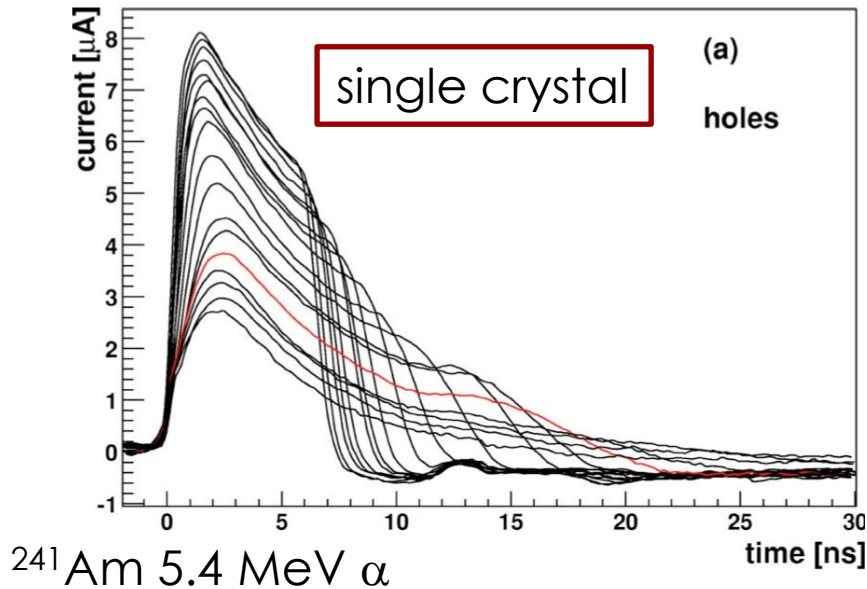
- Impressive progress over the last 20 years.
- Current state of the art for **polycrystalline** CVD diamond  $\delta \sim 250 \mu\text{m}$  ( $\sim 9000 \text{ e/MIP}$ ) **commercially available**.



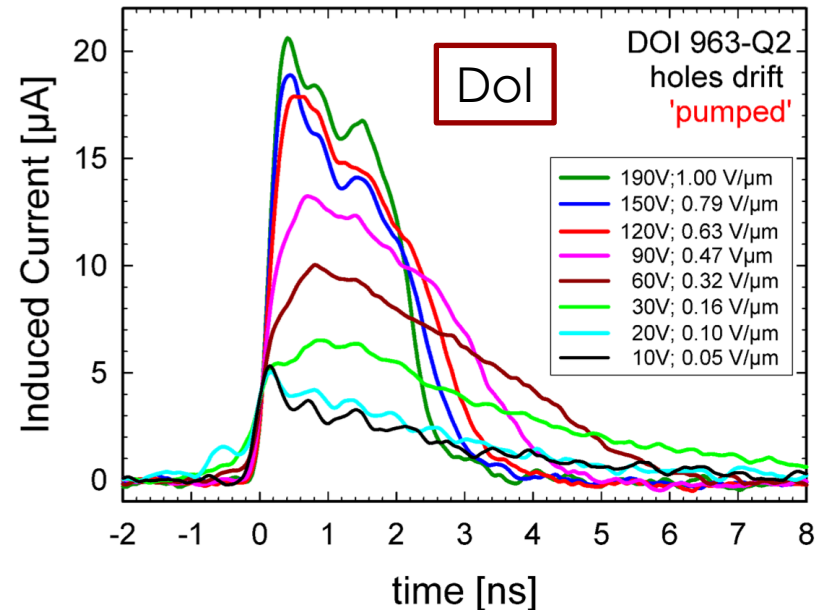
# Development of CVD Diamond for detector applications

- Impressive progress over the last 20 years.
- **Single crystal diamond ~ 100% efficient**
- **Diamond on iridium ~ 97% efficient**

J. Appl. Phys. 97, 073704 (2005)

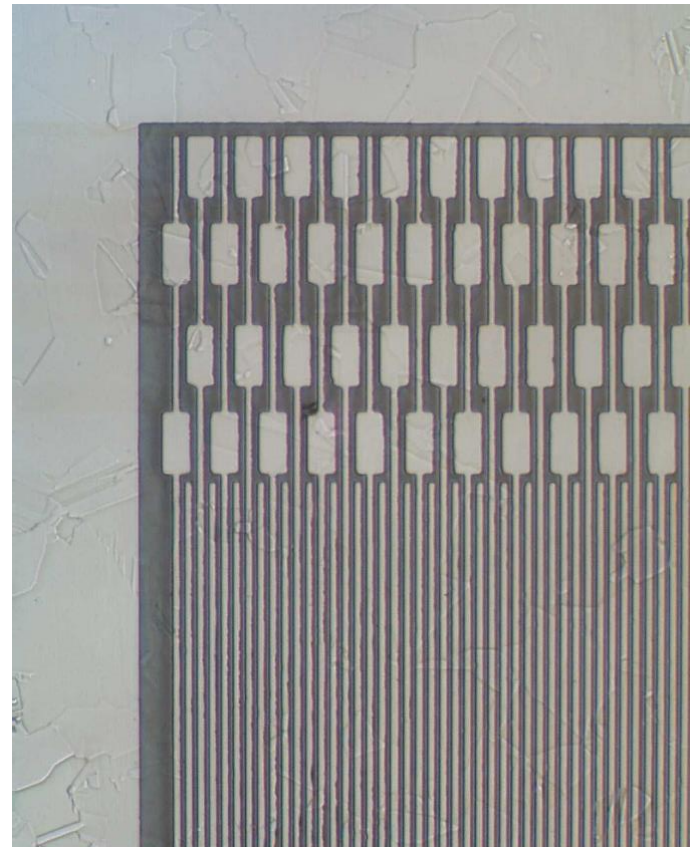


GSI annual report 2013

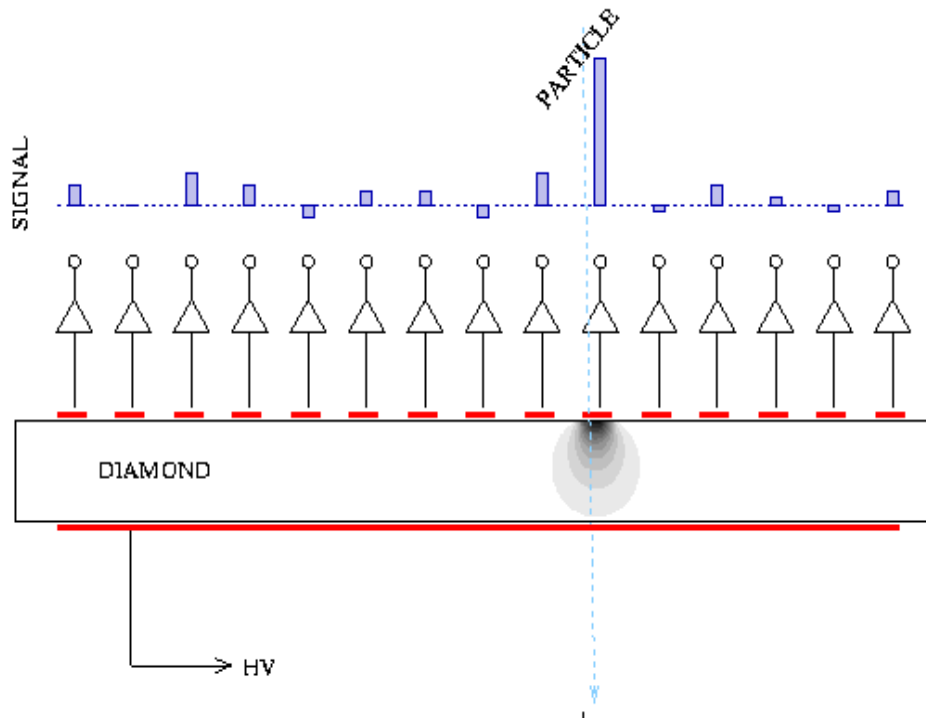


# Strip Detectors

- First position sensitive diamond detectors were strip detectors.
- Many prototypes tested starting around 1994

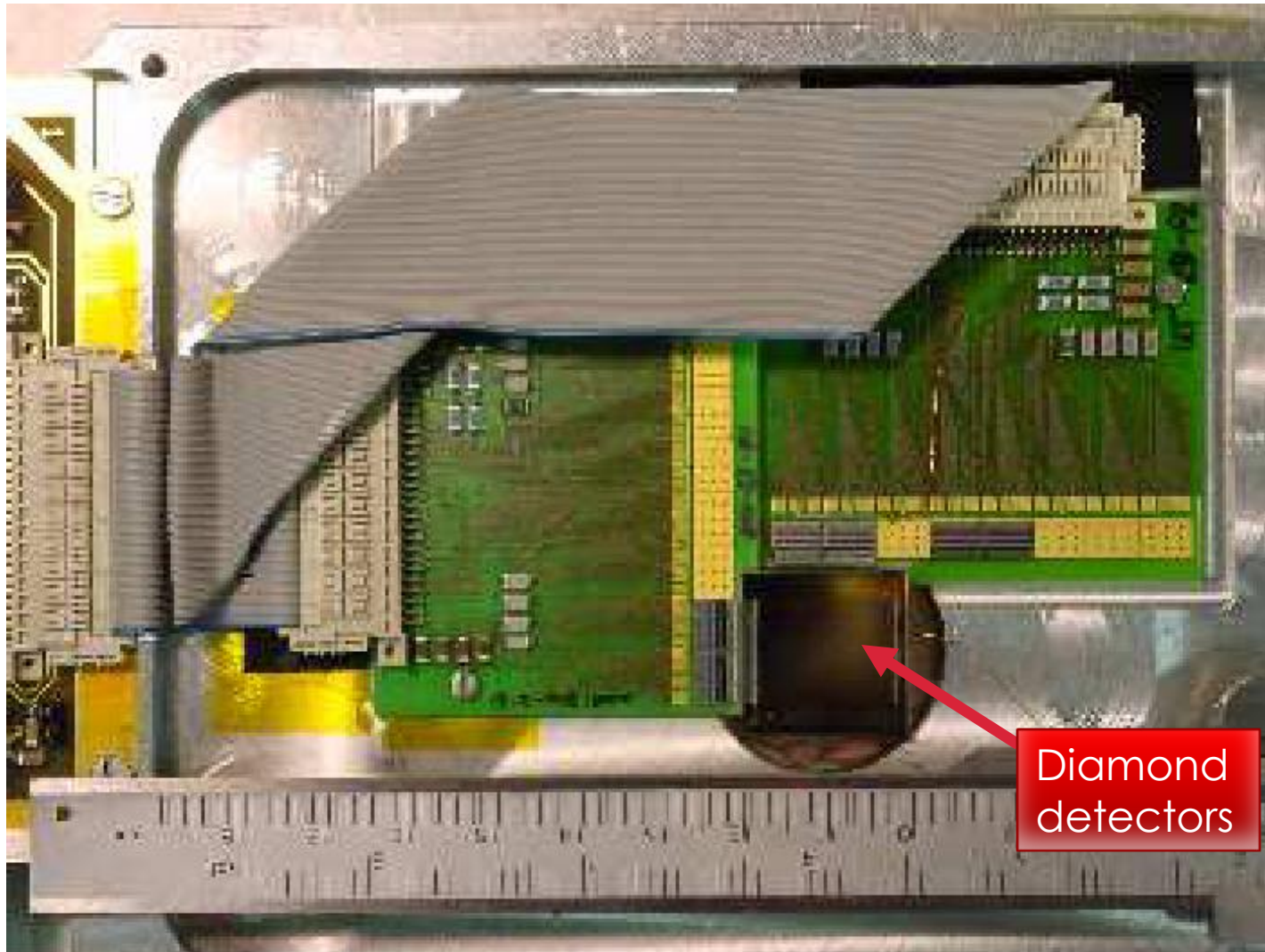


# Principle

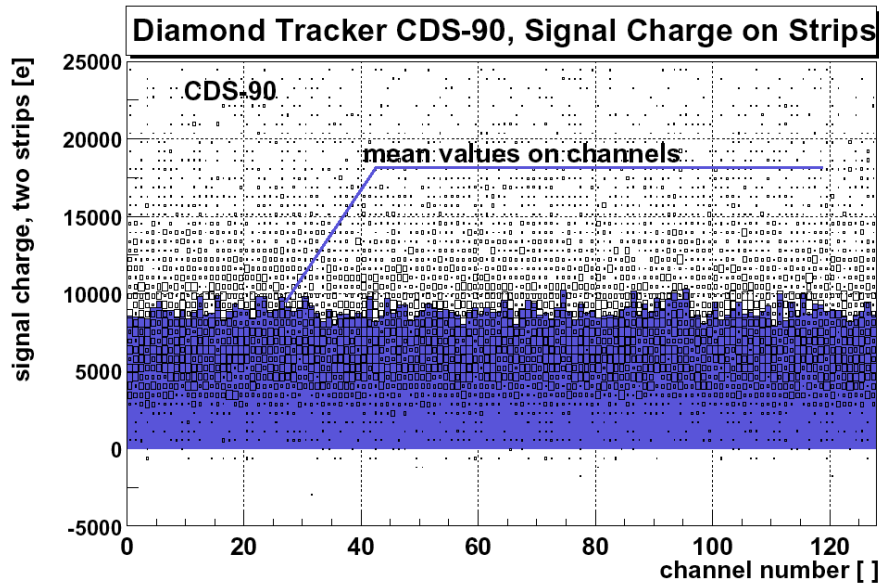


- The charge signal is picked up by the strip(s) next to the particle track.
- The charge is shared by multiple strips if the charge collection is incomplete.
- The position of the particle track can be reconstructed by calculating the charge weighted impact point  
**(Center of Gravity)**

- A Diamond Testbeam Telescope

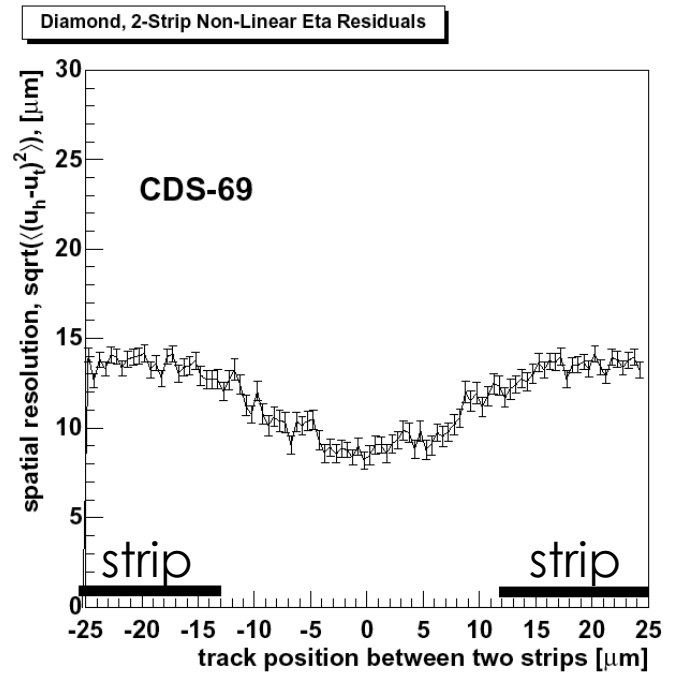


### PH Distribution on each Strip



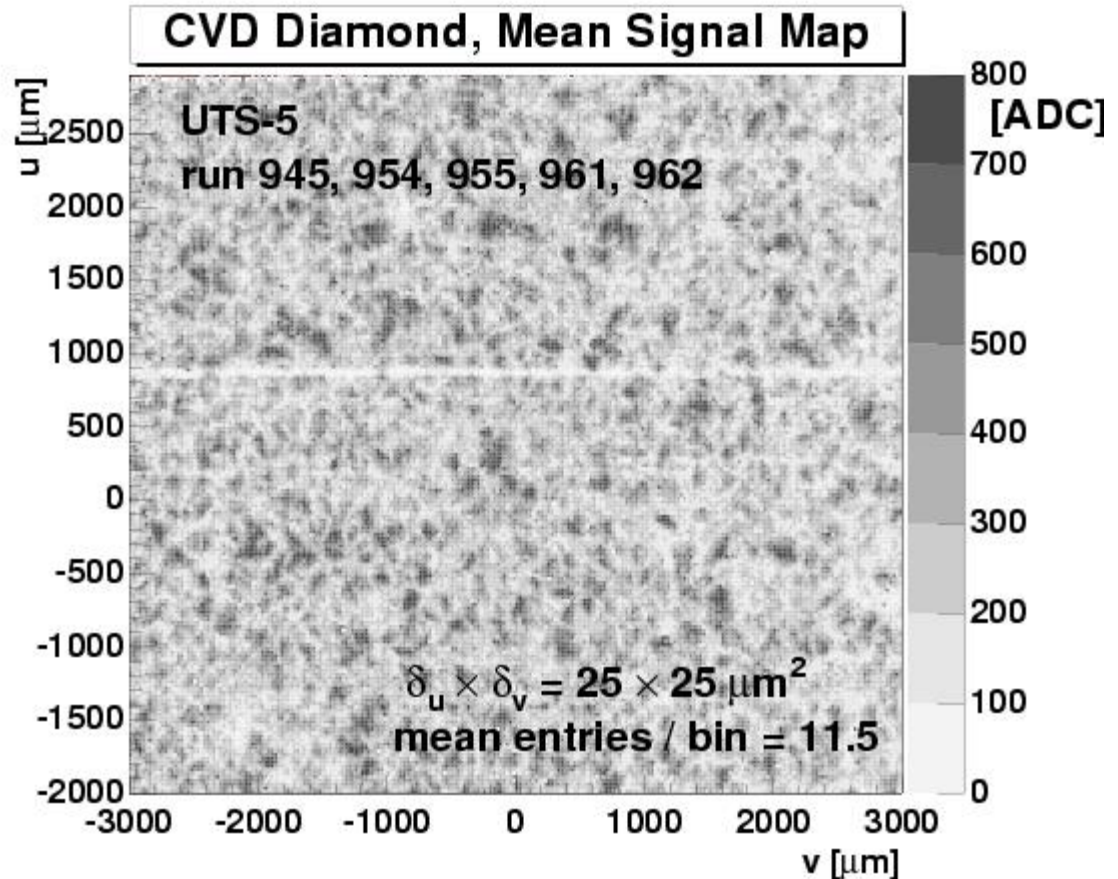
~10ke mean signal

### Residual versus Track Position



## Uniformity in Charge Collection of CVD Diamonds

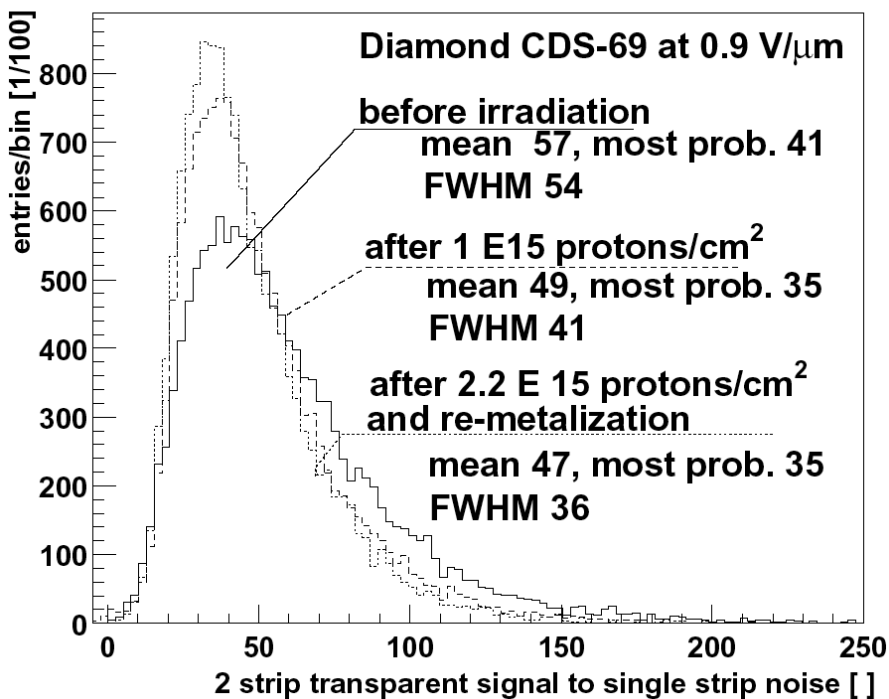
- Measured with MIPS
- Polycrystalline CVD diamond exhibits non-uniform signal response due to crystallite structure.
- Similar patterns observed as with photon beam measurement



# Irradiated Strip Detectors

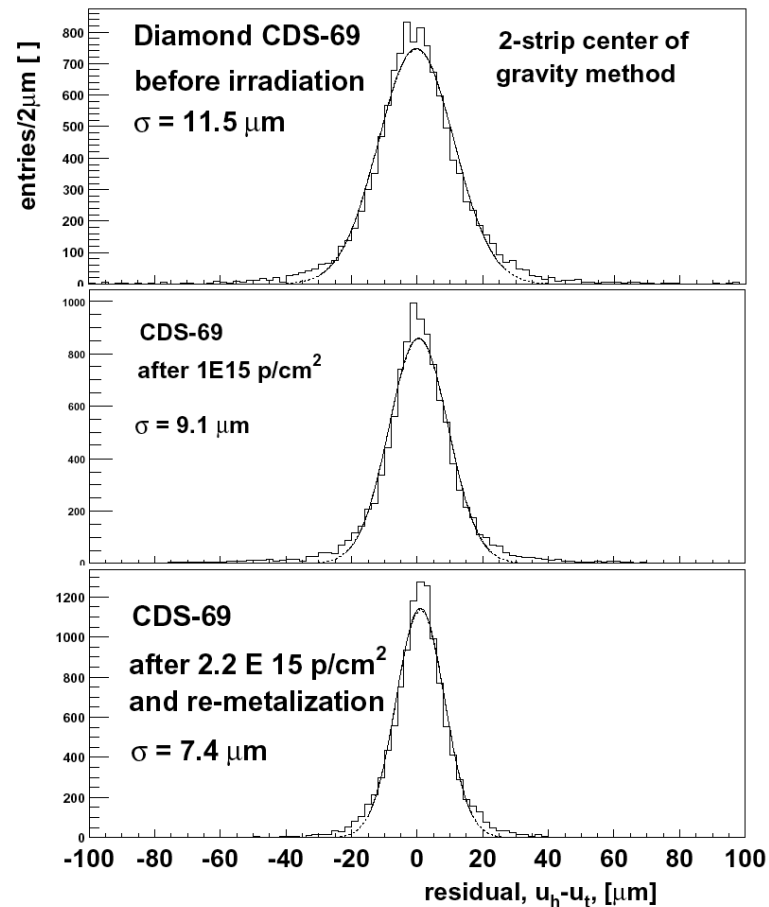
■ Proton Irradiation

Signal from Irradiated Diamond Tracker



15% loss of S/N after 2e15 p cm<sup>-2</sup>

Residual Distributions, Proton Irradiated Diamond



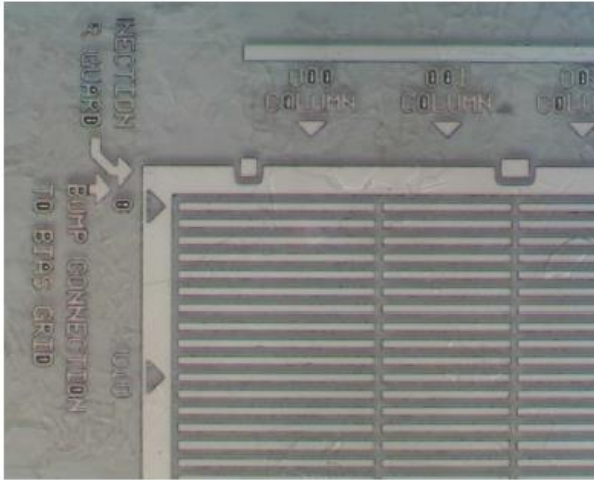
35% improvement in resolution

# Pixel Detectors

- Several prototypes of Diamond pixel detectors have been developed and tested since around 1996.
- Read-out chips use ROC (CMS), FE-I4 (ATLAS)
- More recently tested 3D pixel detectors (see later).
- Some historic examples in the following.

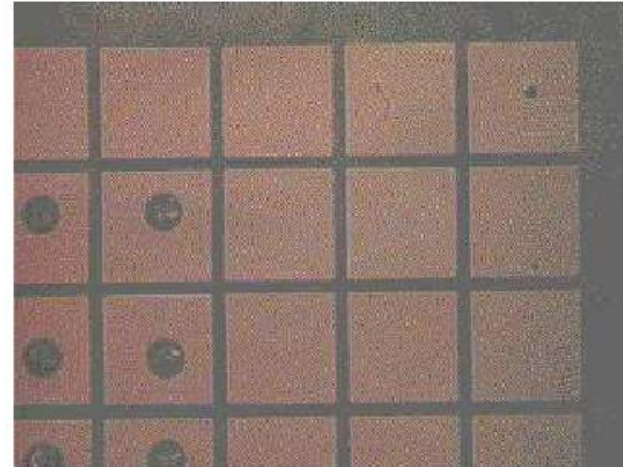
- Diamond Pixel Detectors

ATLAS FE/I Pixels (Al)



- ◆ Atlas pixel pitch  $50\mu\text{m} \times 400\mu\text{m}$
- ◆ Over Metalisation: Al
- ◆ Lead-tin solder bumping at IZM in Berlin

CMS Pixels (Ti-W)



- ◆ CMS pixel pitch  $125\mu\text{m} \times 125\mu\text{m}$
- ◆ Metalization: Ti/W
- ◆ Indium bumping at UC Davis

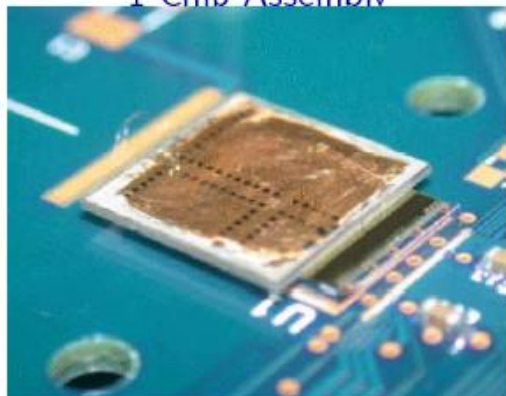
→ Bump bonding yield  $\approx 100\%$  for both ATLAS and CMS devices



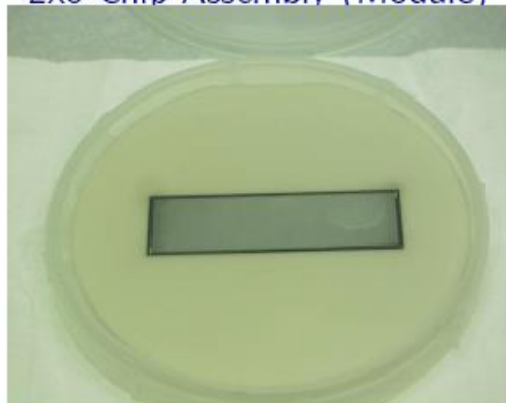
# Diamond Pixel Detectors

## Results from an ATLAS pixel detector

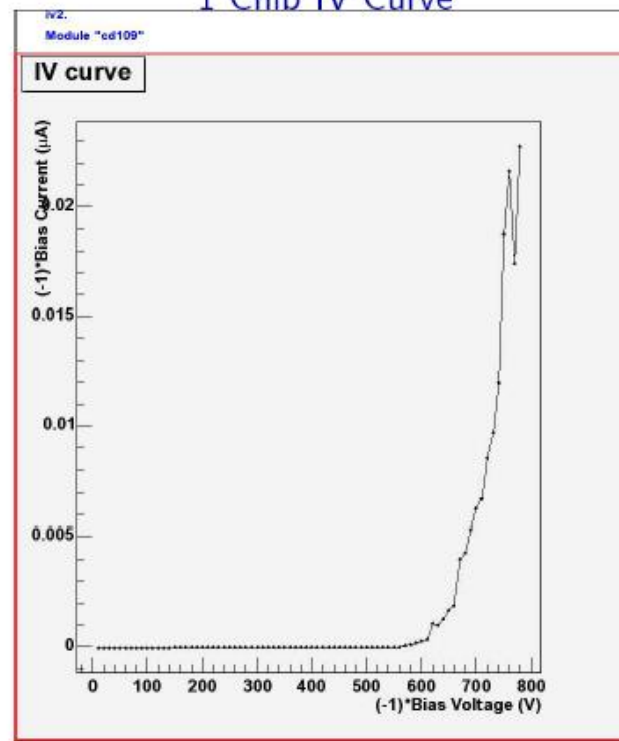
1 Chip Assembly



2x8 Chip Assembly (Module)



1 Chip IV Curve

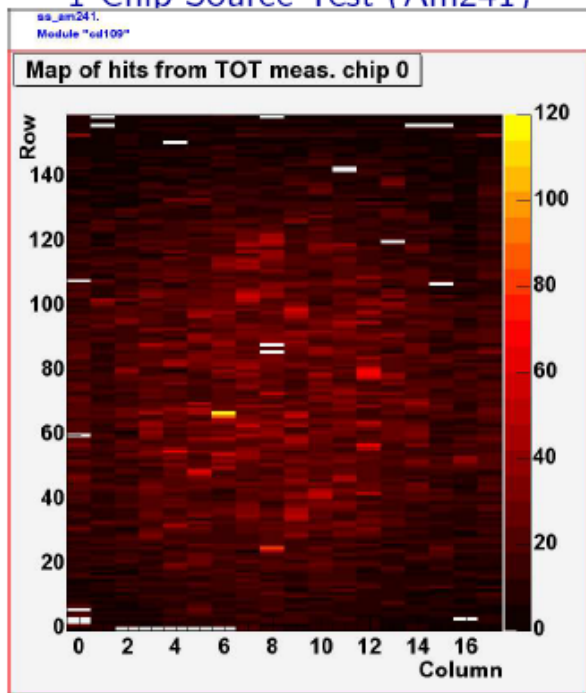




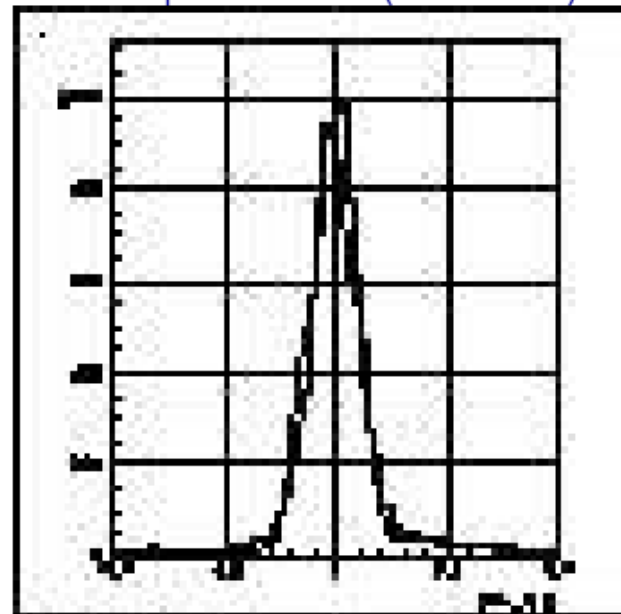
# Diamond Pixel Detectors

## Results from an ATLAS pixel detector

1 Chip Source Test (Am241)



1 Chip Beam Test (Resolution)



Americium 241 deposits  $\approx 4600e$

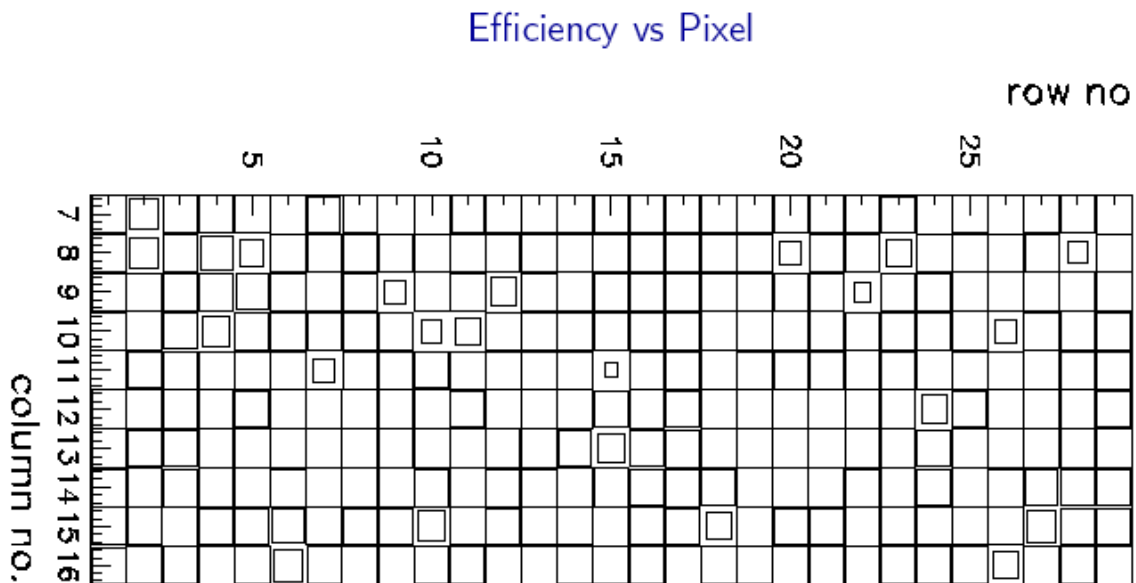
Spatial Resolution  $\approx \text{pitch}/\sqrt{12}$  (pitch  $50\mu\text{m} \times 400\mu\text{m}$ )



## Diamond Pixel Detectors



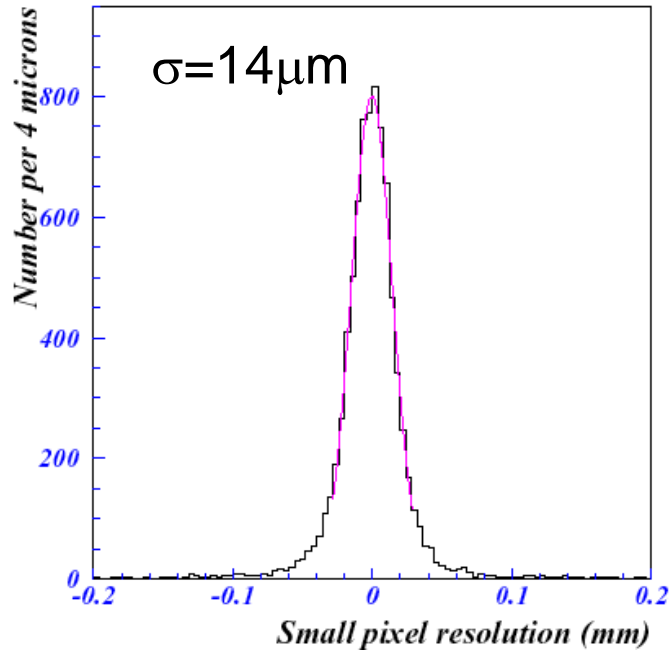
Results from a CMS pixel detector



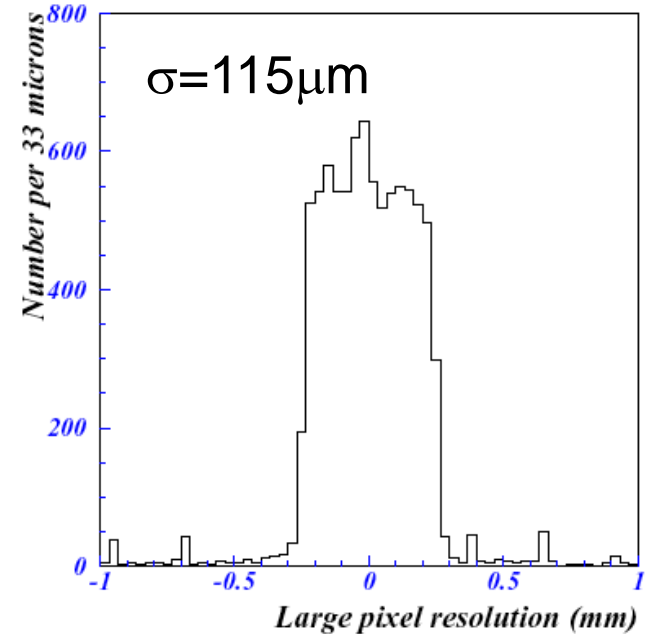
- Inefficient pixels due to bump bonding and/or electronics - shown in pulser tests
- Excellent correlation between beam telescope and pixel tracker data!

- Results from Atlas Diamond Pixel Detectors

Spatial Resolution – Short Direction

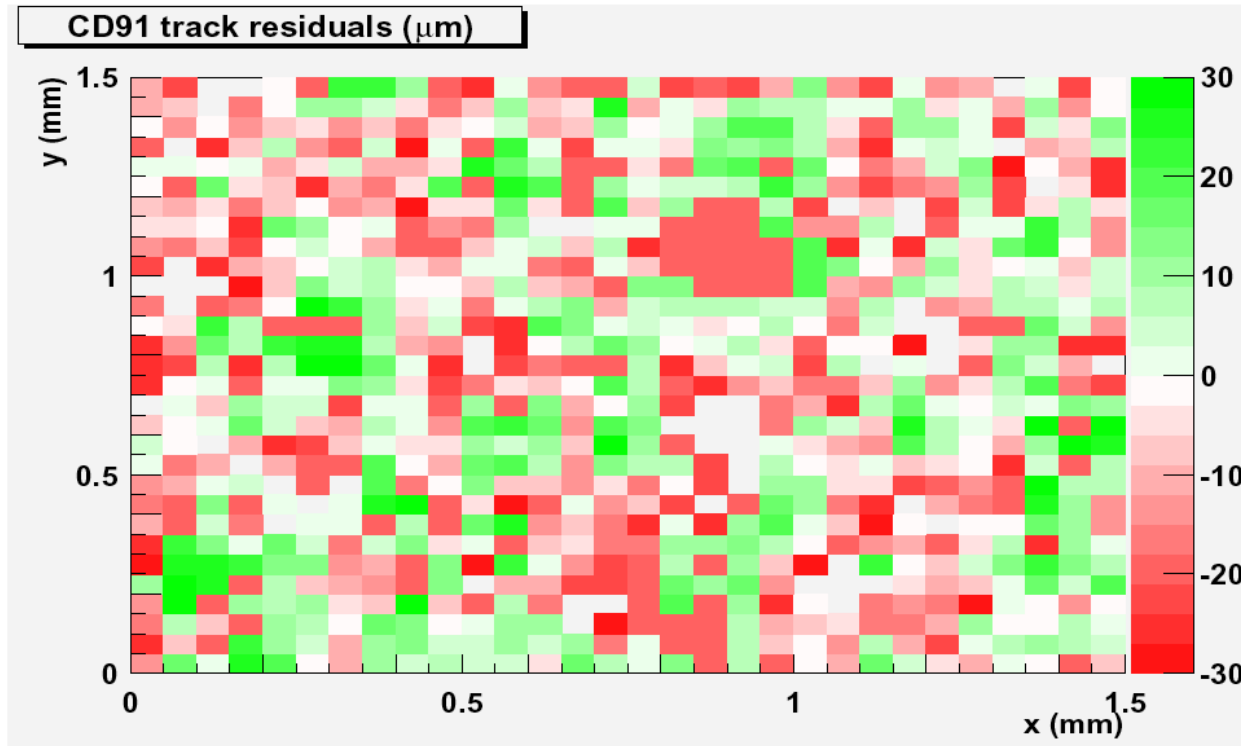


Spatial Resolution – Long Direction



- Efficiency = 80%
- Resolution = digital

- Results from Atlas Diamond Pixel Detectors



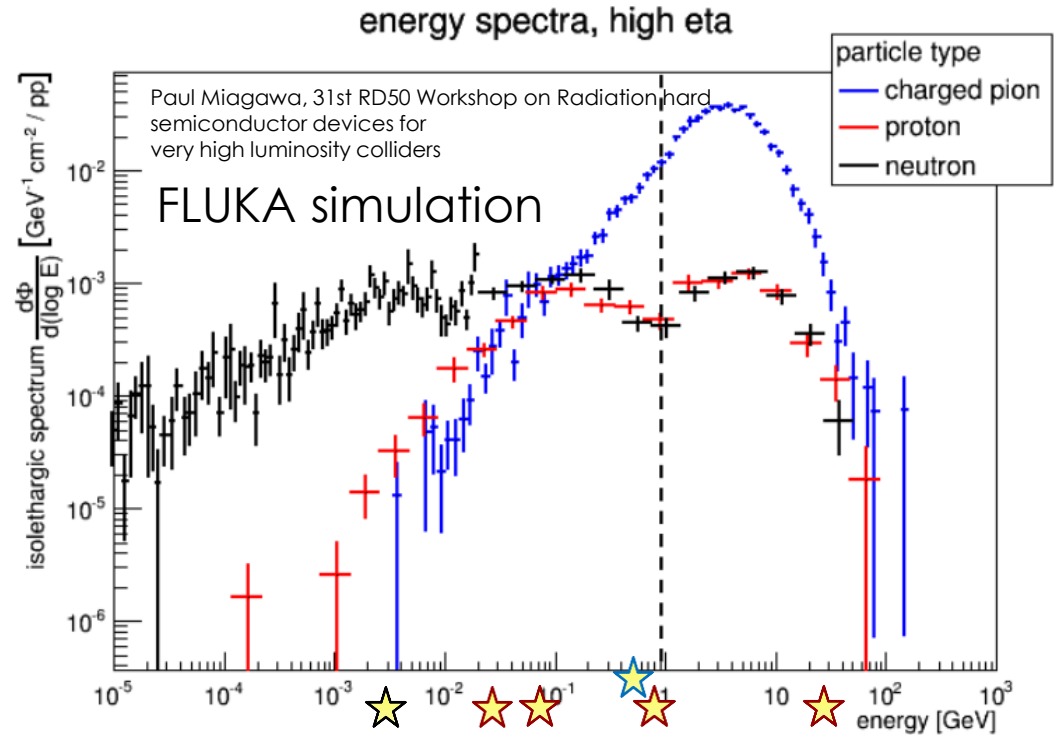
Tommaso Lari (INFN)  
Alexander Oh (CERN)  
Norbert Wermes (University Bonn)

- Large track residuals
- Non-uniformity of response qualitatively reproduces by modeling

# Radiation Tolerance

# Tests of Radiation Tolerance

- Irradiate with **proton, pions** and **neutrons**.
  - Energies within the expected radiation profile at HL-LHC.
  - HL-LHC fluence requirement about  $2e16$  neq.



	Proton ★	Pion ★	Neutron ★
Energy	25MeV – 24GeV	300 MeV	1-10 MeV
Fluence	$1.27e16$ p $\text{cm}^{-2}$	$6e14$ $\pi$ $\text{cm}^{-2}$	$1.3e16$ n $\text{cm}^{-2}$

- Assume simple effective model for radiation damage:

Radiation damage constant  
is fitted with simple model:

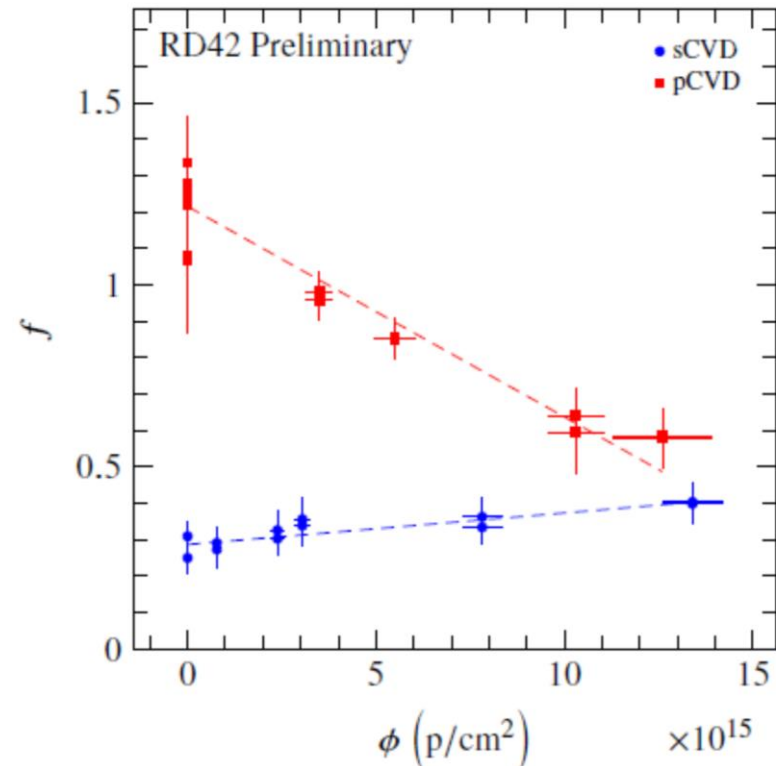
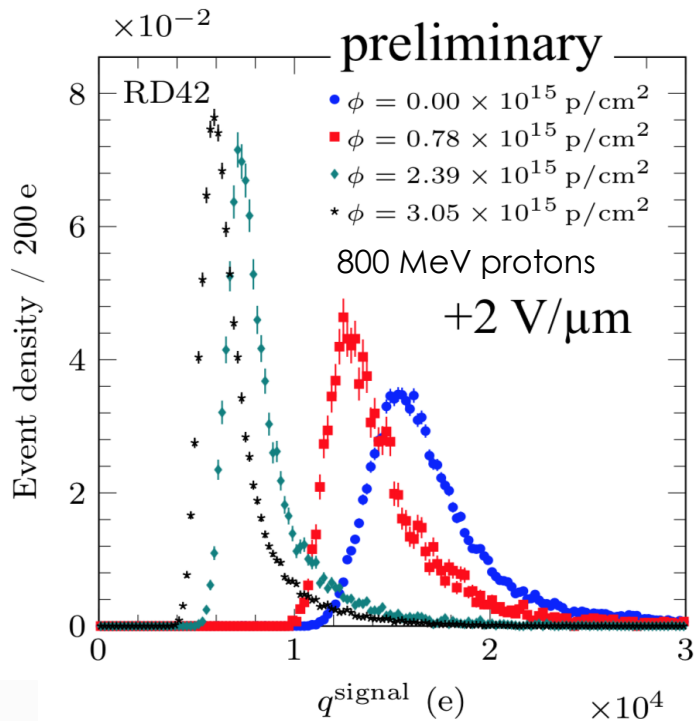
$$\frac{1}{\lambda} = \frac{1}{\lambda_0} + k_{\lambda} \Phi$$

damage constant

particle flux

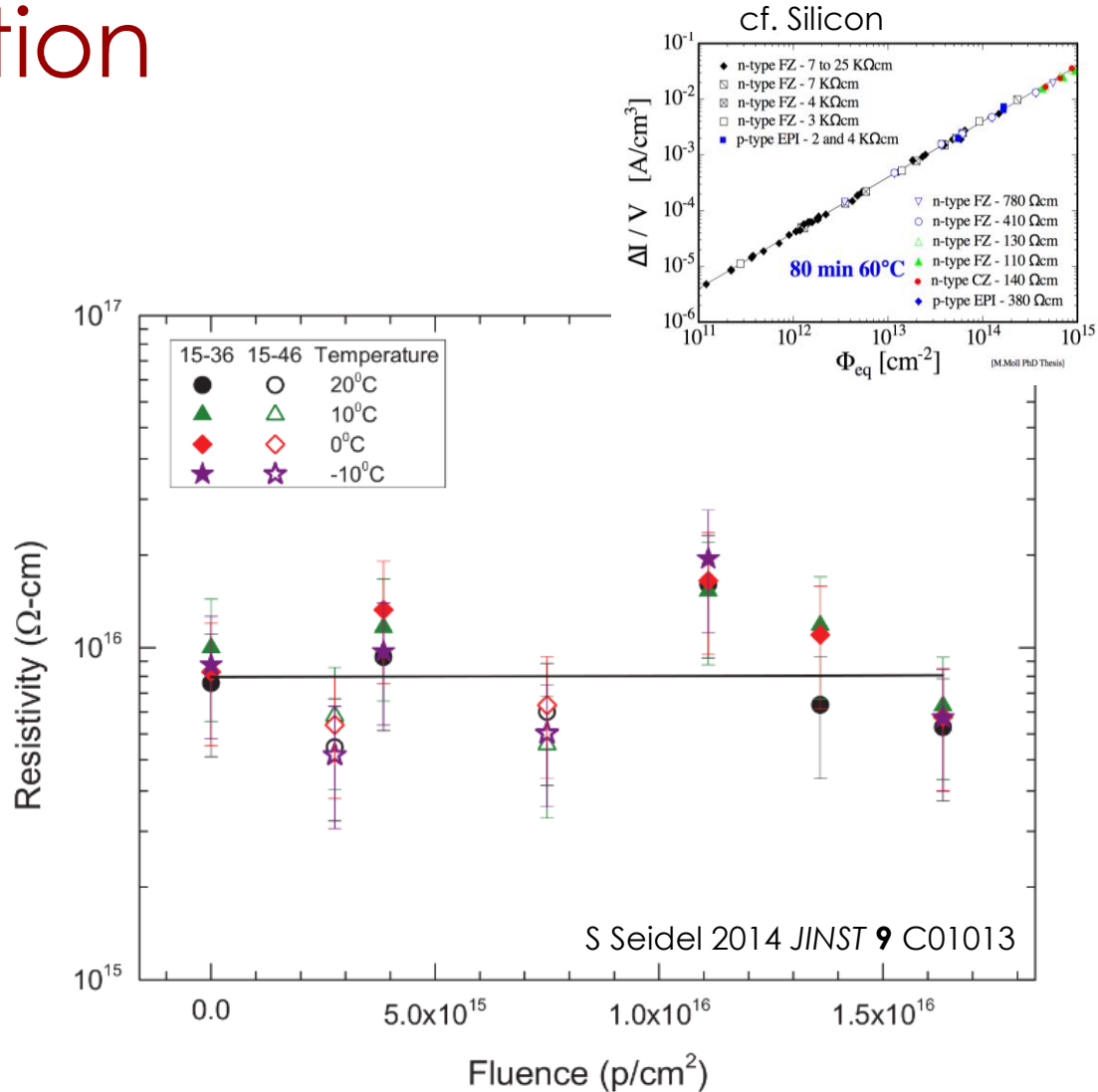
# Radiation Tolerance: Characterization

- Typical Landau Spectra after irradiation of pCVD.
- For pCVD see reduction of **FWHM** / **MP** with irradiation.
  - Expected from polycrystalline nature of material!
  - Single crystal material almost flat.



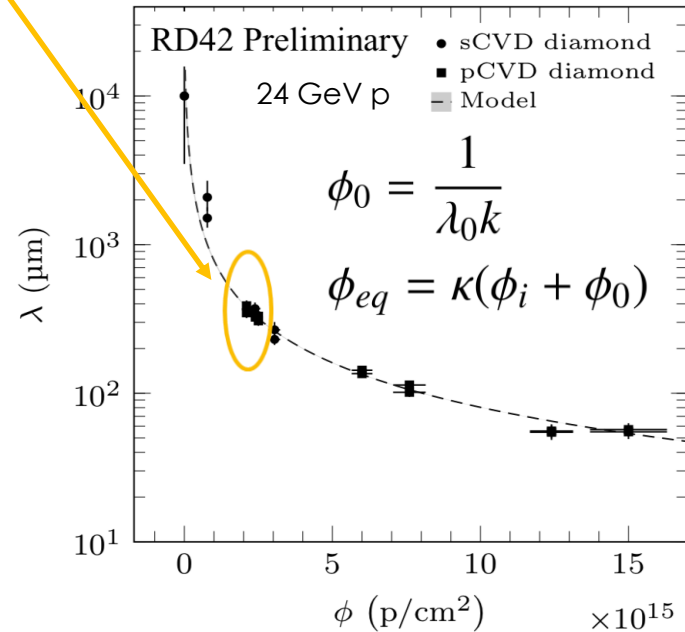
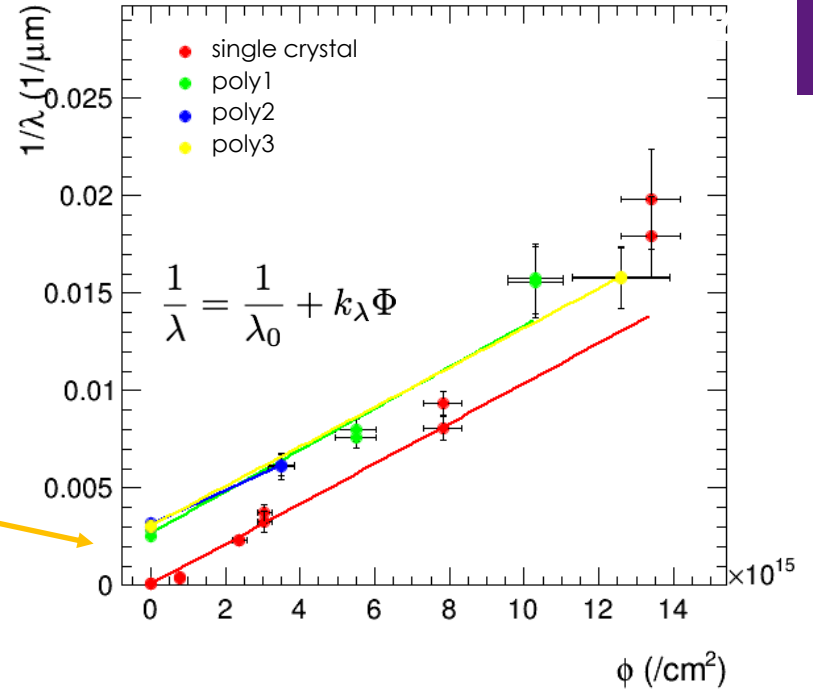
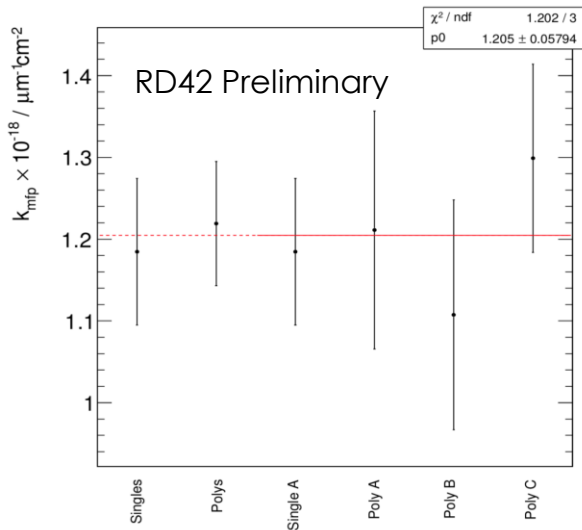
# Radiation Tolerance: Characterization

- Resistivity
  - No dose dependence.
  - Due to large bandgap no significant temperature dependence at RT or below.



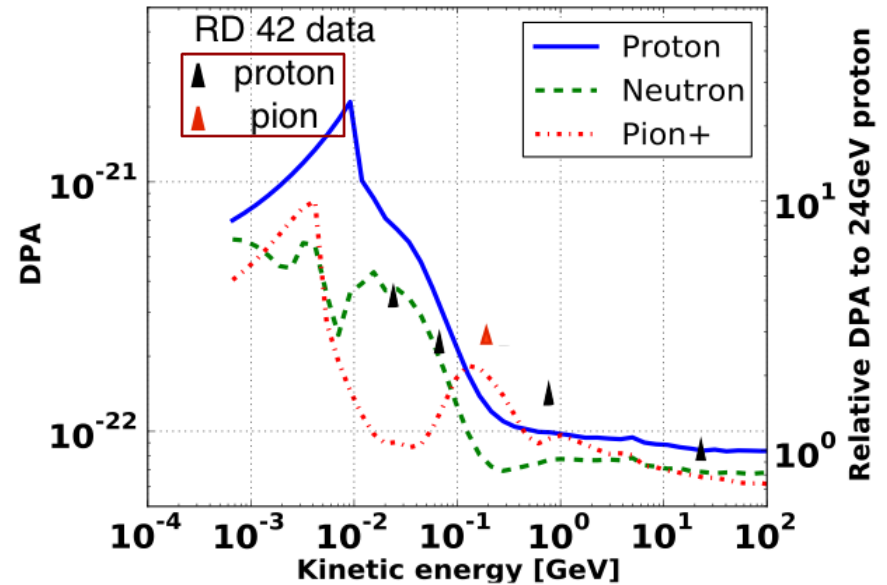
# Radiation Tolerance: Characterization

- Damage factor  $k$  is determined for each sample.
- **pCVD** diamonds are offset by  $\lambda_0$  to account for initial finite carrier lifetime.
- Final damage factor averaged over all samples.



# Radiation Hardness

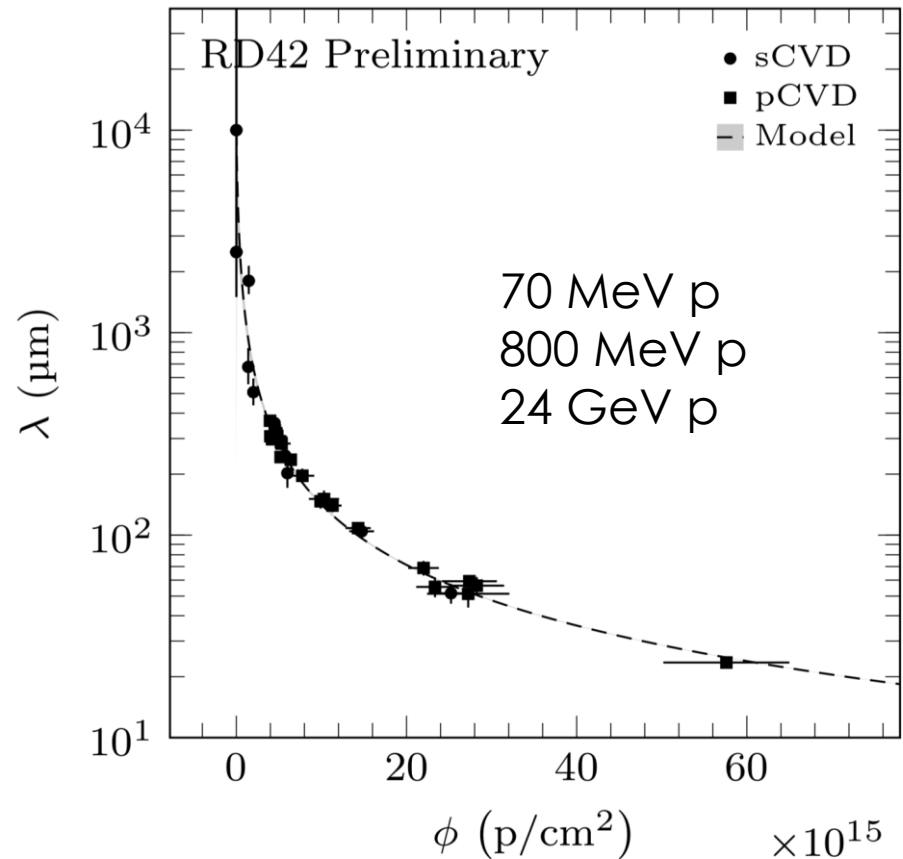
- Describe radiation damage using Norget-Robinson-Torrens theorem to predict displacements per atom (DPA).
- (M. Guthoff et al., arXiv:1308.5419)
- Diamond displacement energy: 43.3 eV
- Reasonable agreement for  $E > 100 \text{ MeV}$ .



# Radiation Tolerance

## ■ 24 GeV protons

- $k_\lambda = 0.67 \pm 0.04 \times 10^{-18} \text{ cm}^2 \mu\text{m}^{-1}$
- polycrystalline diamond sample offset by  $\Phi \sim 5 \times 10^{15}$  to account for existing traps.
- Poly and single crystal diamond show consistent damage constants.



L. Baeni ETHZ Thesis

<https://www.research-collection.ethz.ch/handle/20.500.11850/222412>

# Radiation Tolerance

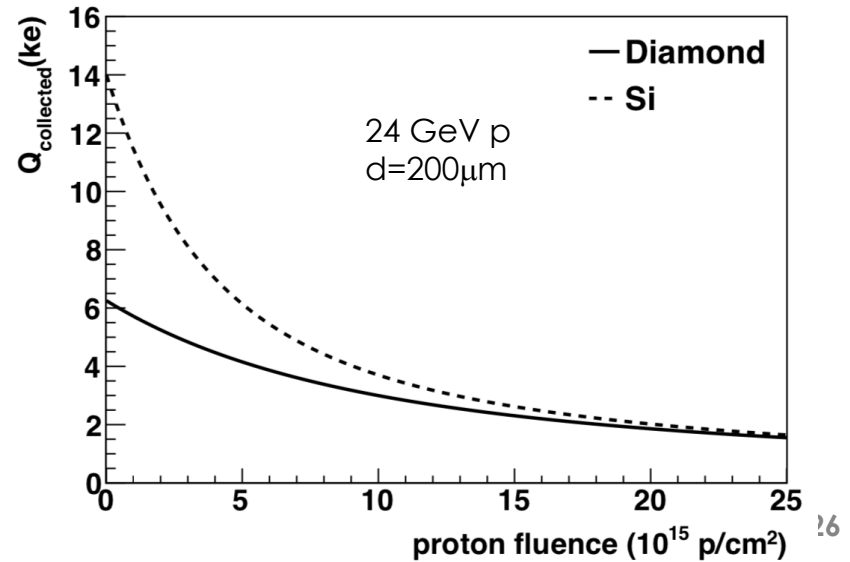
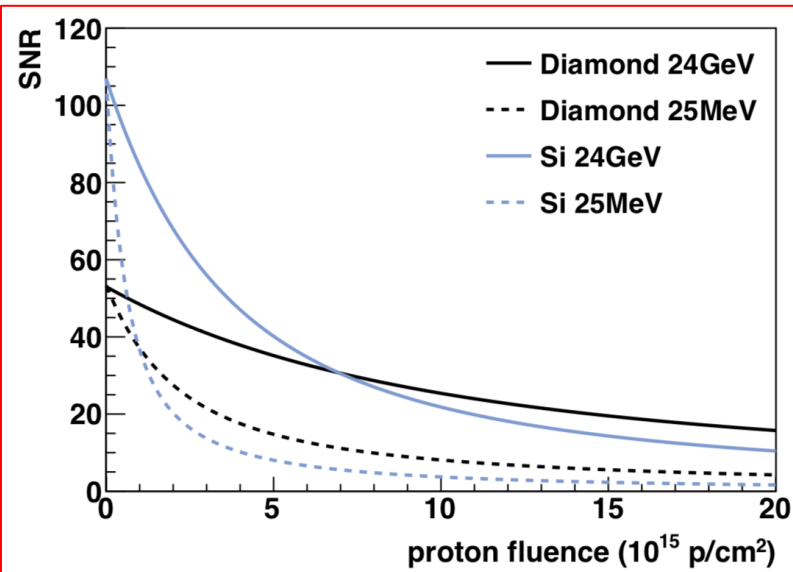
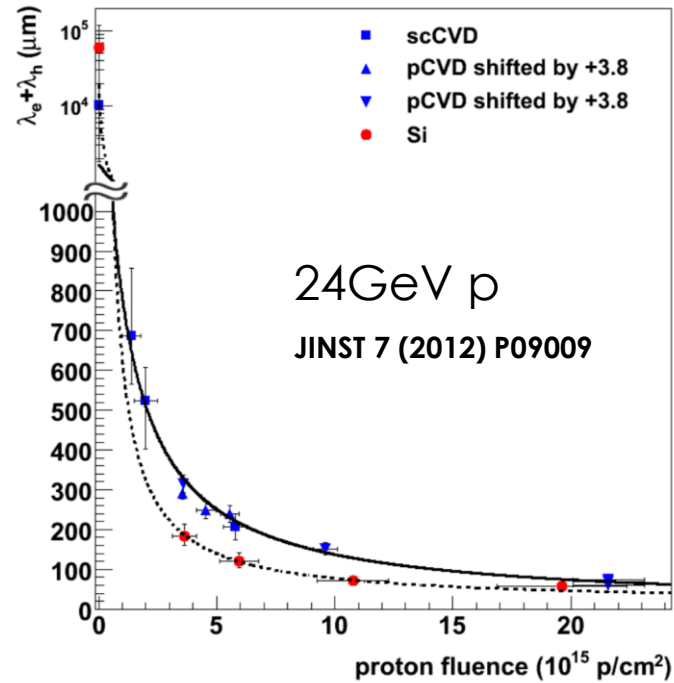
- Summary of RD42 irradiation results:

Particle Species	Relative Damage Constant, $\kappa$
24 GeV p	1
800 MeV p	$1.54 \pm 0.13$
70 MeV p	$2.5 \pm 0.4$
25 MeV p	$4.5 \pm 0.6$
fast neutrons	$4.5 \pm 0.5$

\*normalized to 24GeV protons

# Radiation Tolerance: Comparison to Si

- k factors typically 2-3 times higher for Silicon.
- A comparison to Si needs to take into account:
  - leakage current
  - capacitance
- Possible figure of merit  
Signal to noise ratio:

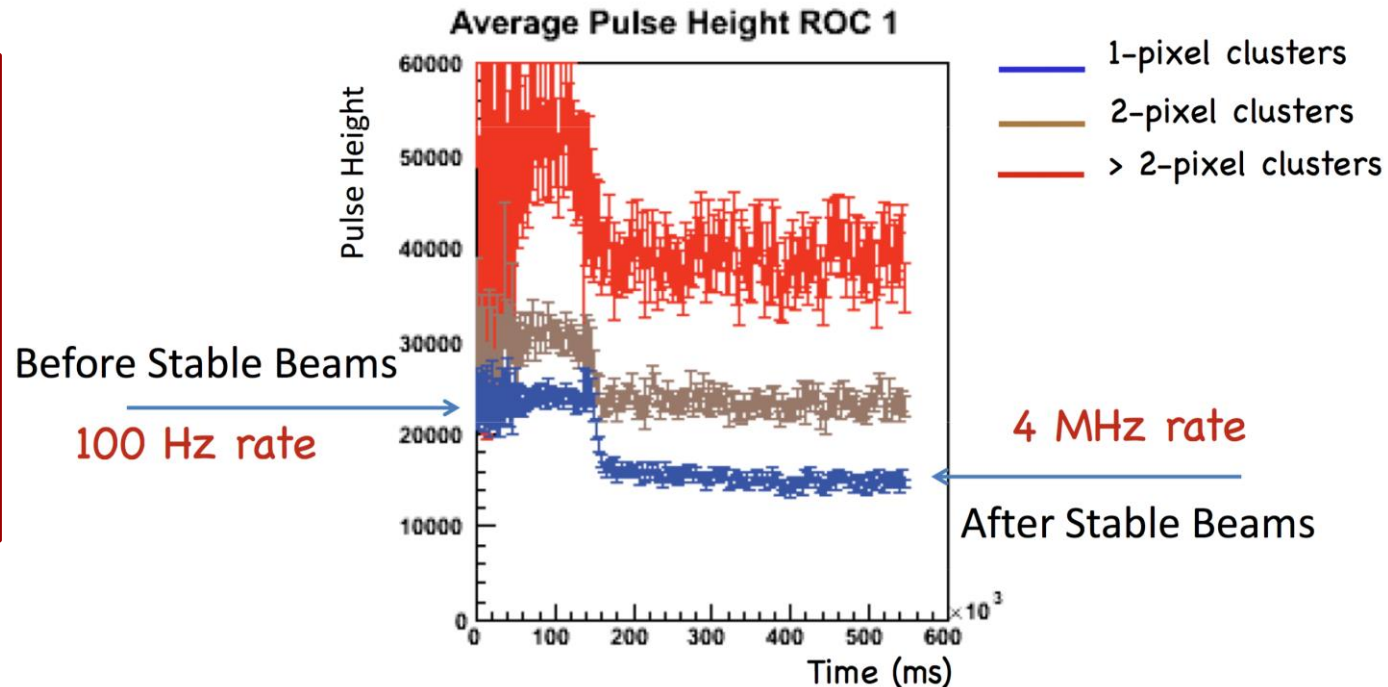


# High rate capability

# High Rate tests

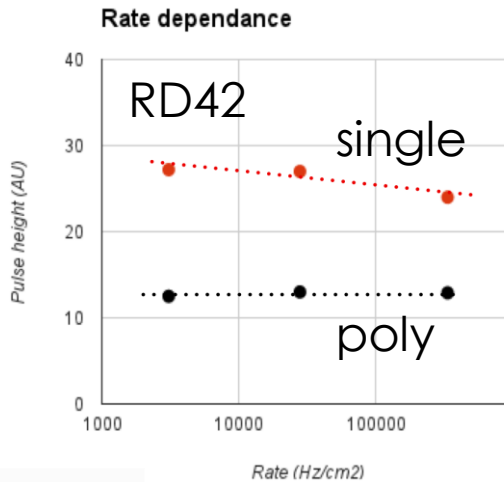
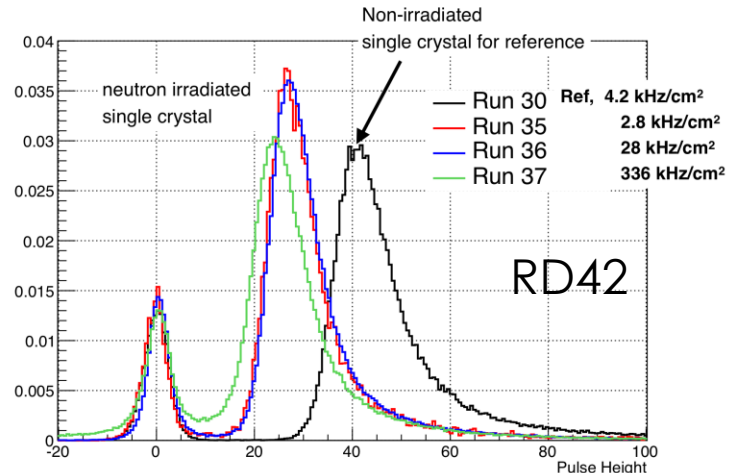
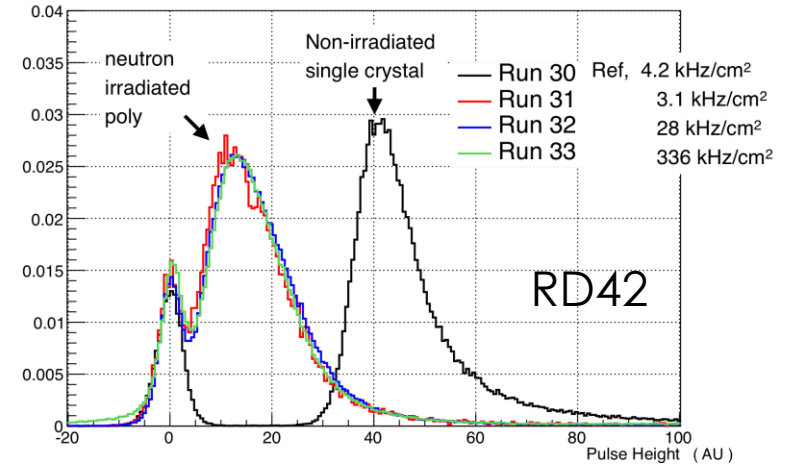
- Tests the pulse height as function of particle rate.
- Test single and poly crystalline diamond.
- Irradiated and un-irradiated.

Investigations triggered by indication of rate dependence of of single crystal diamond pixel detector installed in CMS in 2012.



# High Rate tests

- single and poly sample irradiated with  $5 \times 10^{13}$  reactor n.
- Tested with 250MeV pions.
- Slight rate dependence observed in irradiated **single crystal** sample.
- No rate dependence observed for irradiated **polycrystalline** sample.



# END OF PART 1

- In part 2 next week we look at:
  - 3D Diamond detectors
  - Application of diamond detectors in HEP

## Advanced UK Instrumentation Training

# Diamond Detectors

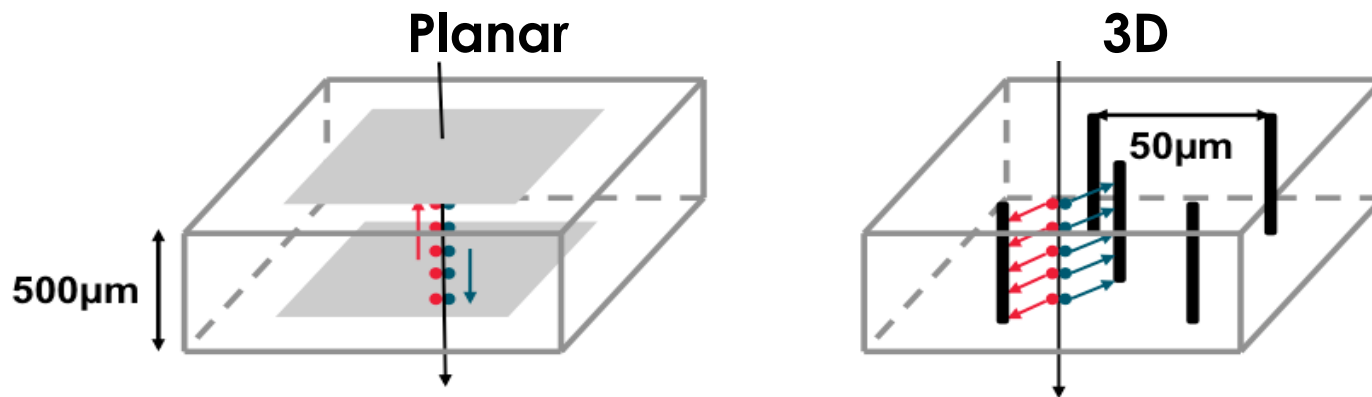
Alexander Oh  
University of Manchester

# PART 2

- 3D Diamond detectors
- Application of diamond detectors in HEP

# 3D diamond detectors

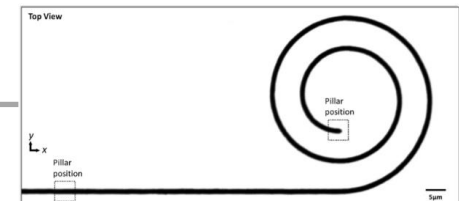
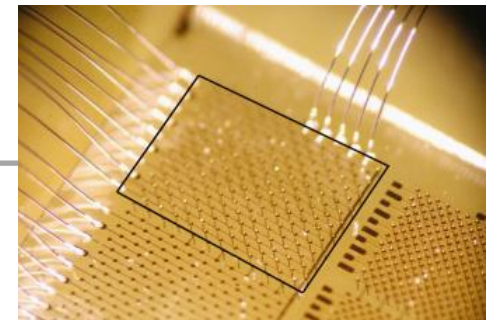
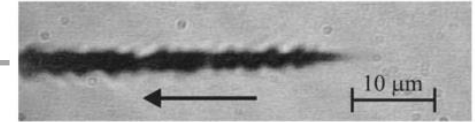
# 3D Diamond Detectors



- Electrode spacing determines drift distance to induce 1e charge.
- 3D has shorter electrode spacing compared to planar.
- Charge carriers need less drift distance (and time) in 3D than in planar to induce equal signal.
- Influence of traps and resulting limited lifetime suppressed in 3D.

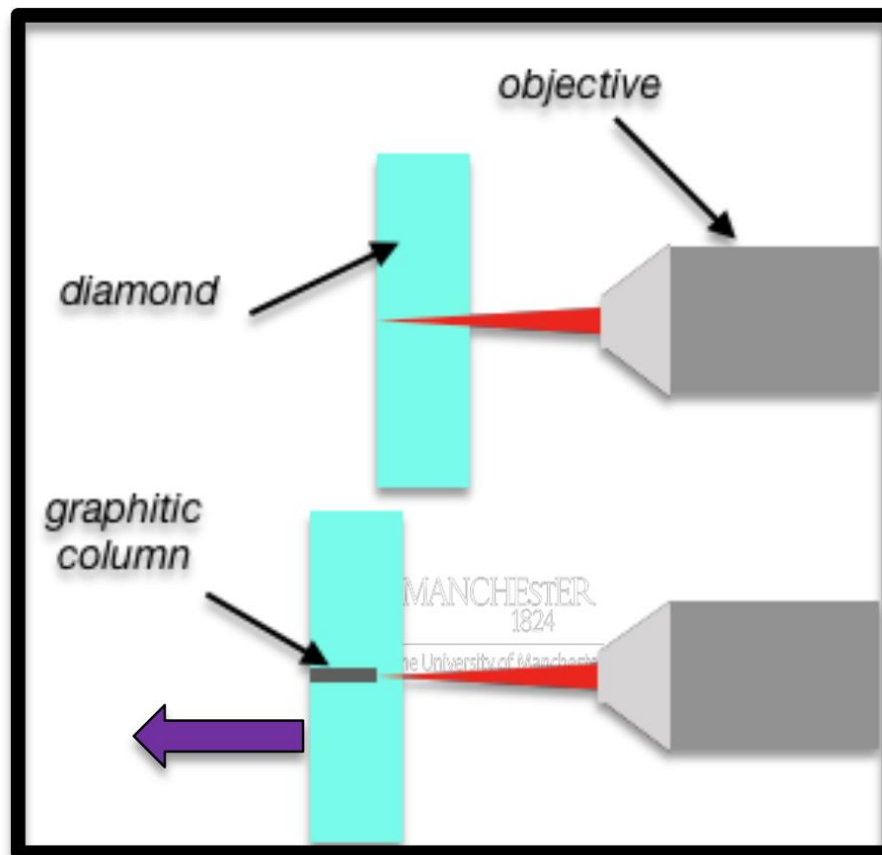
# 3D Diamond Research - A relatively young field

- Laser induced phase change in diamond.
  - E.g. T.V. Kononenko et al, Diamond & Related Materials 18 (2009) 196–199  
“*Femtosecond laser microstructuring in the bulk of diamond*”
- 3D “Pad” detector
  - A. Oh, B. Caylar, M. Pomorski, T. Wengler, Diamond and Related Materials, 38 , (2013), “*A novel detector with graphitic electrodes in CVD diamond*”
  - S. Lagomarsino et al, Appl. Phys. Lett. 103, 233507 (2013), “*Three-dimensional diamond detectors: Charge collection efficiency of graphitic electrodes*”
- 3D “strip array” detector with position resolution.
  - E.g. F. Bachmaier et al, NIM A, 786, (2015) 97-104,  
“*A 3D diamond detector for particle tracking*”
- Radiation damage studies.
  - E.g. S. Lagomarsino et al, Applied Physics Letters 106, 193509 (2015)  
“*Radiation hardness of three-dimensional polycrystalline diamond detectors*”
- Improvements in graphitization process.
  - E.g. B. Sun et al., Applied Physics Letters 105, 231105 (2014), “*High conductivity micro-wires in diamond following arbitrary paths*”
- 3D pixel detectors
  - RD42, CERN-LHCC-2018-015 ((2018), *Development of Diamond Tracking Detectors for High Luminosity Experiments at the LHC, HL-LHC and Beyond*
  - L. Anderlini et al, Front. Phys., 04 November 2020, *Fabrication and Characterisation of 3D Diamond Pixel Detectors With Timing Capabilities*



# Fabrication

- Conductive columns are created by changing diamond into a graphitic material with a short laser pulse:

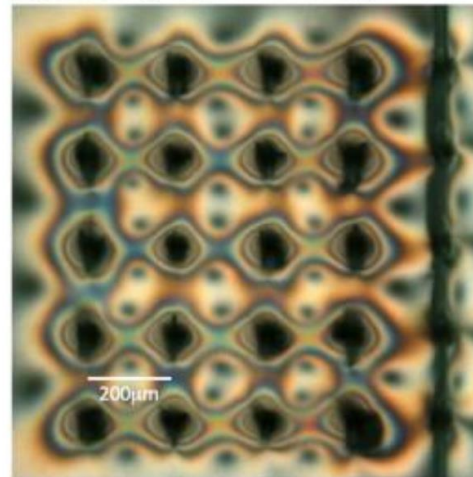


Laser graphitisation of diamond

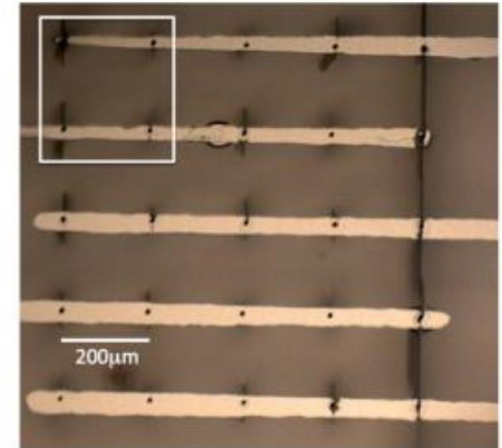
# FIRST 3D DIAMOND DEVICE

- Collaboration of **Manchester**, CEA LIST and CERN
- Published **2013**
- Single crystal substrate
- First device made at LIST using **nano-second** pulse nitrogen laser with beam spot diameter of **10 $\mu$ m**

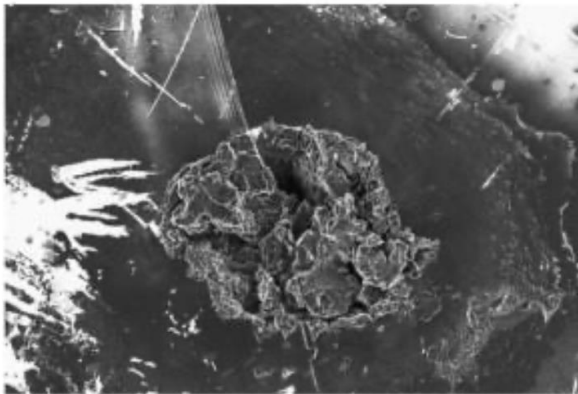
(a) Birefringence microscopy.



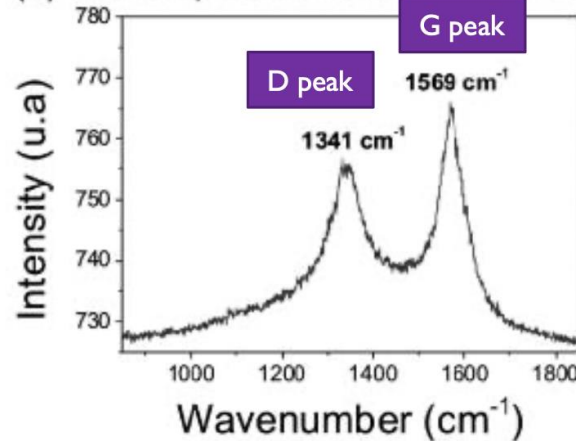
(b) Photograph after metallisation.



(a) SEM picture of a graphitic column.

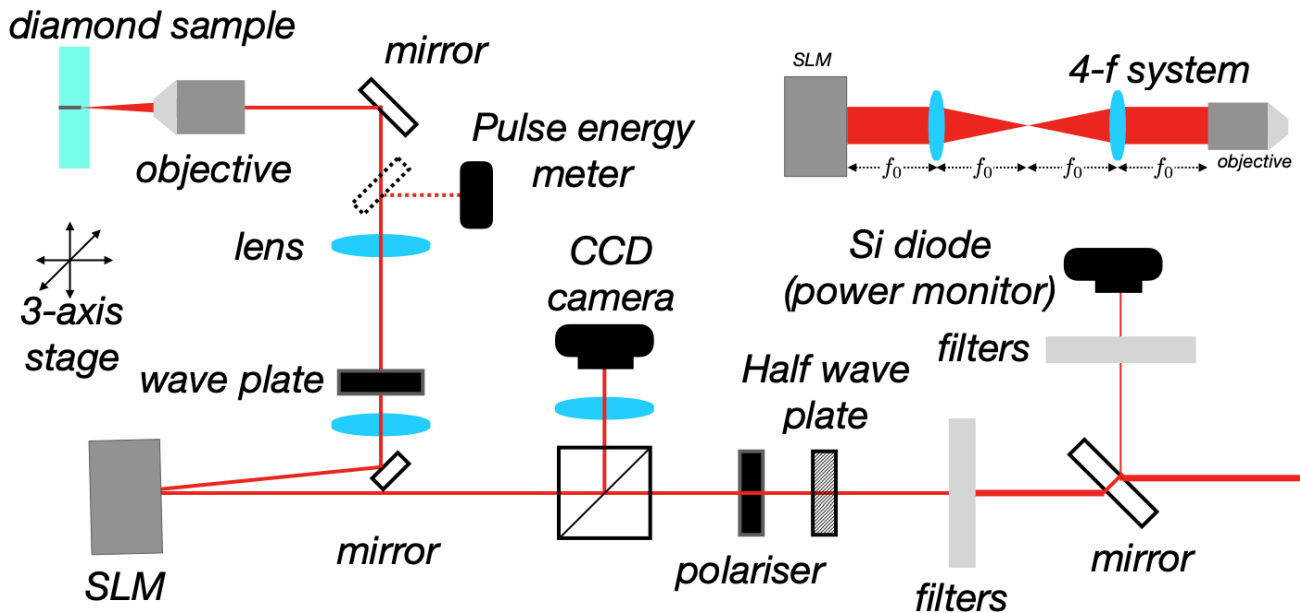


(b) Raman spectrum on the graphitic column.



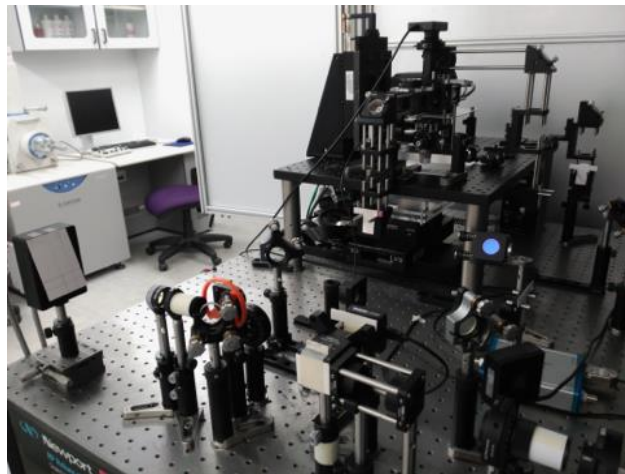
Oh, A., Caylar, B., Pomorski, M., & Wengler, T. (2013). A novel detector with graphitic electrodes in CVD diamond. *Diamond and Related Materials*, 38, 9–13.

# Laser Set-up in Manchester



Laser specs:

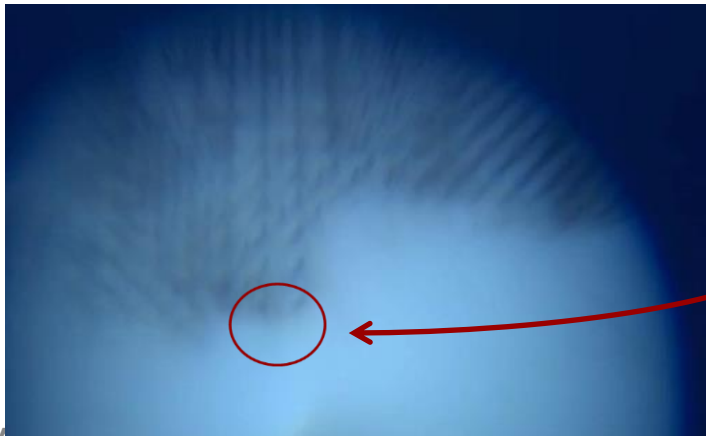
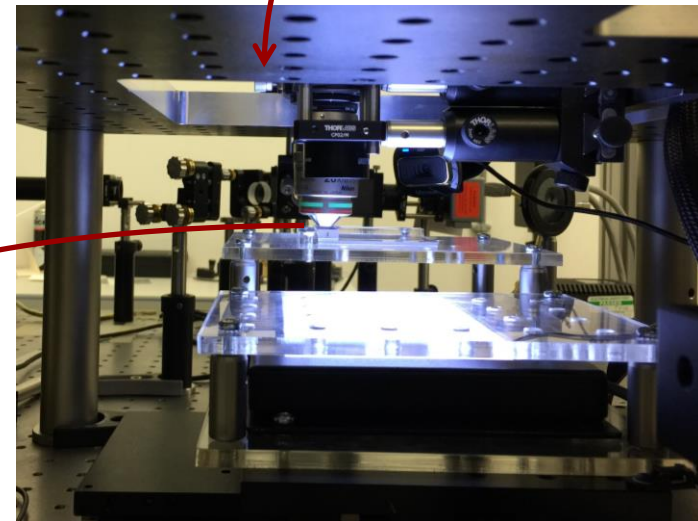
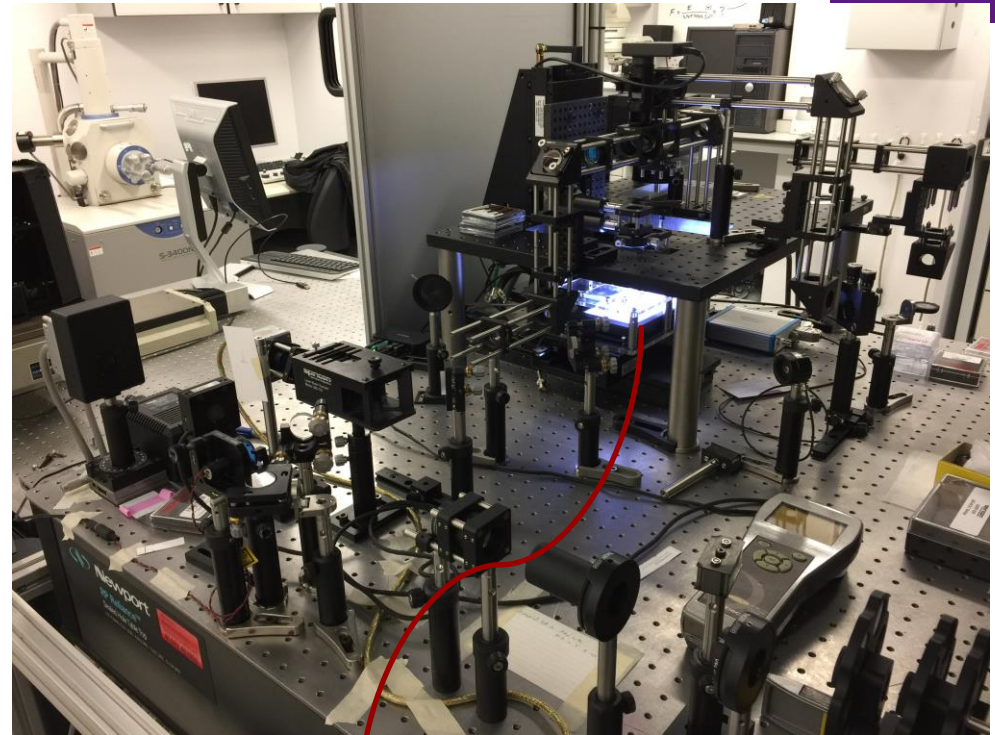
- Wavelength: 800 nm
- Repetition rate: 1 kHz
- Pulse duration: 100 fs
- Max power: 1 W



Just moved to MECCDI!

University of Manchester, Laser Processing Research Center.

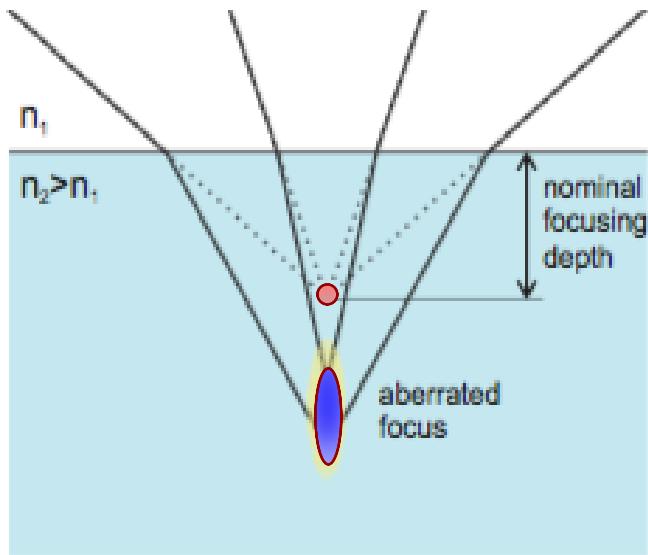
- Wavelength = 800 nm
- Repetition rate = 1 kHz
- Pulse duration = 100 fs
- Spot size = 10 $\mu$ m
- Pulse Energy ~ 1  $\mu$ J
- **Spatial light modulator**



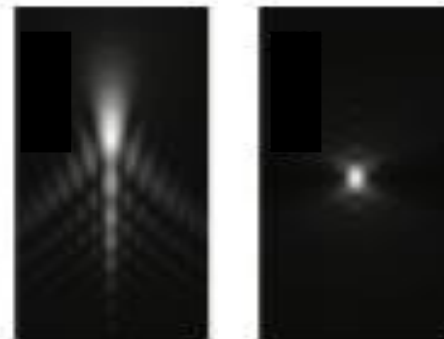
# SLM – Phase Spatial Light Modulation

- Comparison SLM vs standard process.

	Std.	SLM
Resistivity	1 $\Omega\text{cm}$	0.1 $\Omega\text{cm}$
Diameter	$\sim 3\mu\text{m}$	$\sim 1\mu\text{m}$
Diamond to graphite ratio	$\sim 4$	$\sim 0.2$



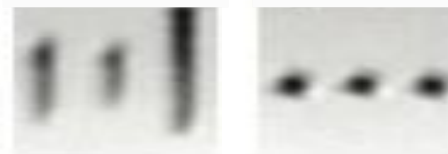
Simulated depth = 40 $\mu\text{m}$



Measured depth = 40 $\mu\text{m}$



depth = 80 $\mu\text{m}$

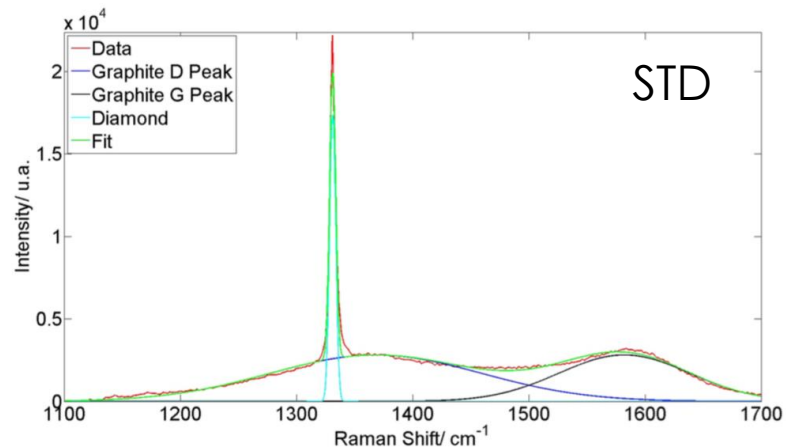
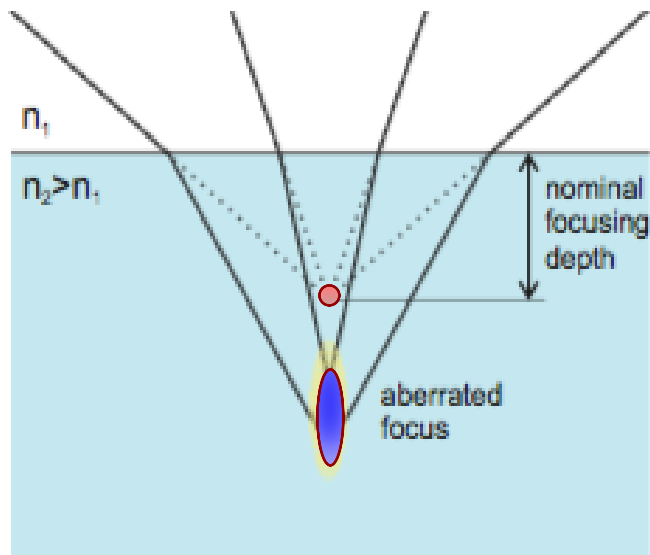


depth = 130 $\mu\text{m}$

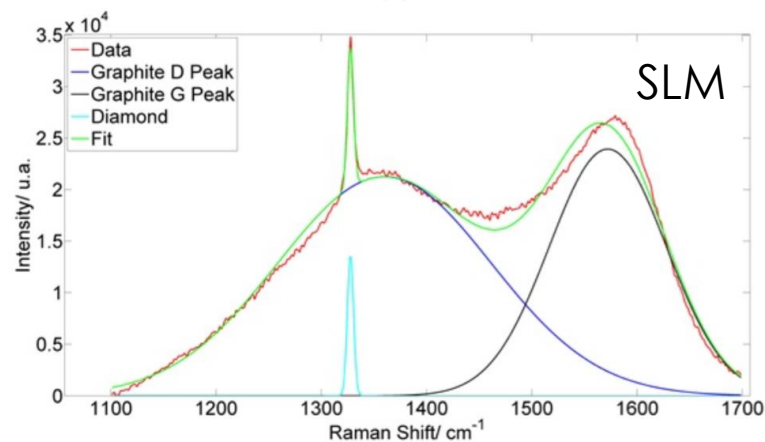


- Comparison SLM vs standard process.

	Std.	SLM
Resistivity	1 Ωcm	0.1 Ωcm
Diameter	~3μm	~1μm
Diamond to graphite ratio	~4	~0.2

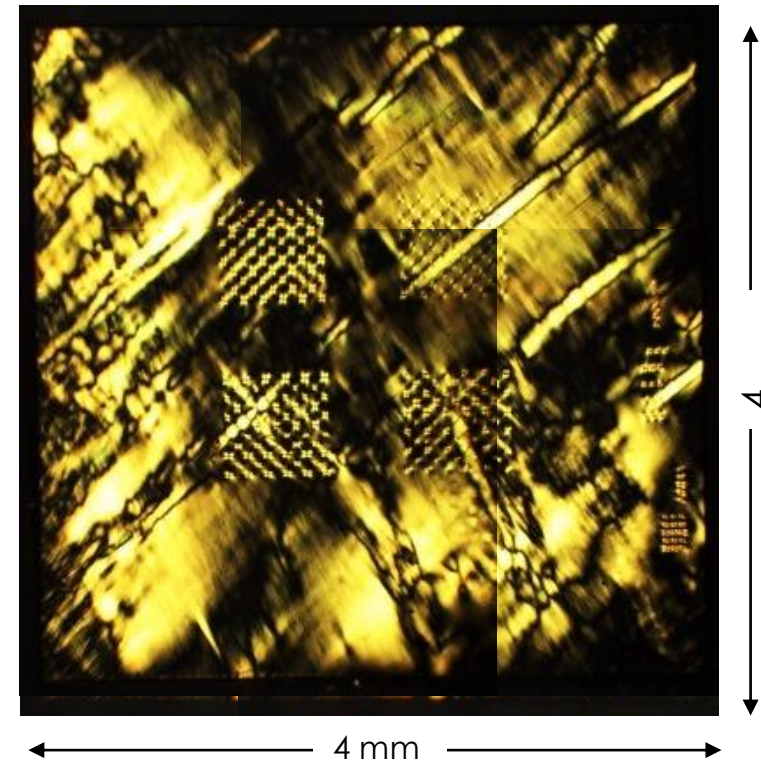
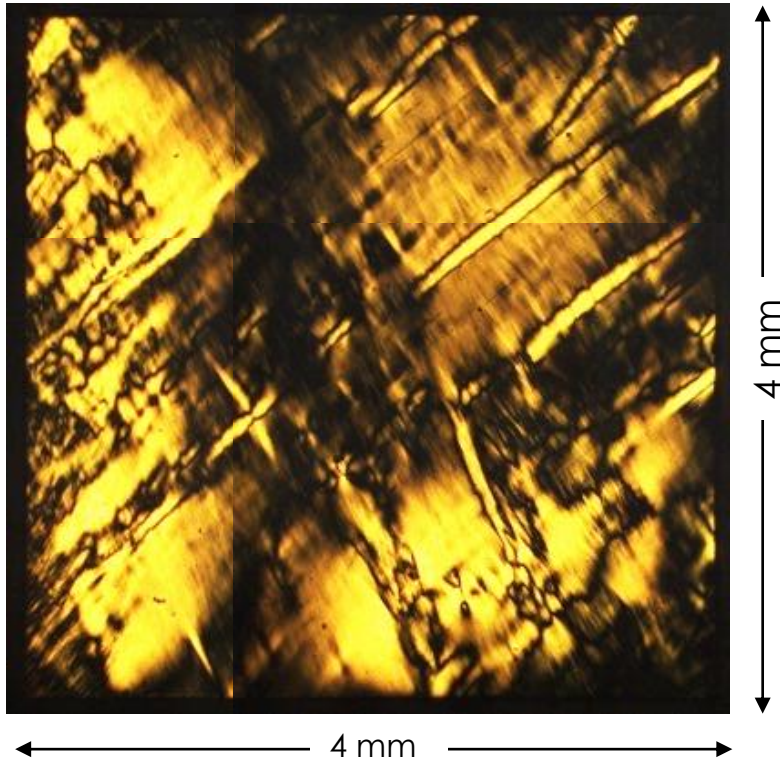


(a)



# X-polariser image

68

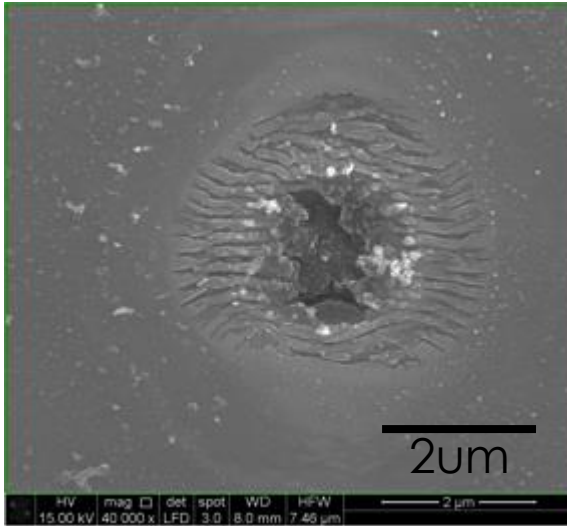


- Optical grade scCVD diamond.

- Post processing.

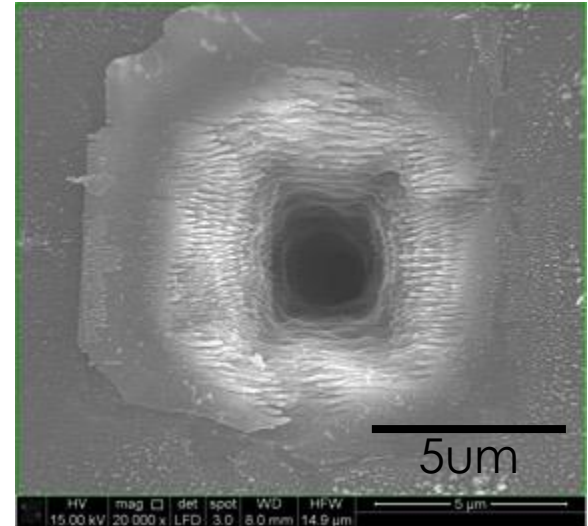
# SEM surface image

- Seed surface

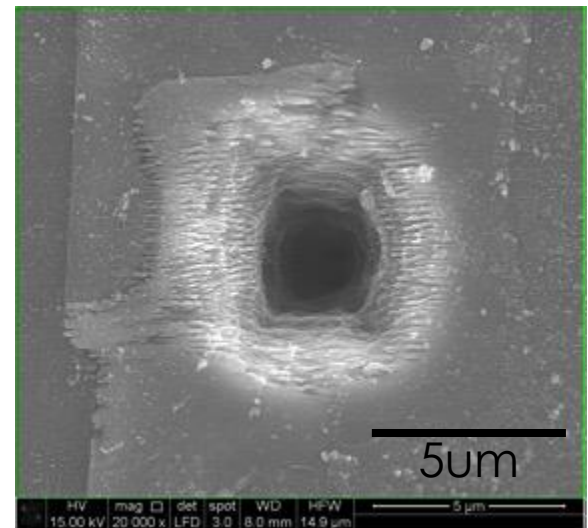
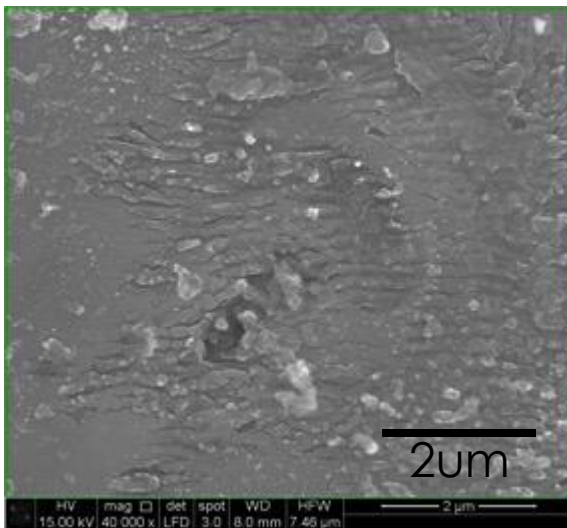


**With SLM**  
10um/s  
400nJ

- Exit surface

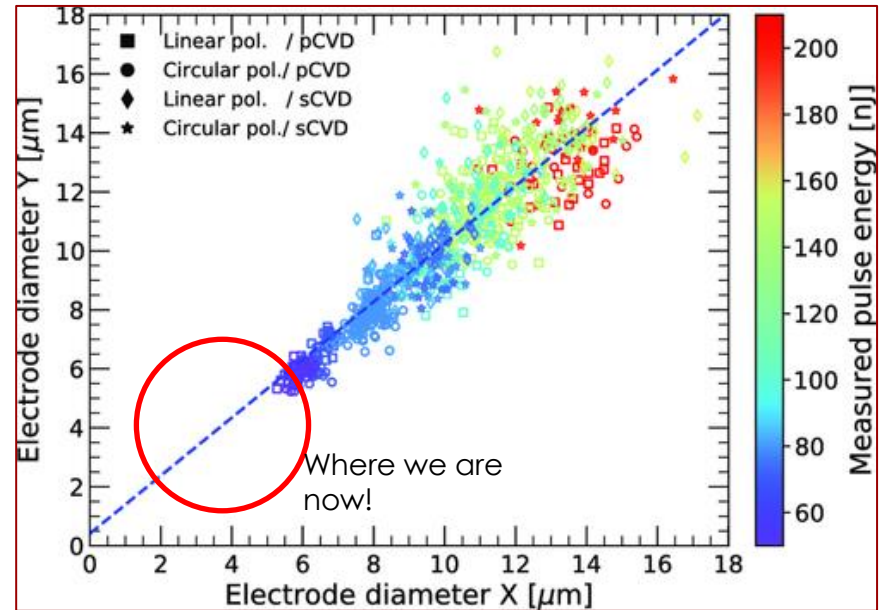


**Without SLM**  
10um/s  
400nJ

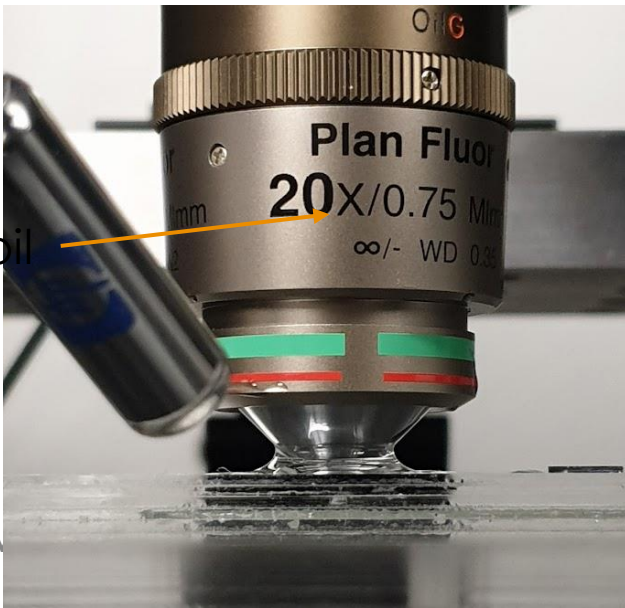


# Making the thinnest column

- More energy = thicker column
- Non-linear breakdown of diamond
  - More focused beam spot at depth makes thinner column
  - Immersion Oil helps to reduce refraction loss from air-diamond interface
    - SLM still key!

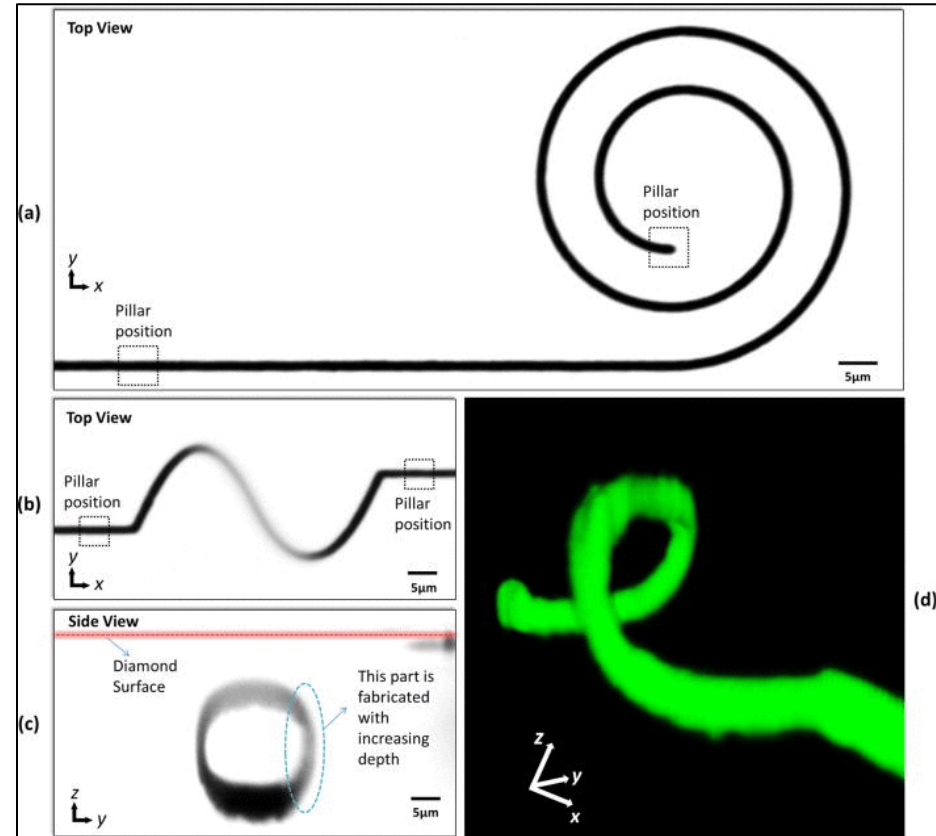


Lopez Paz, I., Allegre, O., Li, Z., Oh, A., Porter, A. and Whitehead, D. (2019), Study of Electrode Fabrication in Diamond with a Femto-Second Laser. Phys. Status Solidi A, 216: 1900236.



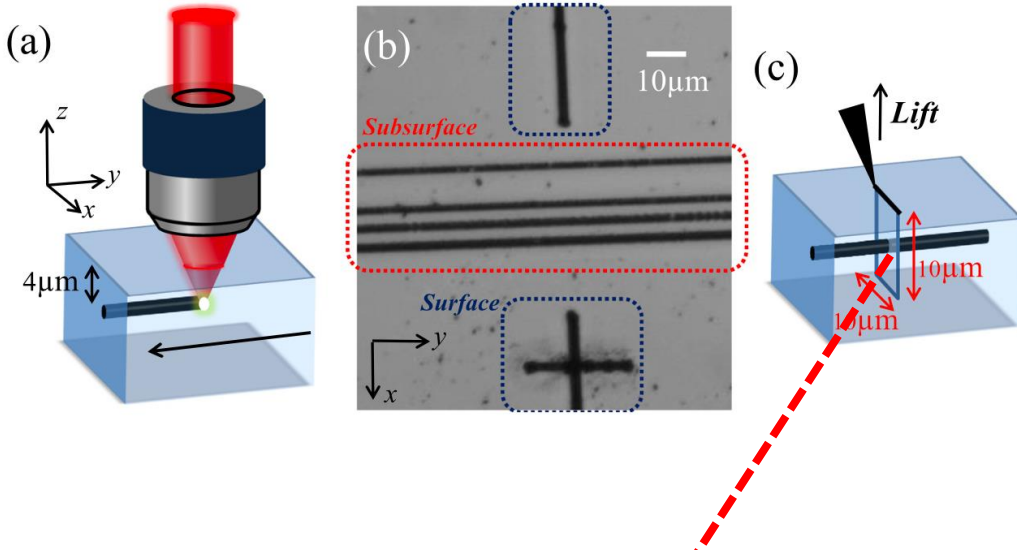
# Moving sideways

- Also have the possibility to move in **arbitrary** direction
- Wavefront correction needs to be tailored in real-time
  - For vertical columns have mainly spherical corrections
  - For horizontal processing, the correction is  $\sim$ elliptical
  - Gets even trickier at depth  $>200\mu\text{m}$

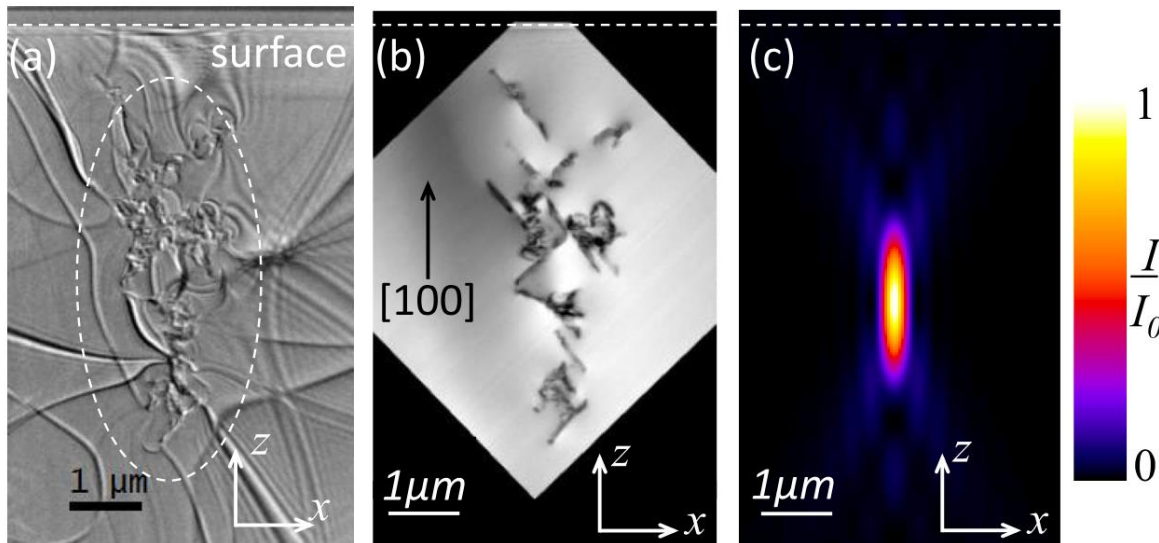


Sun, B., Salter, P. S., & Booth, M. J. (2014). High conductivity micro-wires in diamond following arbitrary paths. *Applied Physics Letters*, 105(23), 231105.

# Internal structure



Patrick S. Salter et al.,  
APPLIED PHYSICS LETTERS 111,  
081103 (2017)



- Prepare sample with horizontal graphitic wires.
- STEM image of wire cross section.
- Optical and spectral data points to micro-cracks and nano-clusters of  $sp^2$  bonded carbon.
- Micro wires are not macroscopic structures!

# Parameter space scan

73

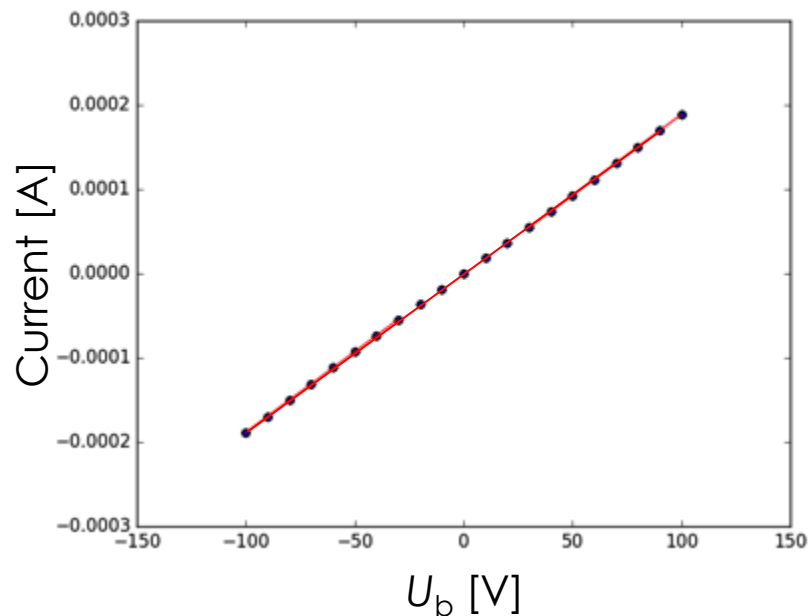
Patrick Salter, Oxford

Iain Haughton, AO, Manchester

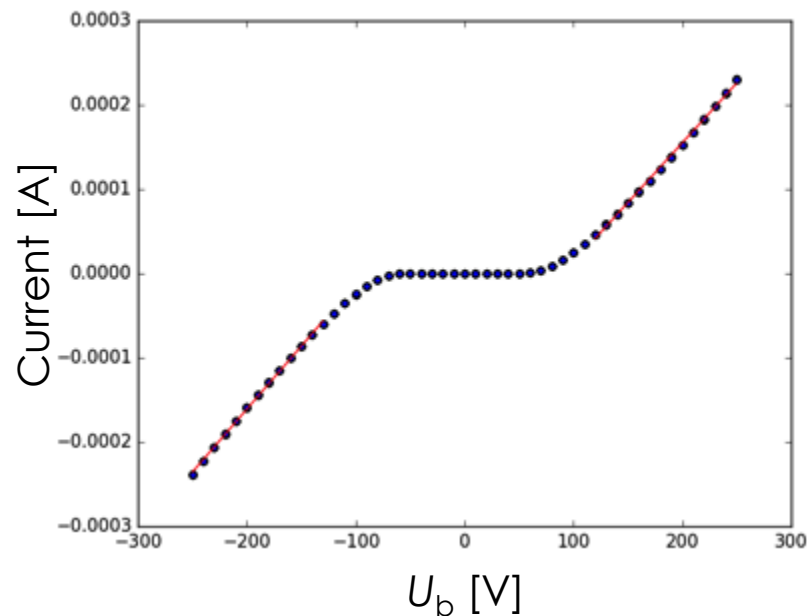
		Laser translation speed			
		5um/s	10um/s	20um/s	30um/s
Laser beam energy	100nJ	x	x		
	200nJ	x	x	x	
	300nJ		x	x	x
	400nJ		x	x	x
	500nJ			x	x
	600nJ				x

- Repeat **with** and **without** SLM correction.

- Ohmic and barrier potential curves observed.



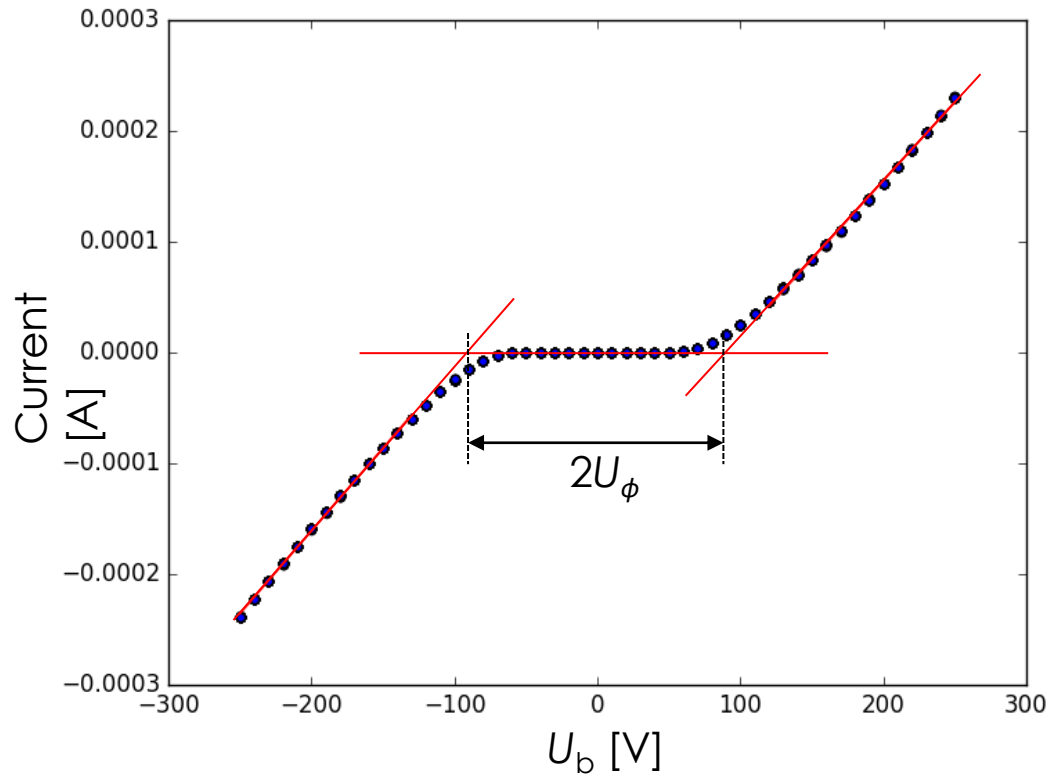
Continuous.



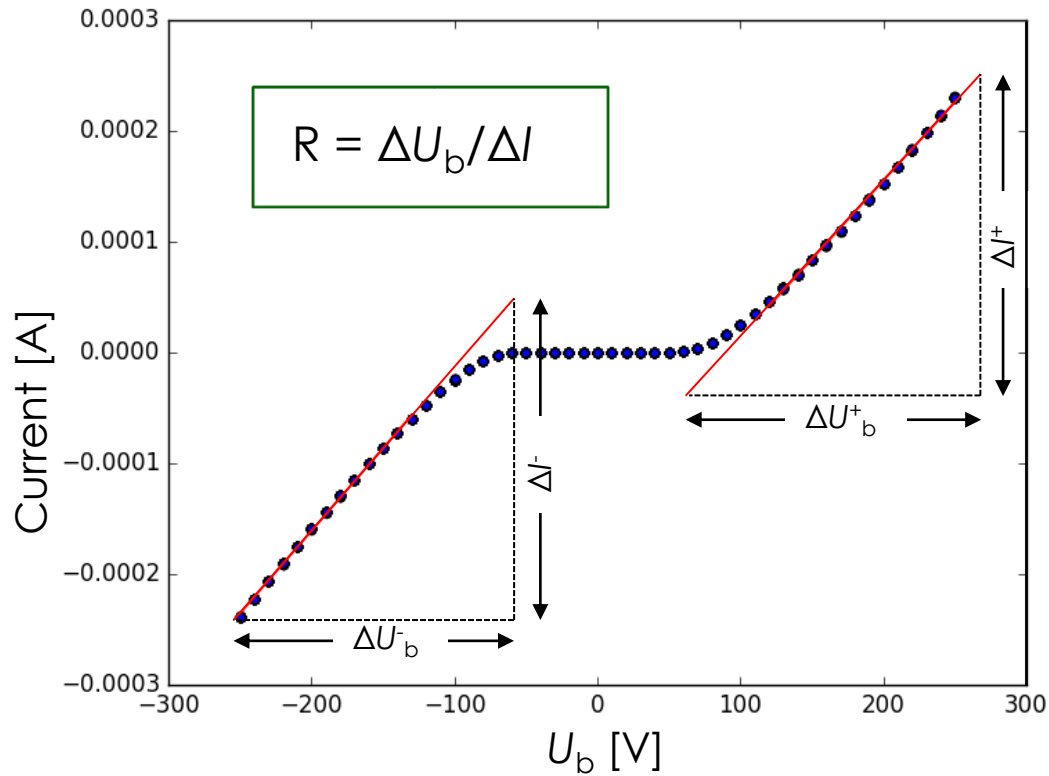
Bulk effect?  
Micro gaps?

# Barrier potential

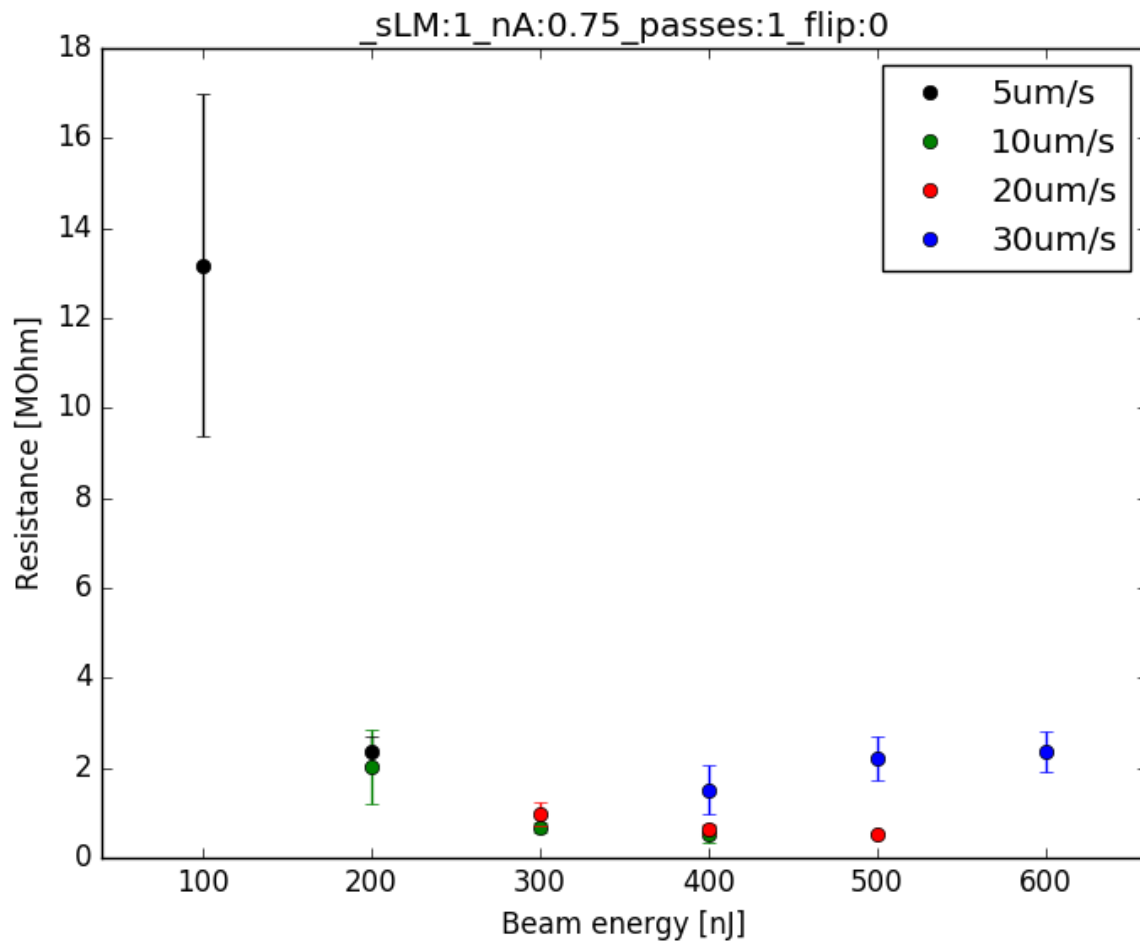
76



## Resistance measurement

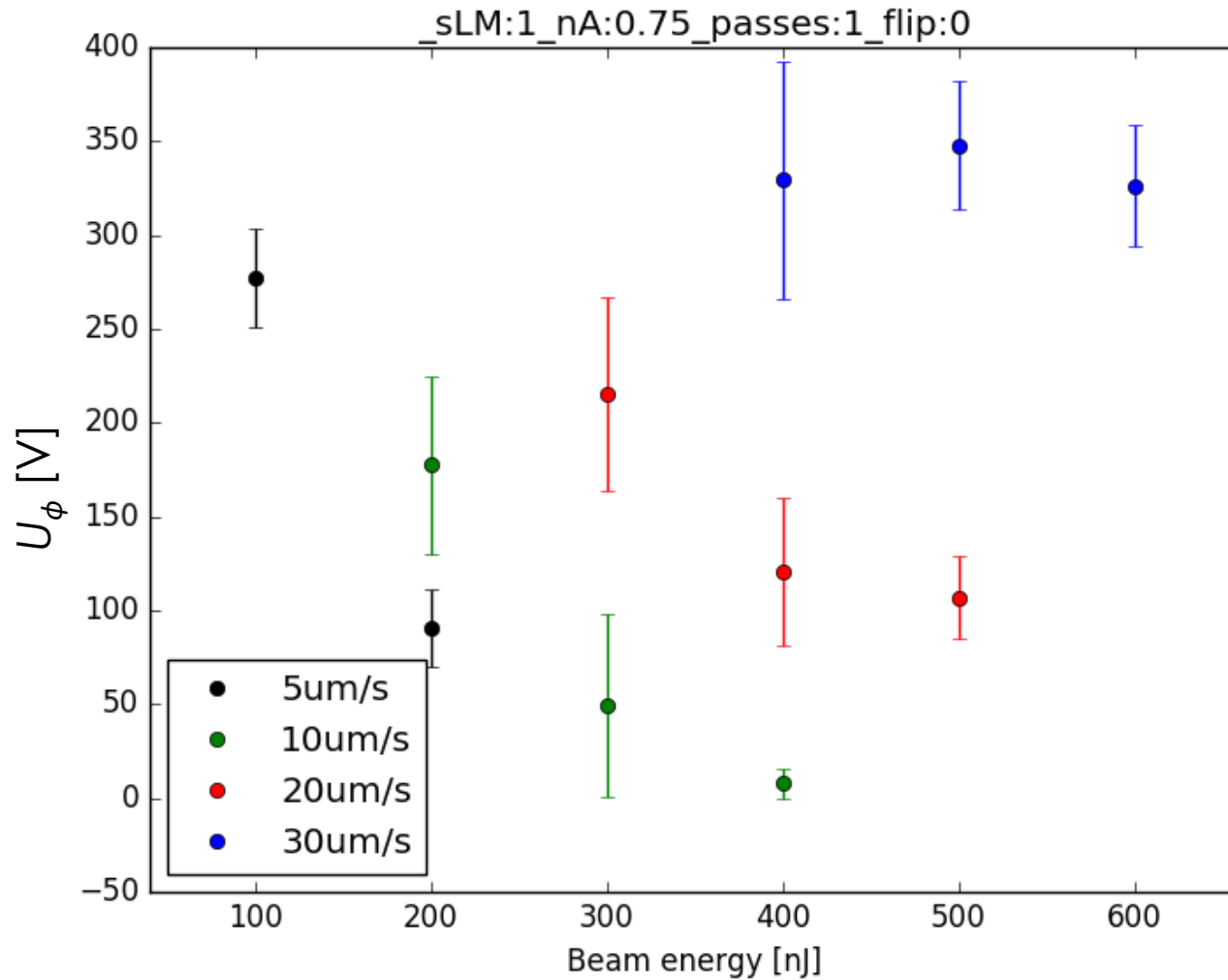


# Resistance



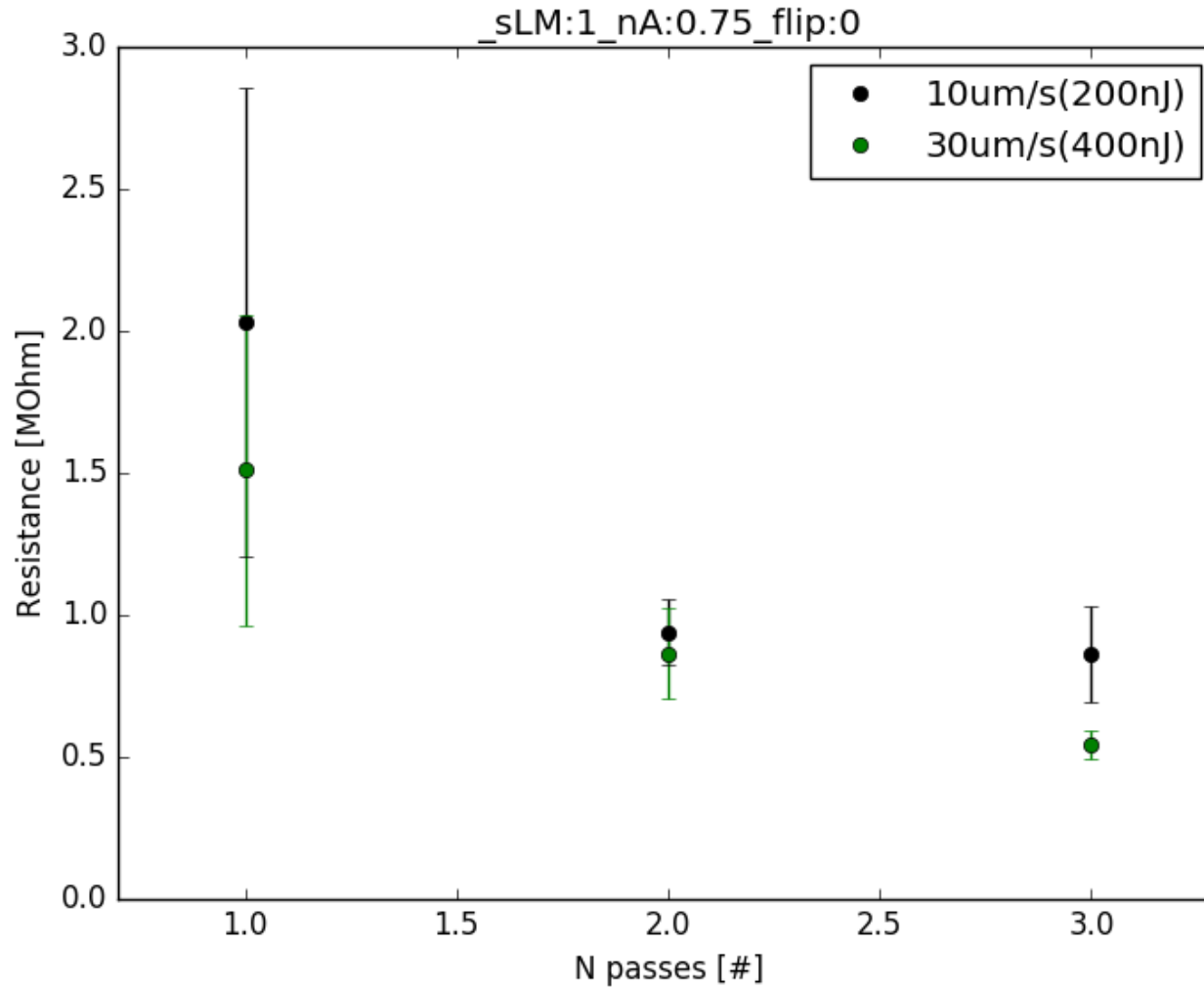
- Resistance increase as power law  
→ multi-photon process.

# Barrier energy



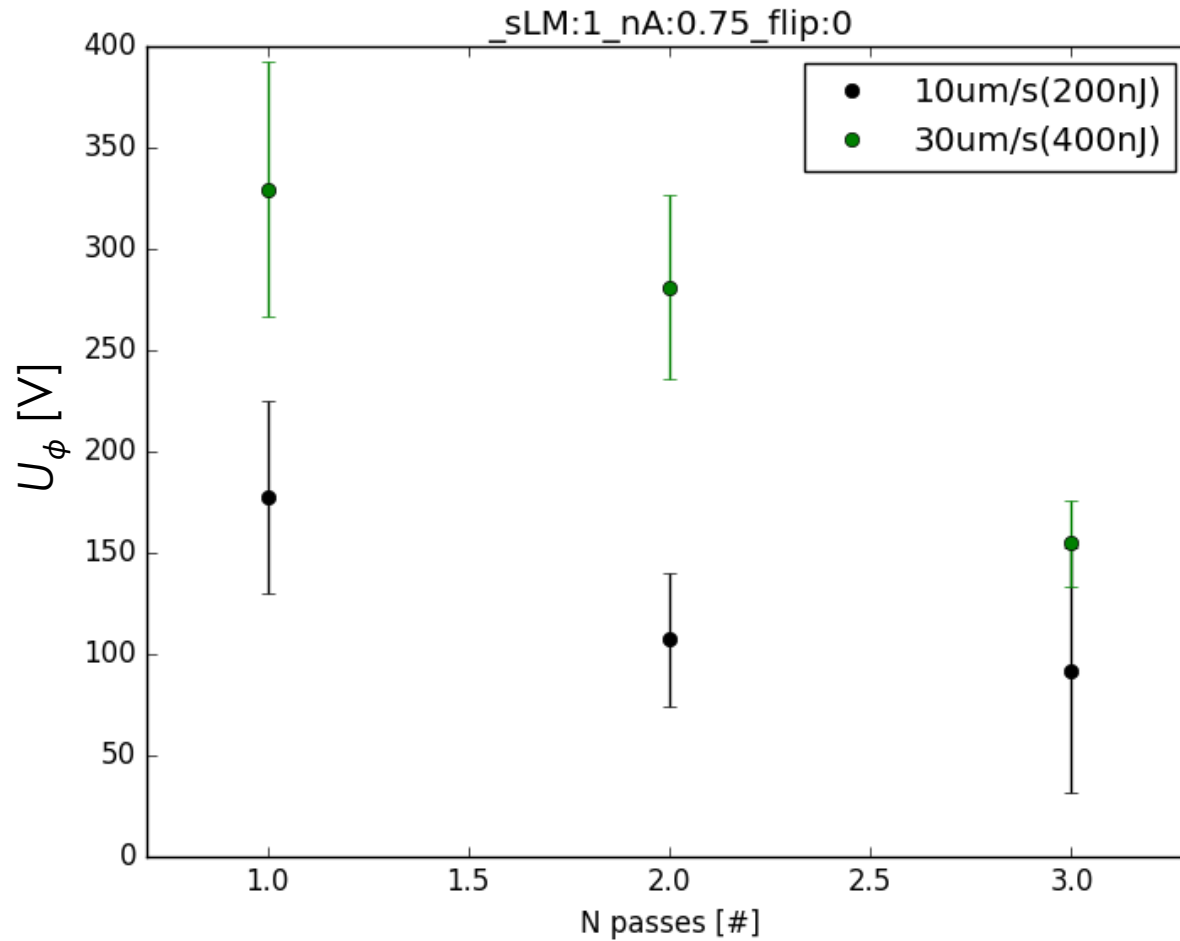
- Reduction in barrier with increased energy.
- Discrepancy at 30  $\mu\text{m/s}$ .

# Multiple passes



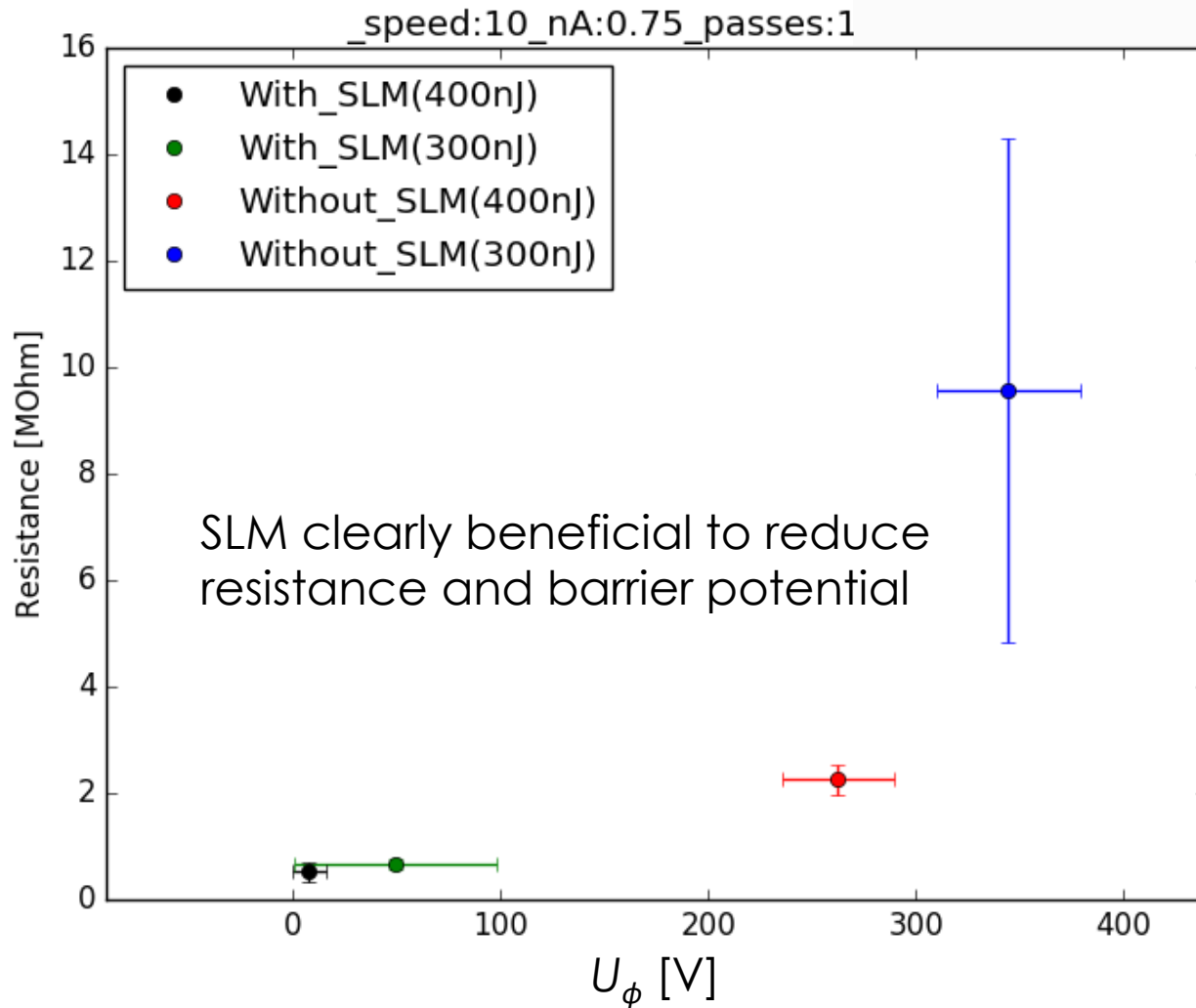
- Multiple passes reduces resistance and increases uniformity of the columns.

# Multiple passes

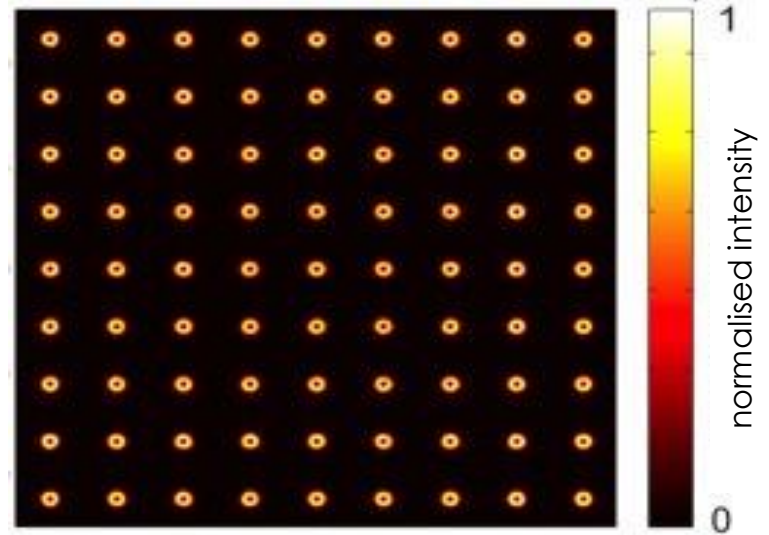
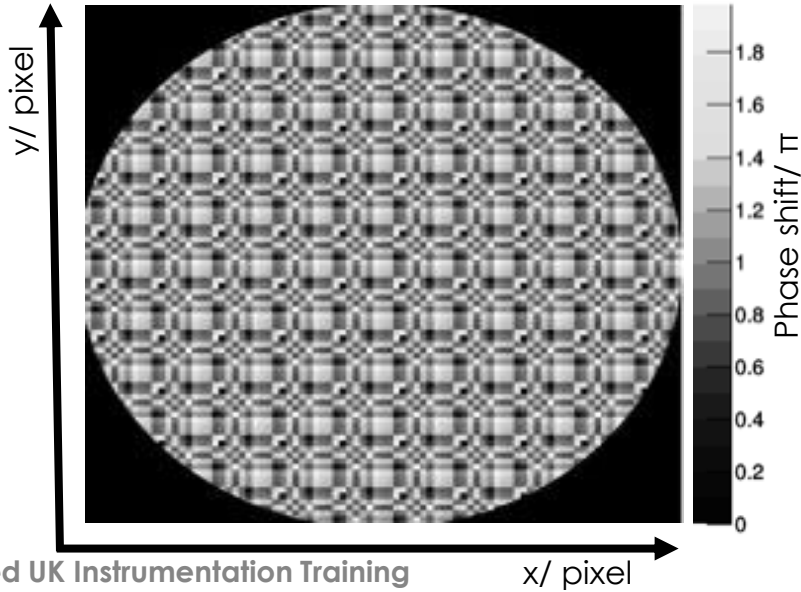
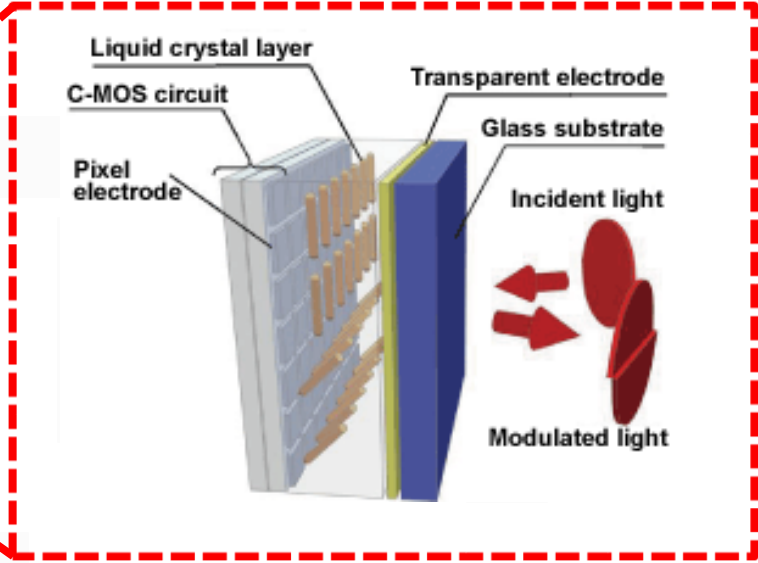


- Multiple passes also reduces  $U_\phi$ .

## With and without SLM



# SLM parallel processing?



# 3D Diamond detector tests with relativistic charged particles

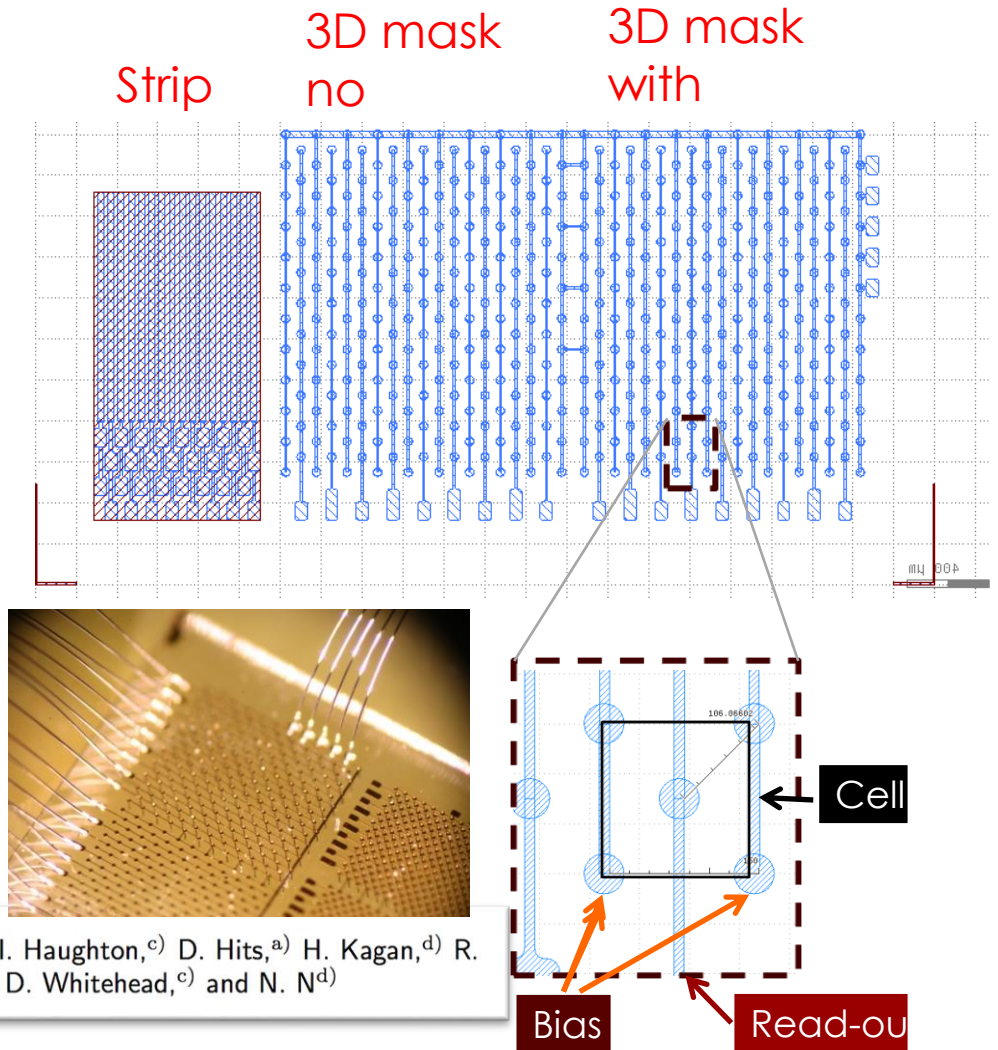
- Types
  - 100x100um cell size ganged to form strips
  - 100x100um cell size, bonded to pixel read-out
  - 50x50um cell size, bonded to pixel read-out
- All detectors made from polycrystalline diamond.
- Beam tests
  - CERN beam line H6 : protons  $\sim 120$  GeV/c
  - PSI : pions  $\sim 250$  MeV/c

Thanks for material from the RD42 collaboration!

# 3D Diamond prototype

## ■ Proto-type

- Strip detector with back side contact
- 3D metal only pattern
- 3D metal + graphitic columns
- Cubic cell base size  $150\mu\text{m}$
- 99 cells
- Measure response with 120 GeV protons.
- Paper published NIMA "A 3D diamond detector for particle tracking", NIM A, 786 (2015)

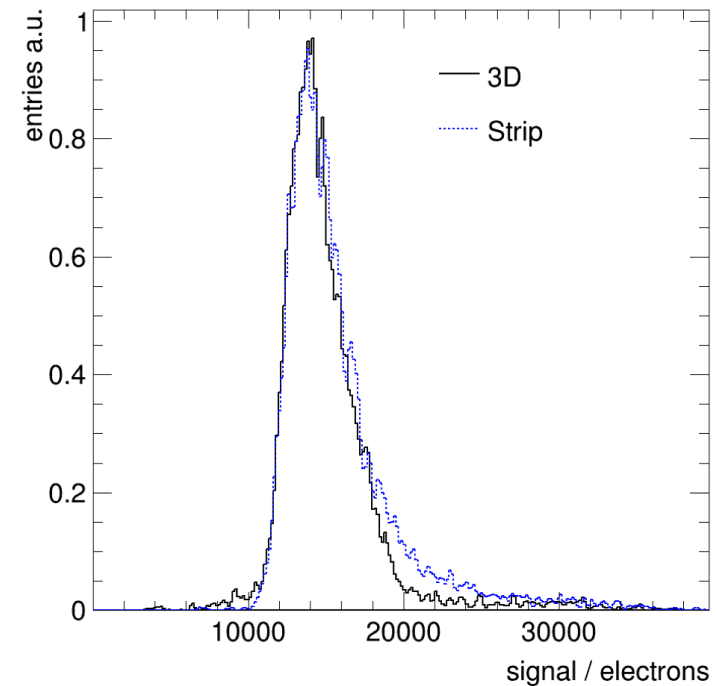
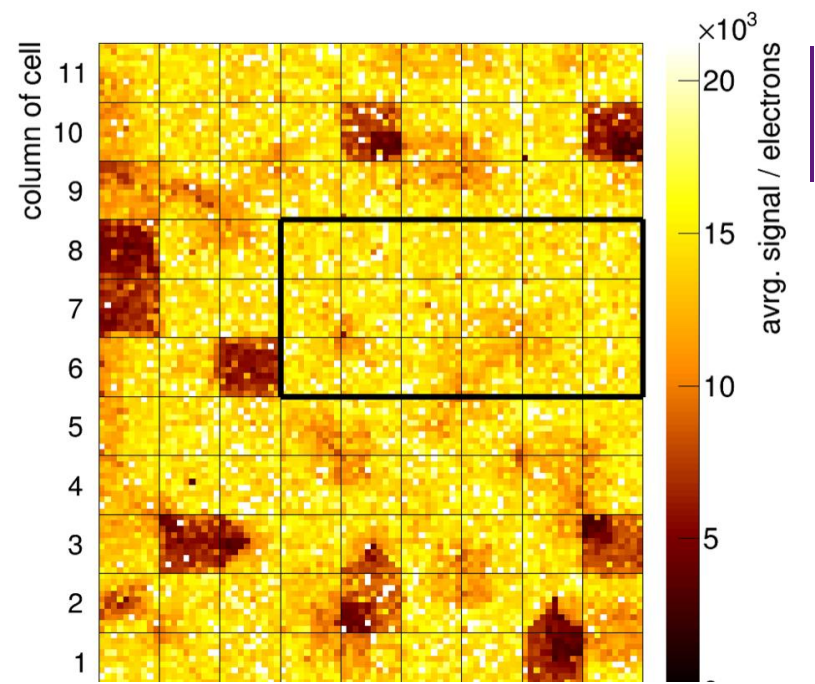


F. Bachmair,<sup>a)</sup> L. Baeni,<sup>a)</sup> P. Bergonzo,<sup>b)</sup> B. Caylar,<sup>b)</sup> G. Forcolin,<sup>c)</sup> I. Haughton,<sup>c)</sup> D. Hits,<sup>a)</sup> H. Kagan,<sup>d)</sup> R. Kass,<sup>d)</sup> L. Li,<sup>c)</sup> A. Oh,<sup>c)</sup> M. Pomorski,<sup>b)</sup> V. Tyzhnevyy,<sup>c)</sup> R. Wallny,<sup>a)</sup> D. Whitehead,<sup>c)</sup> and N. N<sup>d)</sup>

## Analysis steps

- $U_b(3D)=40V$
- $U_b(\text{strip})=500V$
- Identify **continuous region** of intact cells for analysis.
- Exclude contribution of negative signals.
- **Average charge**  
Strip: 16.8ke  
3D: 15.9ke
- **MP:**  
Strip: 14.7ke  
3D: 15ke

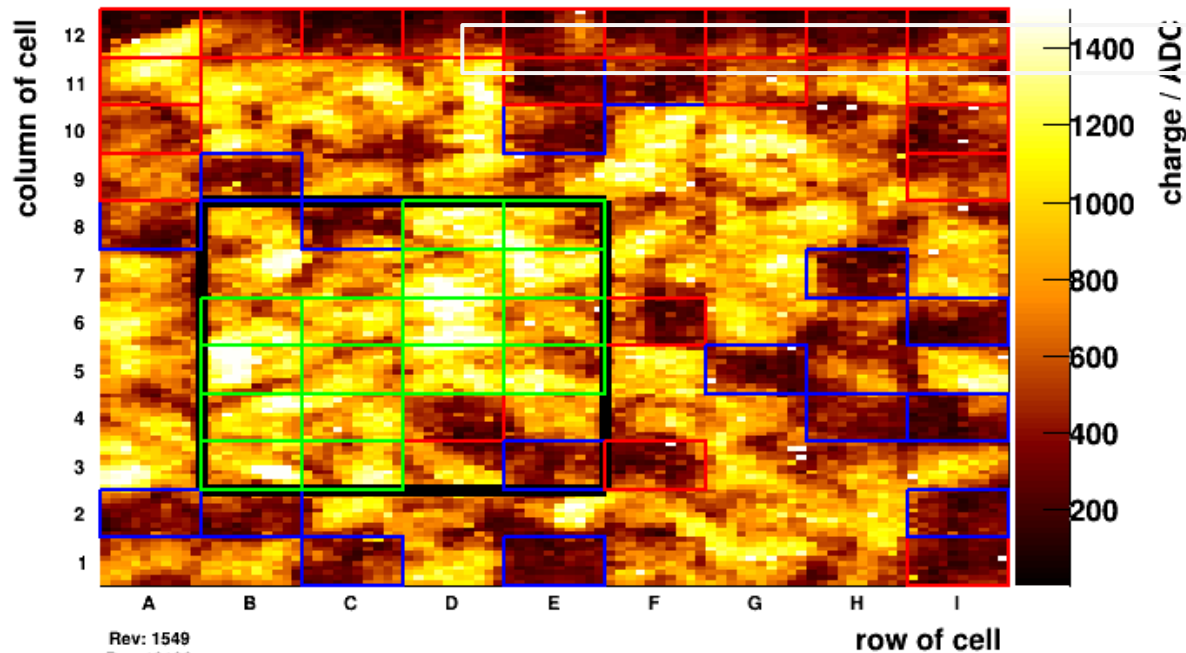
3D and Strip show comparable response.  
Conclusion -> 3D works!



# Test of first 3D **pCVD** diamond detectors

hPulseHeightVsDetectorHitPositionXY\_trans

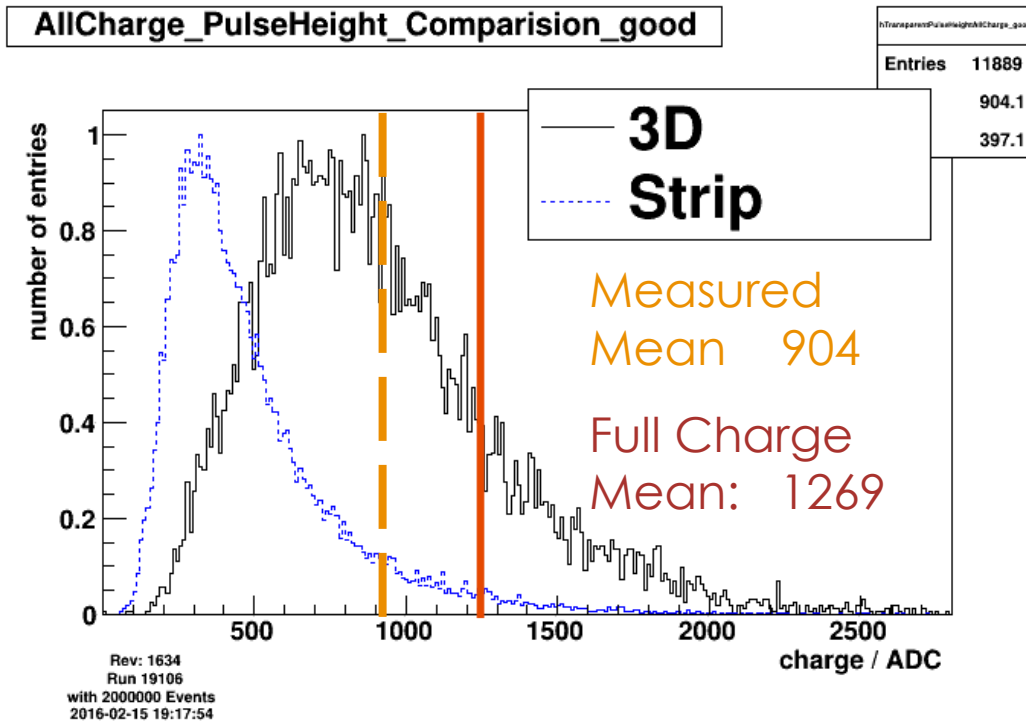
- $U_b(3D)=75V$
- $U_b(\text{strip})=500V$
- Selected 16 adjacent cells



Rev: 1549  
Run 19106  
with 2000000 Events  
2016-02-02 13:34:21

# Test of first 3D **pCVD** diamond detectors

- Red line estimate the Mean for Full Charge Collection (100%)



71% of Full Charge Collection, corresponding to ~13 ke.

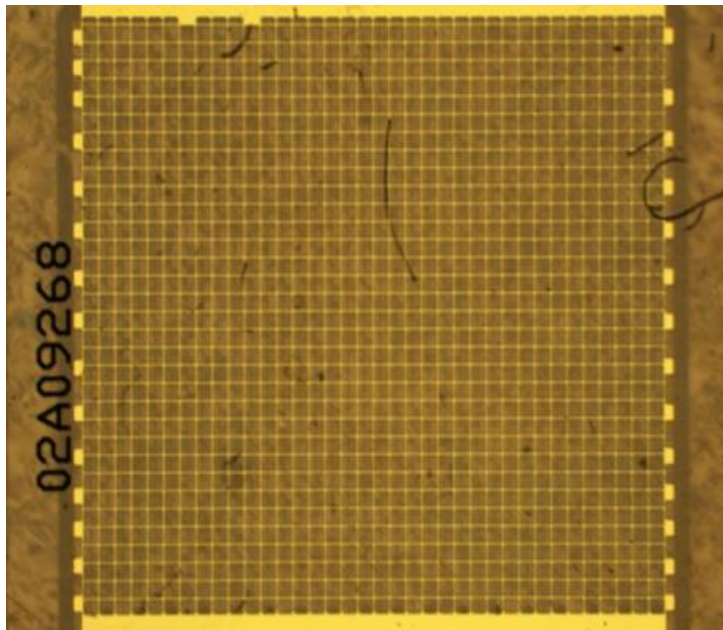
Highest charge collection ever measured for pCVD diamonds

# Large area 3D, pCVD, 100x100

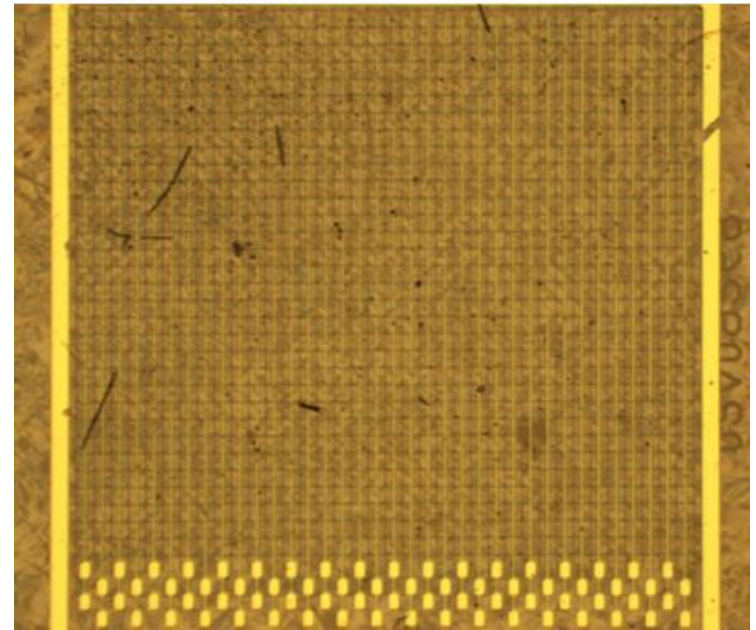
In May/Sept 2016 tested the first full 3D device fabricated in pcCVD with three dramatic improvements:

1. An order of magnitude more cells (1188 vs 99).
2. Smaller cell size (100um vs 150um).
3. Higher column production efficiency (>99% vs ~90%).

HV side

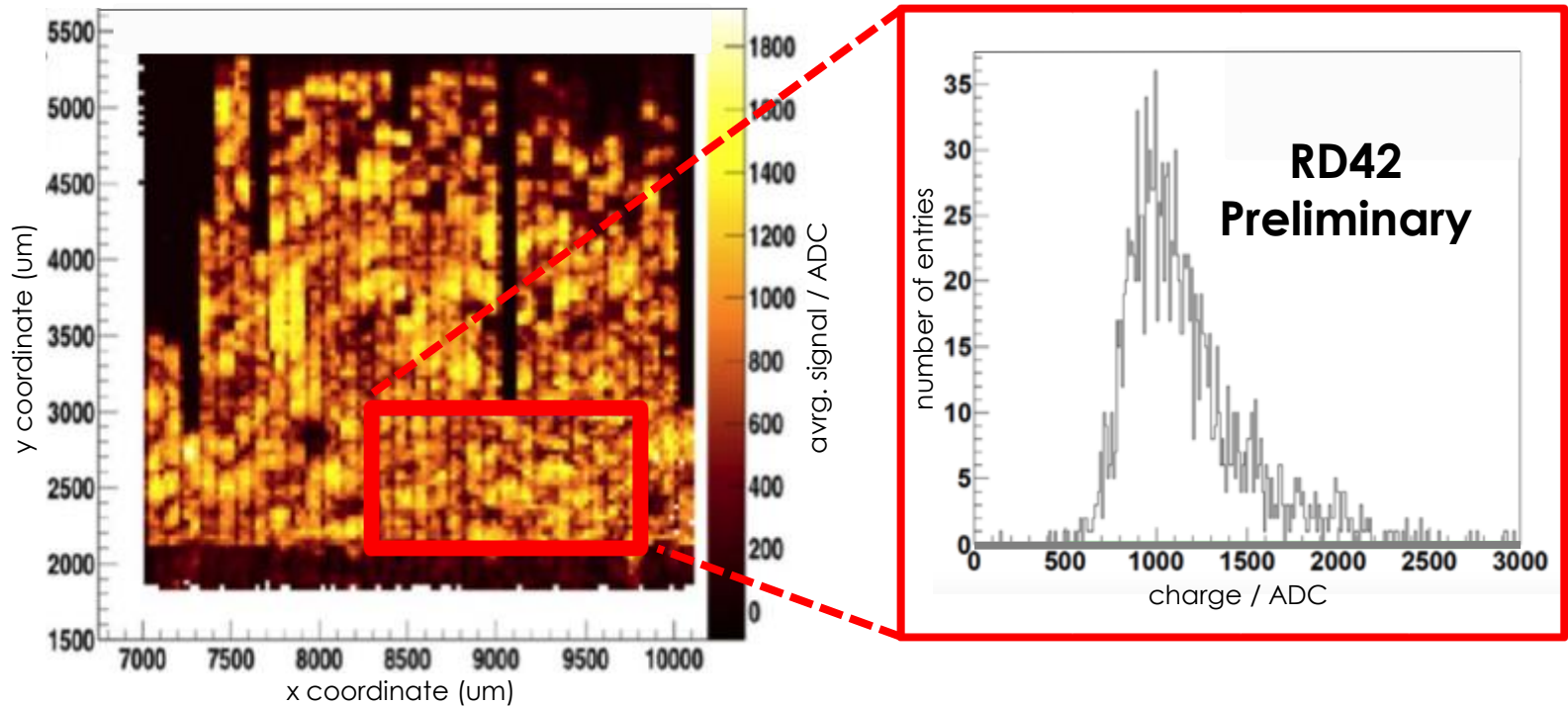


Readout side



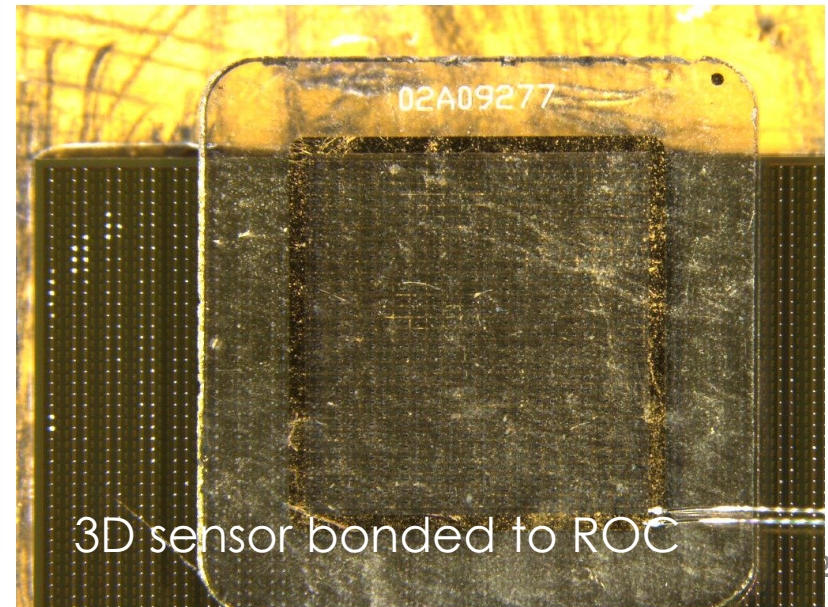
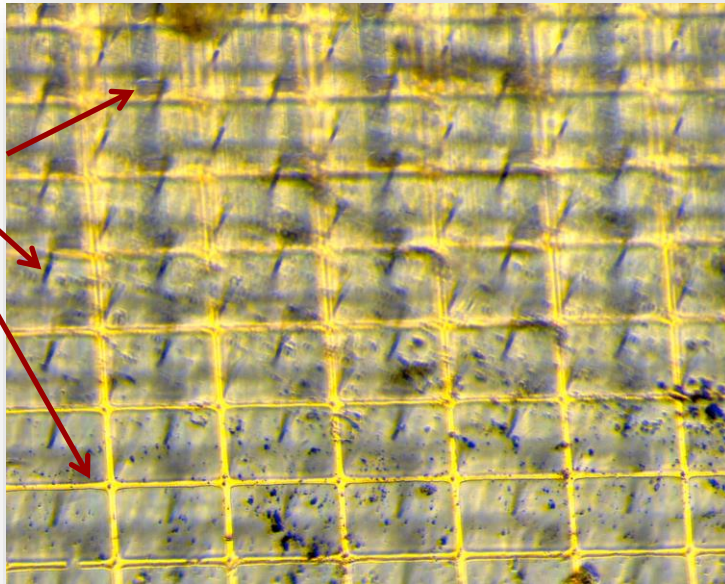
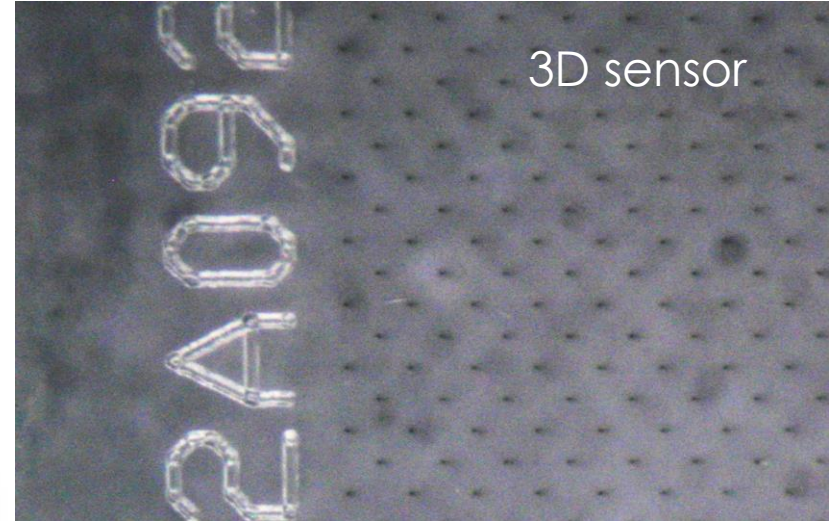
# Large area 3D, pCVD, 100x100

- Largest charge collection to date in pcCVD diamond!
  - >85 % of charge collected in continuous region, about twice as much as planar.



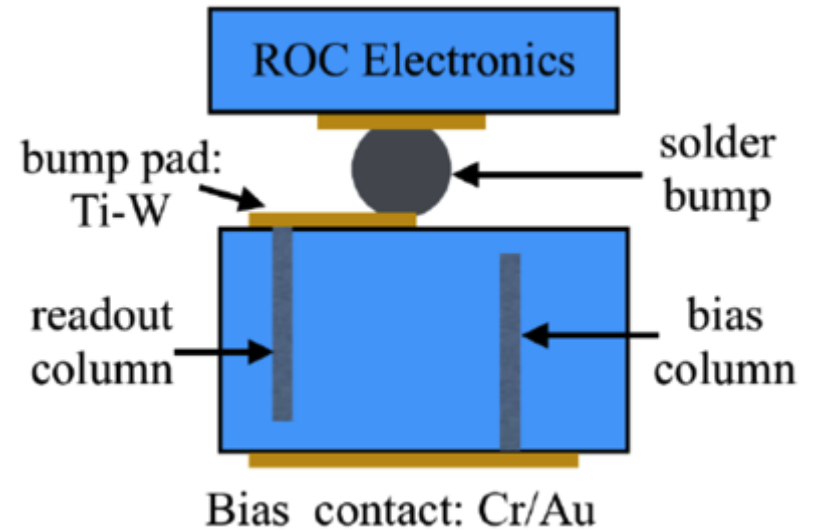
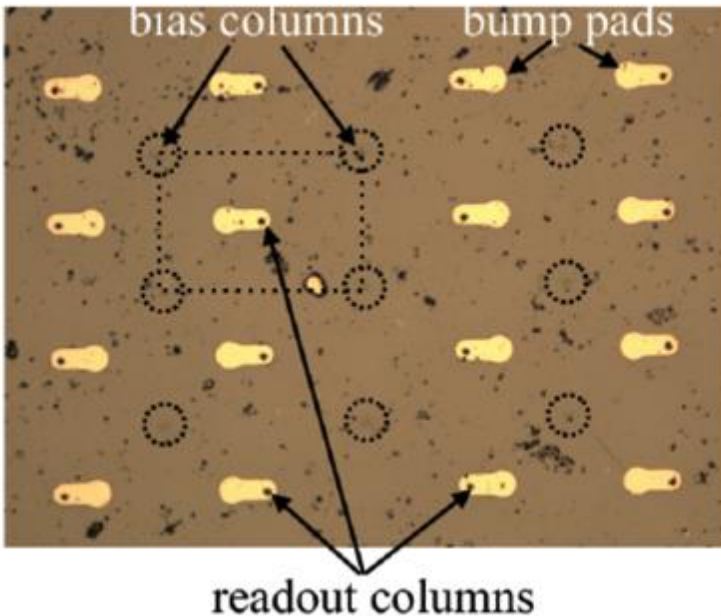
# Pixel 3D, pCVD, 100x100

- First assembly with ROC chip produced.
  - Bump bonded in Princeton.
  - Cr-Au on bias side.
  - Ti-W under-bump metal.
  - Indium bumps on sensor.



# Pixel 3D, pCVD, 100x100

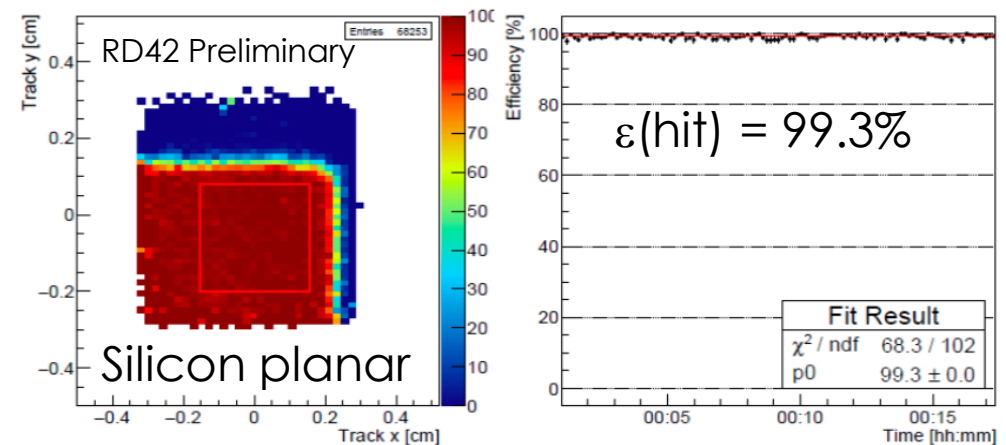
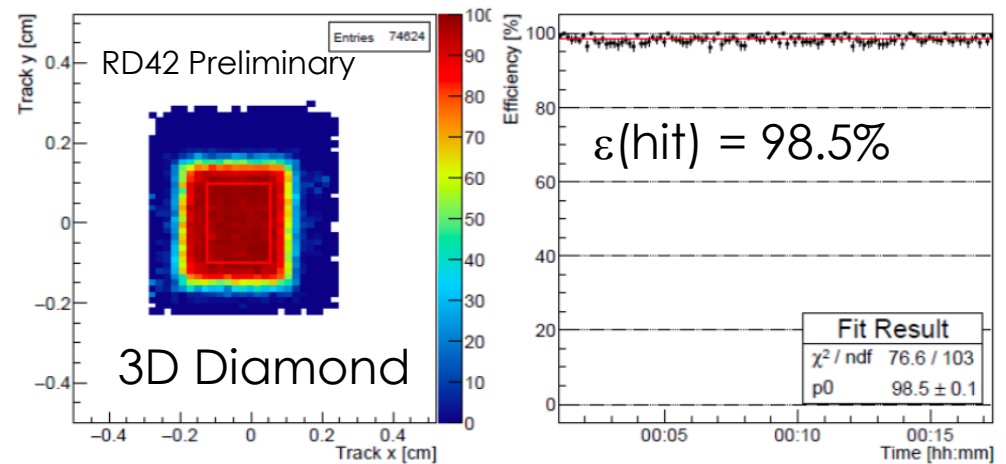
- Production of first pixel device using CMS readout electronics.



- Active region 3x3 mm with cell size  $\sim 100 \times 100$   $\mu\text{m}$ .

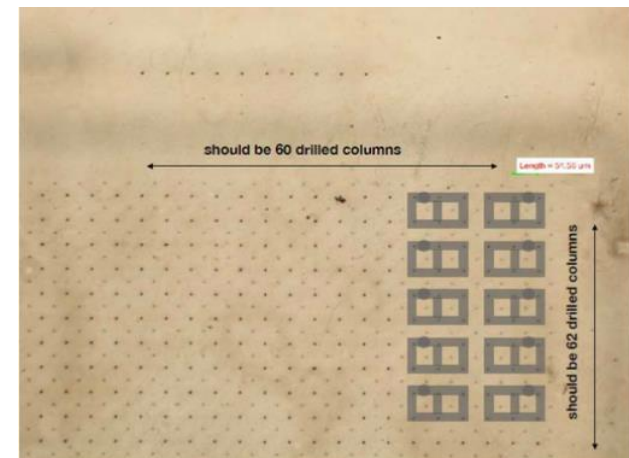
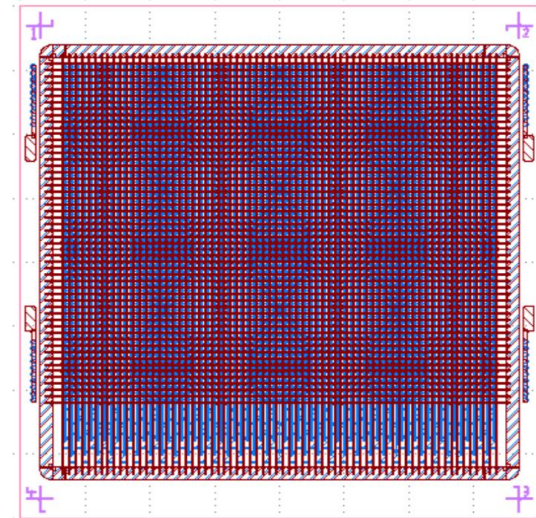
# Pixel 3D, pCVD, 100x100

- 3D diamond device and Silicon reference planar device.
- Pixel threshold 1500e.
- Check hit efficiency over time.
- Device works!



# Next generation 3D Diamond

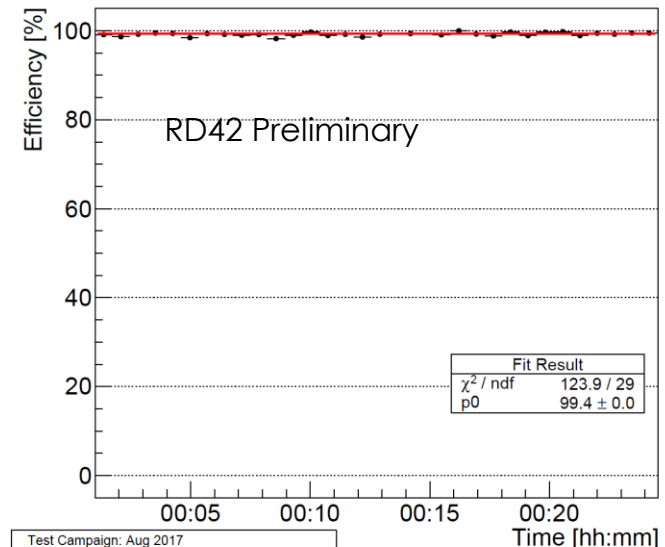
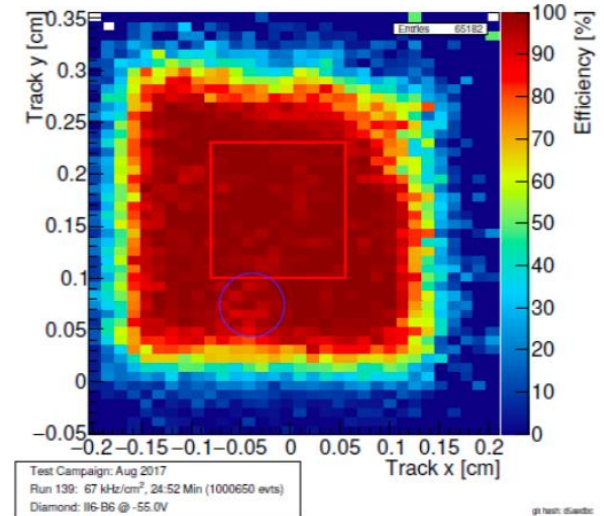
- Produced 3500 Cell pixel prototype, 50x50um cell size.
- Sample production:
  - Oxford (2x cubic cells)
  - Manchester set-up in progress (expected production date end of month.)
  - Bump bonding
    - For ROC (CMS) Princeton.
    - For FE-I4 (ATLAS) IFAE.
- Data taking in August 2017 at PSI.



# First 50x50 $\mu\text{m}$ cell 3D Diamond (2017)

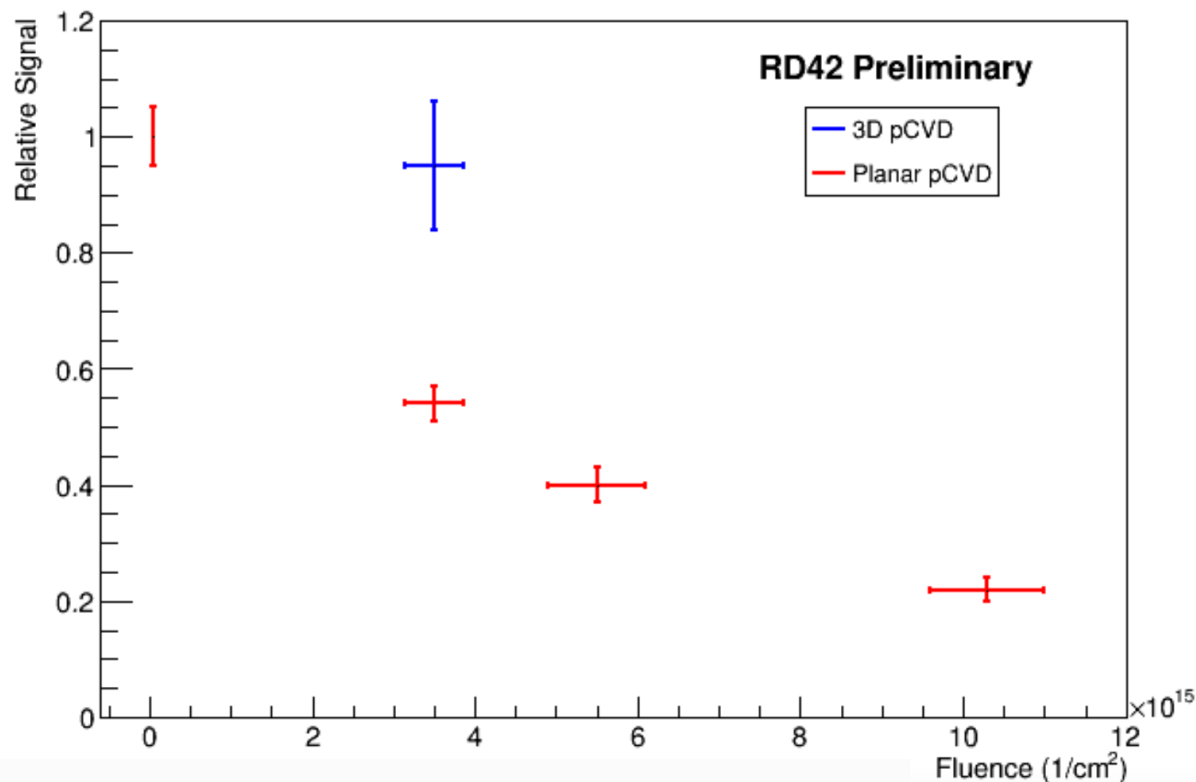
- Readout with CMS pixel readout.
- Bump bonding issue in upper right edge (Indium bump deposition machine not working properly)
- 6 columns (3x2) ganged together.
- Preliminary hit efficiency **99.2%**
- Preliminary: Collect **>90%** of charge!
- Rate dependence tested with 10 kHz/cm<sup>2</sup> and 10 MHz/cm<sup>2</sup> -> no dependence observed.

RD42 Preliminary



# 3D diamond radiation tolerance

- Tested a 3D device irradiated to  $3.5 \times 10^{15}$  p/cm<sup>2</sup> and compare to a planar diamond device at same fluence.
- Signal reduction:  
Planar  $45 \pm 5\%$   
3D  $5 \pm 10\%$
- Assuming scaling is similar 3D should operate at  $10 \times 10^{17}$  p/cm<sup>2</sup>



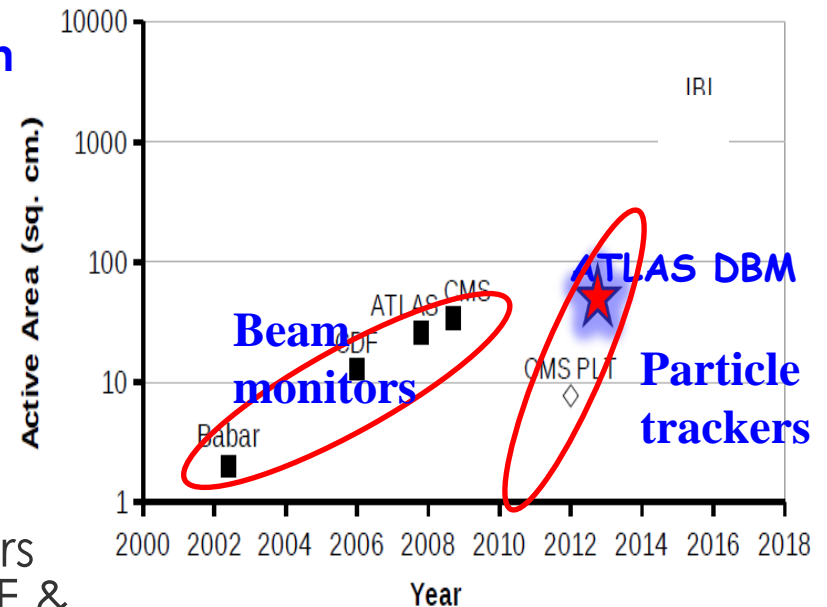
# Applications in HEP

# Applications in HEP

- Vertex detectors with CVD Diamond are not considered yet as an option for LHC.
- For Beam monitoring CVD Diamond is used at CMS and ATLAS at the LHC.
- BaBar and Belle test already CVD Diamond in their beam monitoring system.

# Diamond in current HEP experiments

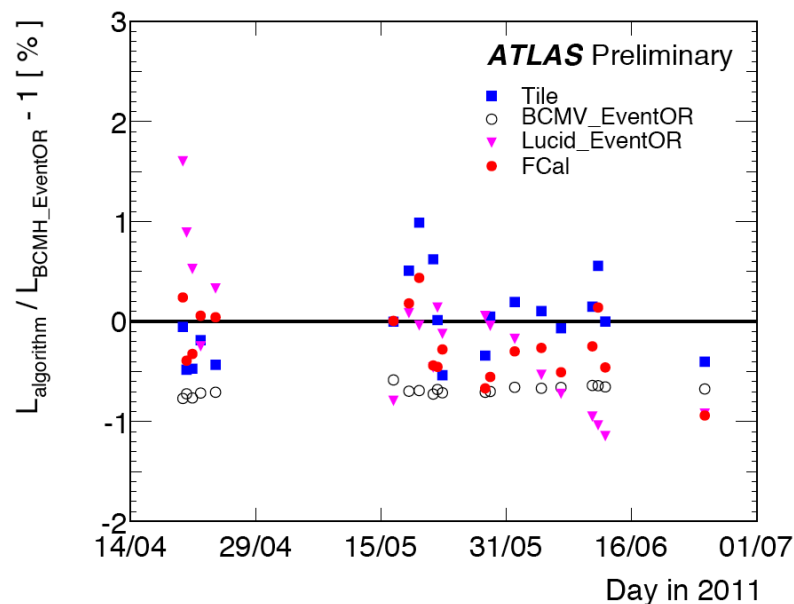
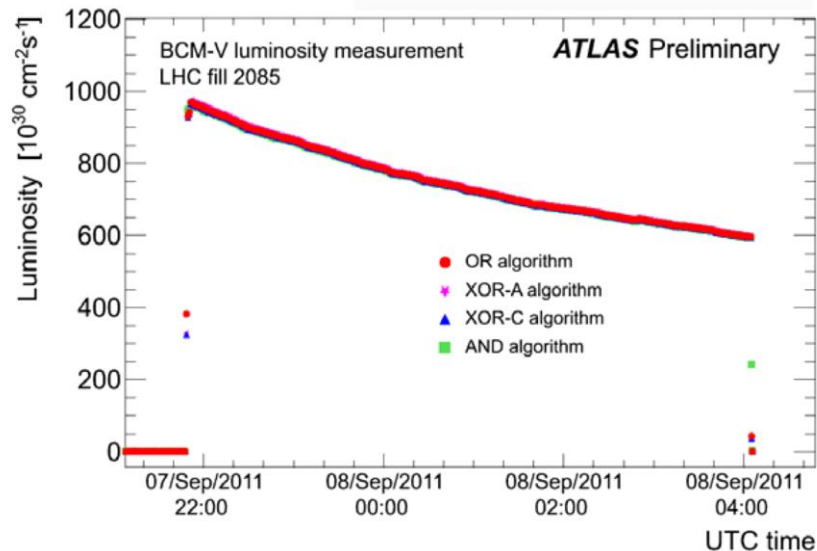
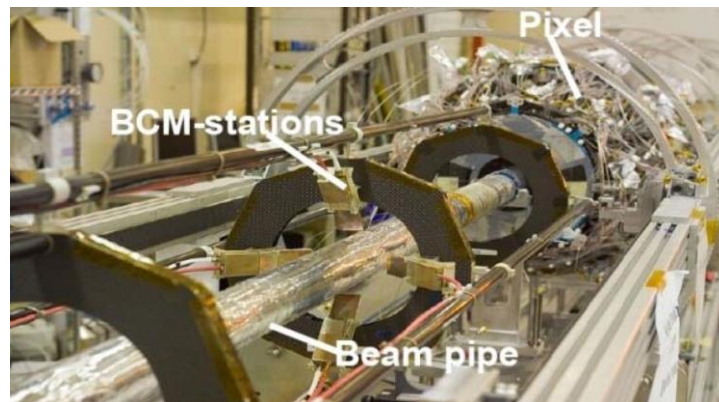
- **Beam monitors** to protect experiments against **beam losses** at the LHC, CERN.
  - For Silicon Vertex systems careful monitoring is crucial.
  - Beam monitors have to be **radiation hard**.
  - Abort beam when monitors signal dangerous beam conditions.
  - False signals must be avoided.
- During run-1 **diamond beam monitors operated** in ATLAS, CMS, and LHCb.
- Previously diamond beam monitors were installed in BaBar(SLAC), CDF & D0 (Tevatron).





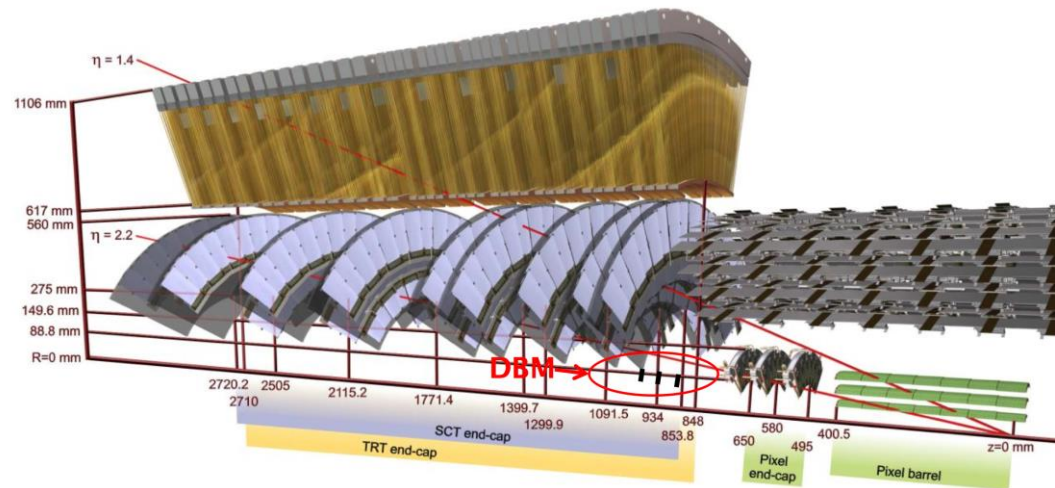
# ATLAS beam conditions monitor

- Single particle counting with  $\sigma=0.7\text{ns}$ .
- Distinguish between collision events and out-of-time background.
- Good stability
- Used for luminosity determination.



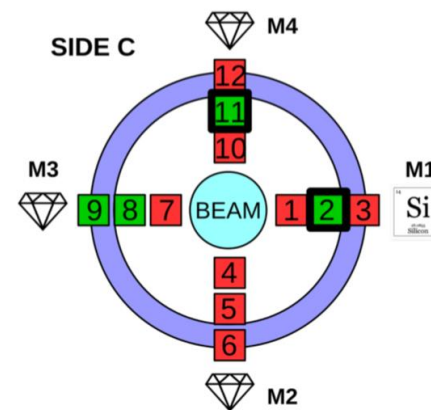
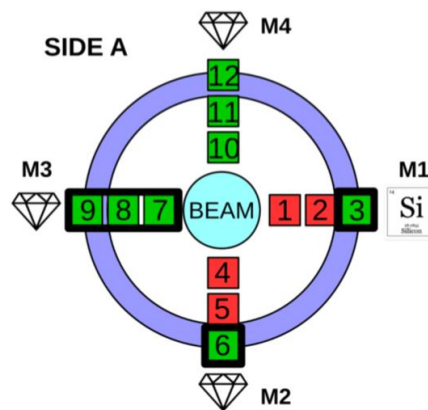
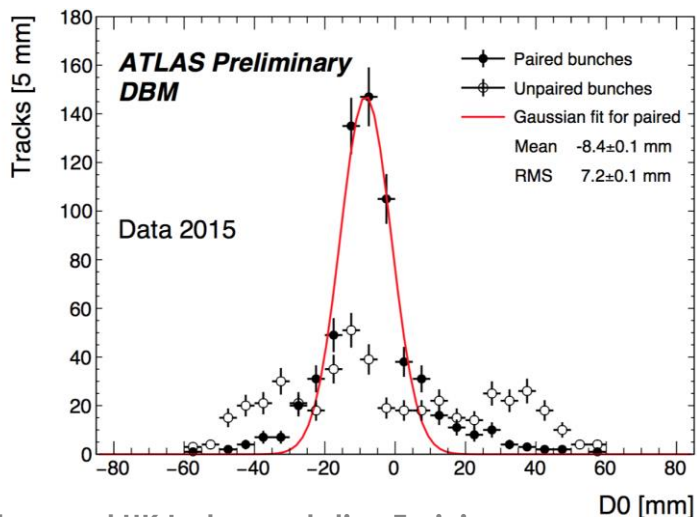
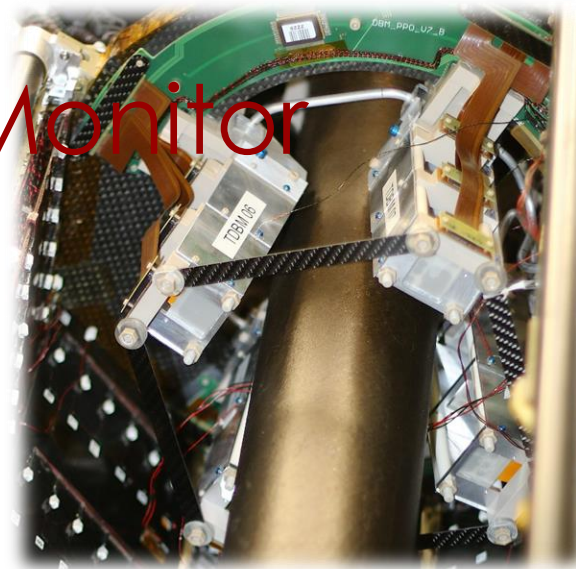
# Run 2: ATLAS Diamond Beam Monitor

- 8 mini-trackers of 3 planes each using pixel-detectors.
- polycrystalline diamond sensors, 18mm x 21mm,  $\delta > 250 \mu\text{m}$ .
- bump-bonded to FE-I4 pixel read-out chip.
  - 336 x 80 pixels
  - pixel size :  $50 \mu\text{m} \times 250 \mu\text{m}$
- Purpose:
  - Bunch-by-bunch luminosity monitor (aim < 1 % per BC per LB)
  - Bunch-by-bunch beam spot monitor



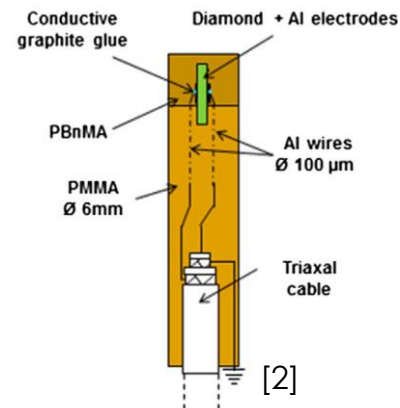
# Run 2: ATLAS Diamond Beam Monitor

- Installed in ATLAS during LS1, but switched off due to unexpected death of Si and Diamond modules.
- DBM recommissioned in 2017/18 with 50% working modules.

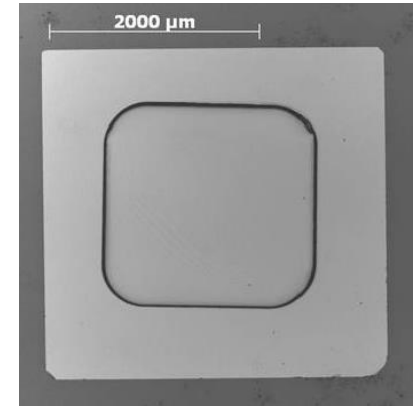


# Examples of diamond detectors in related areas

- Synchrotron labs
  - beam position monitor
- Radiation Therapy
  - small field dosimetry
- Heavy Ion (GSI, FAIR)
  - beam diagnostic
  - particle tracking and TOF
  - hadron spectroscopy



scCVD dosimeter,  
0,4 mm<sup>3</sup> active vol. [2]



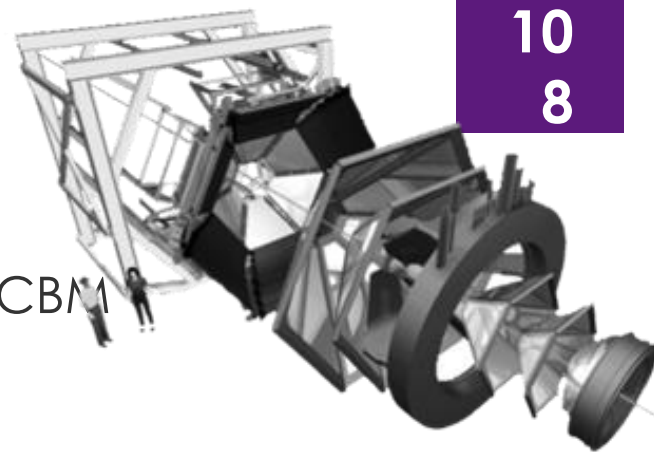
3  $\mu\text{m}$  thick membrane  
in 40  $\mu\text{m}$  thick scCVD [1]

[1] M. Pomroski, CEA-LIST, MRS Fall meeting, Boston 28/11/2012

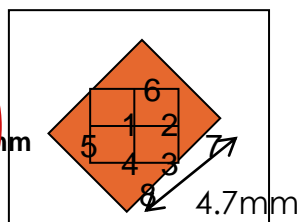
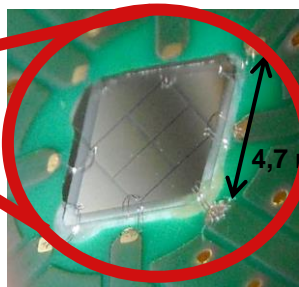
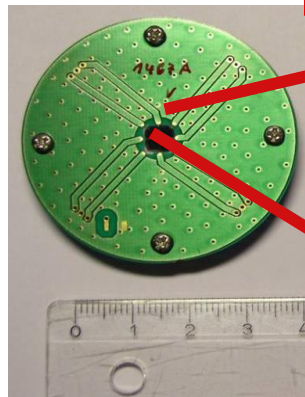
[2] F. Marsolat et al. / Diamond & Related Materials 33 (2013) 63–70 2026

# Detectors for Heavy Ion

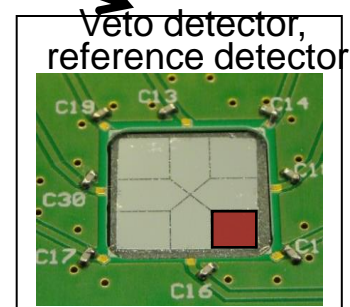
- In-beam START-VETO detectors for HADES and CBM
  - High beam intensities ( $10^7$  #/s).
  - Protons (MIPS) up to very heavy ions (Au, U)
  - Excellent time resolution (30-100 ps)
  - Radiation hard up to  $10^{12}$  /cm Au ions



HI, TO sensor



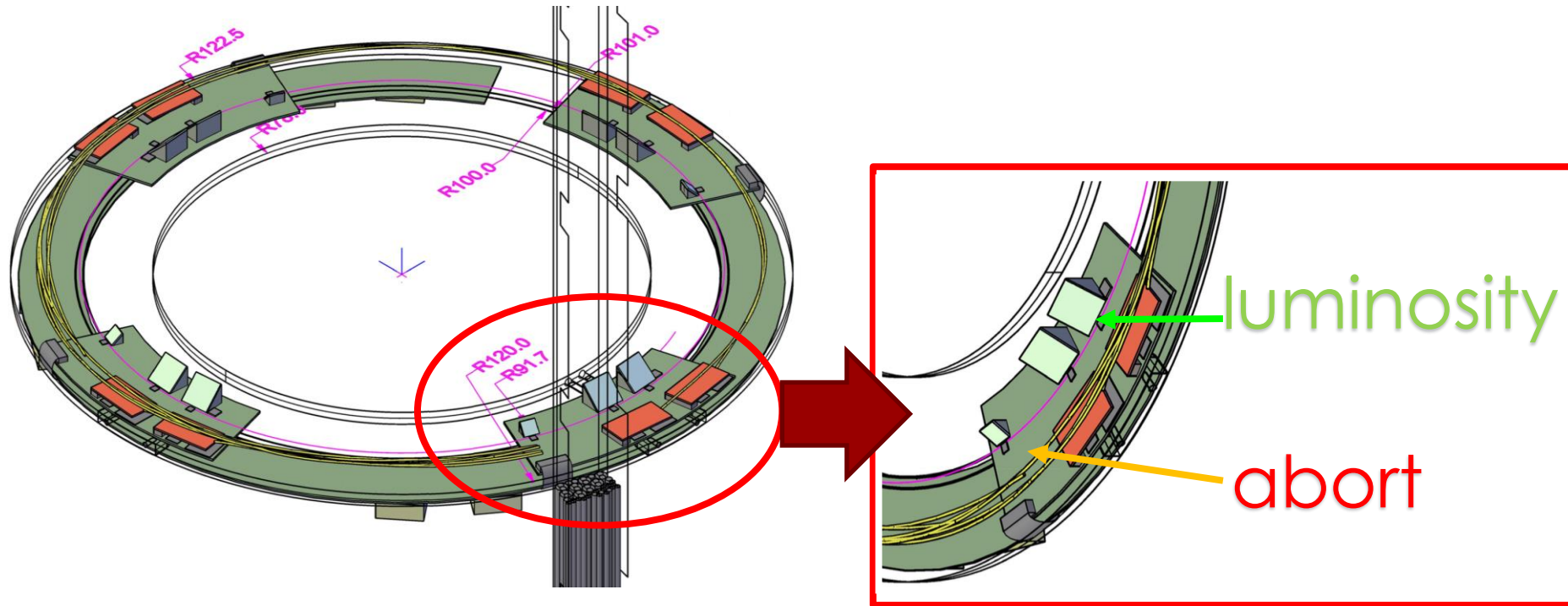
Start: SC diamond,  
70  $\mu\text{m}$  thickness, 4.7mm x  
4.7mm



Veto detector,  
reference detector

Veto: PC diamond,  
100  $\mu\text{m}$  thickness, 20 mm x  
20 mm

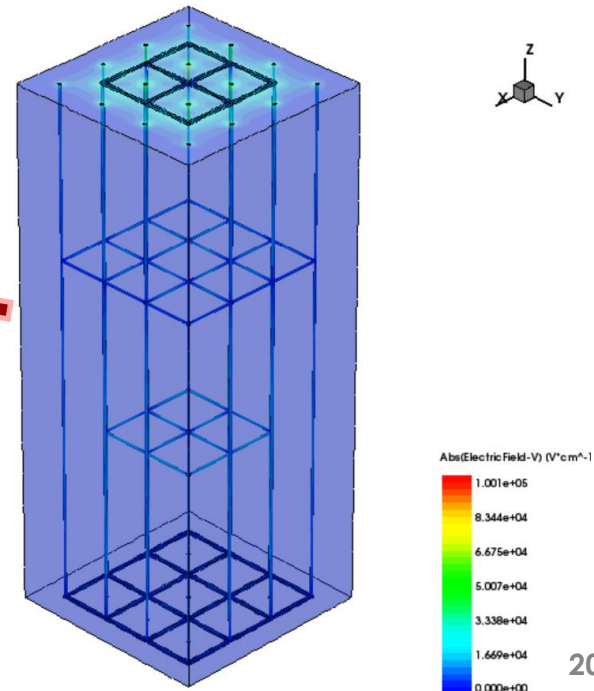
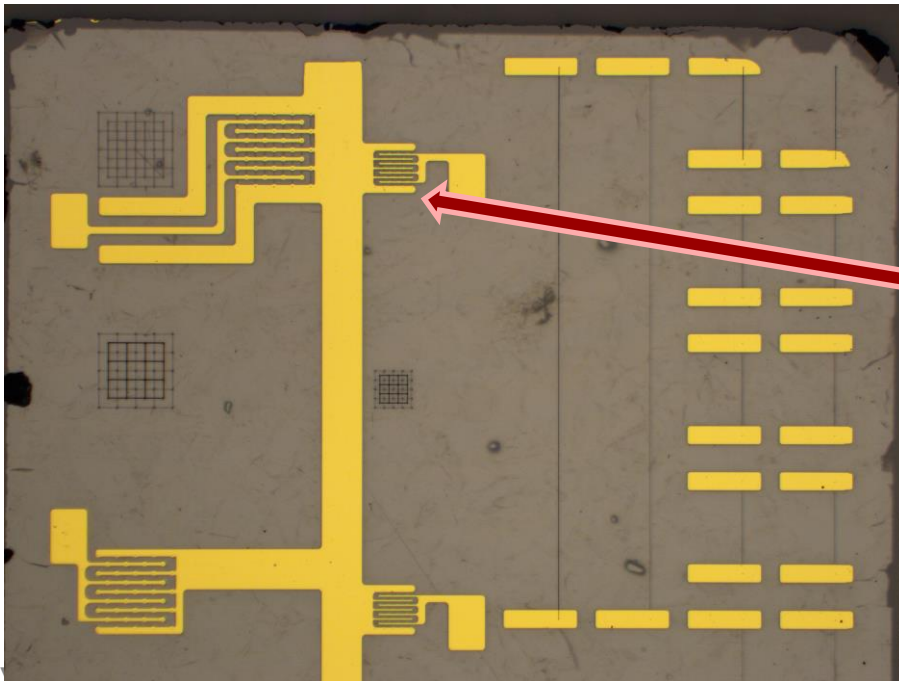
# Upgrade for LHC Phase-2: BCM' modules



# First BCM' 3D test structure with new "cage" design

11  
0

- Fabricated March 2020 (~week of UK Lockdown) first 3D diamond device with horizontal ganging
- Test structure has horizontal wires at depths of 125 and 375  $\mu\text{m}$  in a 500  $\mu\text{m}$  thick substrate ( $\rho$  measurement)
- Metallised 3D detector with alternating ganging (~model) read out in current mode in **RD42 Zagreb Testbeam 06-2021, second version tested April 2022**



# Dark matter

- Dark matter detection via elastic spin-independent interaction with Carbon nuclei.
- Diamond operated as cryogenic calorimeter.
- Reach of first prototypes is comparable to CRESST silicon sensors.
- Promising if scaled up (mass, time, background shielding)



## Light dark matter search using a diamond cryogenic detector

CRESST Collaboration

G. Angloher<sup>1</sup>, S. Banik<sup>2,3</sup>, G. Benato<sup>4</sup>, A. Bento<sup>1,9</sup>, A. Bertolini<sup>1,a</sup>, R. Breier<sup>5</sup>, C. Bucci<sup>4</sup>, J. Burkhardt<sup>2</sup>, L. Canonica<sup>1,13,b</sup>, A. D'Addabbo<sup>4</sup>, S. Di Lorenzo<sup>1</sup>, L. Einfalt<sup>2,3</sup>, A. Erb<sup>6,10</sup>, F. v. Feilitzsch<sup>6</sup>, S. Fichtinger<sup>2</sup>, D. Fuchs<sup>1</sup>, A. Garai<sup>1</sup>, V. M. Ghete<sup>2</sup>, P. Gorla<sup>4</sup>, P. V. Guillaumon<sup>4</sup>, S. Gupta<sup>2</sup>, D. Hauff<sup>1</sup>, M. Jeřkovec<sup>5</sup>, J. Jochum<sup>7</sup>, M. Kaznatcheeva<sup>6</sup>, A. Kinast<sup>6</sup>, H. Kluck<sup>2</sup>, H. Kraus<sup>8</sup>, S. Kuckuk<sup>7</sup>, A. Langenkämper<sup>1</sup>, M. Mancuso<sup>1</sup>, L. Marini<sup>4,11</sup>, B. Mauri<sup>1</sup>, L. Meyer<sup>7</sup>, V. Mokina<sup>2</sup>, M. Olmi<sup>4</sup>, T. Ortman<sup>6</sup>, C. Pagliarone<sup>4,12</sup>, L. Pattavina<sup>4,6</sup>, F. Petricca<sup>1</sup>, W. Potzel<sup>6</sup>, P. Povinec<sup>5</sup>, F. Pröbst<sup>1</sup>, F. Pucci<sup>1</sup>, F. Reindl<sup>2,3</sup>, J. Rothe<sup>6</sup>, K. Schäffner<sup>1</sup>, J. Schieck<sup>2,3</sup>, S. Schönert<sup>6</sup>, C. Schwertner<sup>2,3</sup>, M. Stahlberg<sup>1</sup>, L. Stodolsky<sup>1</sup>, C. Strandhagen<sup>7</sup>, R. Strauss<sup>6</sup>, I. Usherov<sup>7</sup>, F. Wagner<sup>2</sup>, M. Willers<sup>6</sup>, V. Zema<sup>1</sup>

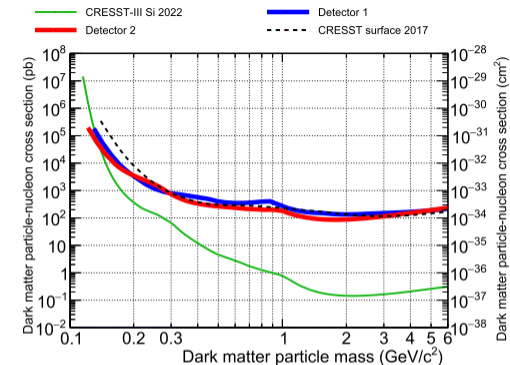


**Fig. 5** Exclusion limits for the elastic spin-independent DM-nucleon scattering cross section at 90% CL, calculated for detector 1 (blue) and 2 (red) using Yellin's optimum interval method. In black, the previous best above ground exclusion limits of CRESST are plotted [17]. In green, the best exclusion limits below 0.160 GeV/c<sup>2</sup> from CRESST underground measurements [4] are plotted as a benchmark reference

# Physics motivation

PHYSICAL REVIEW D 99, 123005 (2019)

- Sensitive to dark matter and ALPs.
- Predictions for 1 kg Y \*

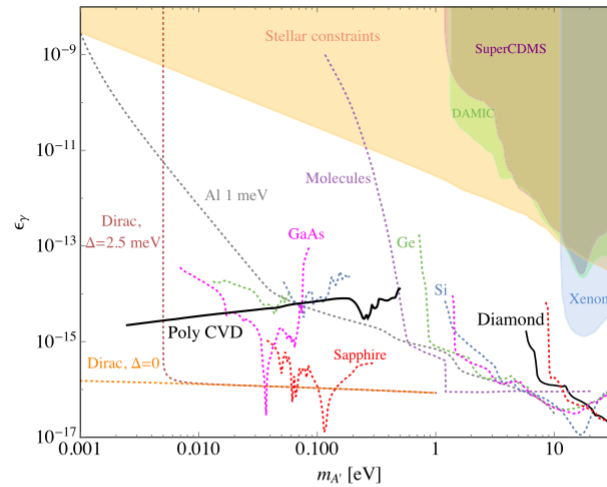


FIG. 4. Projected reach at 95% C.L. for absorption of kinetically mixed dark photons with mass greater than 1 meV. The solid black curves indicate the expected reach for a kilogram-year exposure of diamond. Projected reach for germanium and silicon [45], Dirac materials [10], polar crystals [12], molecules [82], and superconducting aluminum [9] targets are indicated by the dotted curves. Constraints from stellar emission [83,84], DAMIC [85], SuperCDMS [72], and Xenon [84] data are shown by the shaded orange, green, purple, and blue regions, respectively.

\* 1kg high purity synthetic diamond costs O(1 M)

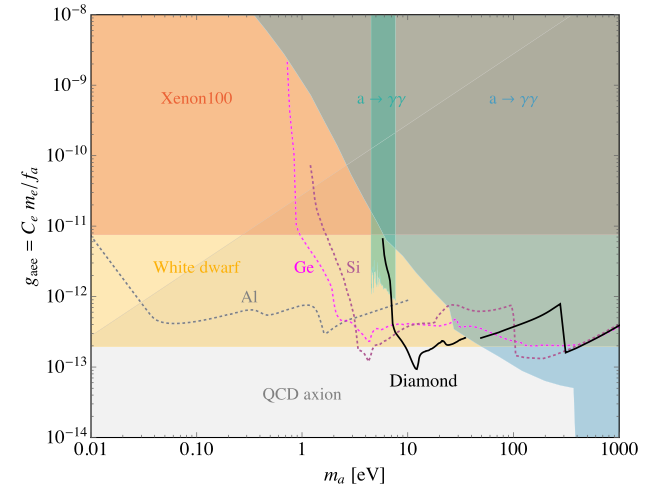


FIG. 5. Projected reach at 95% C.L. for absorption of axionlike particles. The reach of a kilogram-year exposure of diamond is shown by the solid black curve. The reach for semiconductors such as germanium and silicon [45] and superconducting aluminum [9] targets is depicted by the dotted magenta, purple, and gray curves, respectively. Stellar constraints from Xenon100 data [88] and white dwarves [87] are indicated by the shaded red and orange regions, respectively. Constraints from loop-induced couplings to photons are presented in the shaded blue and green regions [89,90]. The QCD axion region of interest is indicated in shaded gray.

# Current Diamond TES landscape

- Relatively new field.
- Diamond proposed as a DM detector.

PHYSICAL REVIEW D **99**, 123005 (2019)

Editors' Suggestion

## Diamond detectors for direct detection of sub-GeV dark matter

Noah Kurinsky,<sup>1,2</sup> To Chin Yu,<sup>3,4</sup> Yonit Hochberg,<sup>5</sup> and Blas Cabrera<sup>3</sup>

<sup>1</sup>*Fermi National Accelerator Laboratory, Batavia, Illinois 60510, USA*

<sup>2</sup>*Kavli Institute for Cosmological Physics, University of Chicago, Chicago, Illinois 60637, USA*

<sup>3</sup>*Department of Physics, Stanford University, Stanford, California 94305, USA*

<sup>4</sup>*SLAC National Accelerator Laboratory, 2575 Sand Hill Road, Menlo Park, California 94025, USA*

<sup>5</sup>*Racah Institute of Physics, Hebrew University of Jerusalem, Jerusalem 91904, Israel*

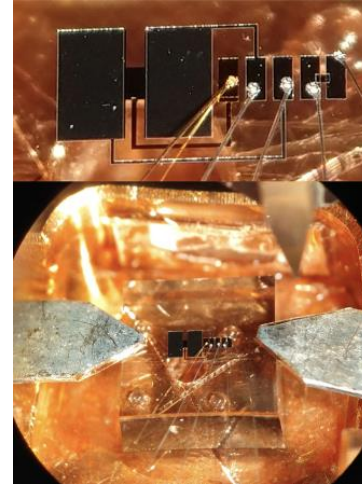
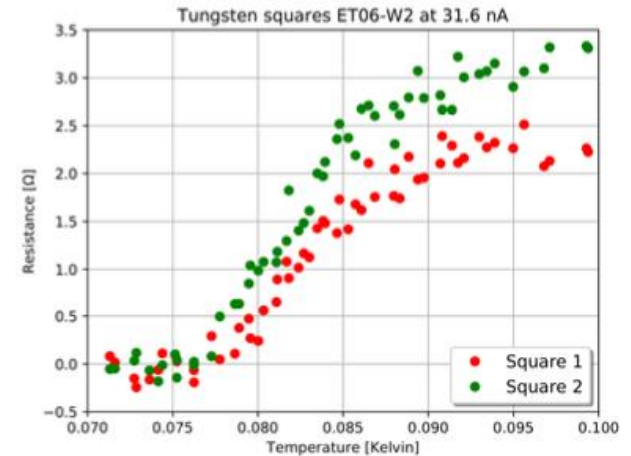
 (Received 5 February 2019; published 10 June 2019)

We propose using high-purity lab-grown diamond crystal for the detection of sub-giga electron volt dark matter. Diamond targets can be sensitive to both nuclear and electron recoils from dark matter scattering in the mega-electron-volt and above mass range as well as to absorption processes of dark matter with masses between sub-electron volts to tens of electron volts. Compared to other proposed semiconducting targets such as germanium and silicon, diamond detectors can probe lower dark matter masses via nuclear recoils due to the lightness of the carbon nucleus. The expected reach for electron recoils is comparable to that of germanium and silicon, with the advantage that dark counts are expected to be under better control. Via absorption processes, unconstrained QCD axion parameter space can be successfully probed in diamond for masses of order 10 eV, further demonstrating the power of our approach.

DOI: [10.1103/PhysRevD.99.123005](https://doi.org/10.1103/PhysRevD.99.123005)

# Why diamond?

- Operation as Transition Edge Sensor (TES)
  - W Al metalisation
- Diamond has high Debye temperature:
  - high thermal conductivity
  - excellent phonons transport.
- Light nucleus ( $A=12$ )
  - probe lower DM masses



Material	$\Theta_D$ in K
Diamant	1860
Si	645
Cr	610
Fe	470
Mo	450
Al	428
Ge	374
Cu	345

# Summary

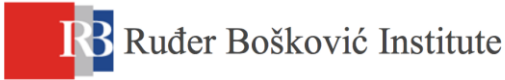
- Diamond systems are used as beam and luminosity monitors in current HEP experiments and foreseen for future experiments.
- Radiation hardness and rate dependence has been studied.
- 3D diamond has been demonstrated to work.
- The understanding of diamond as a detector material is advancing.

# EXTRA MATERIAL

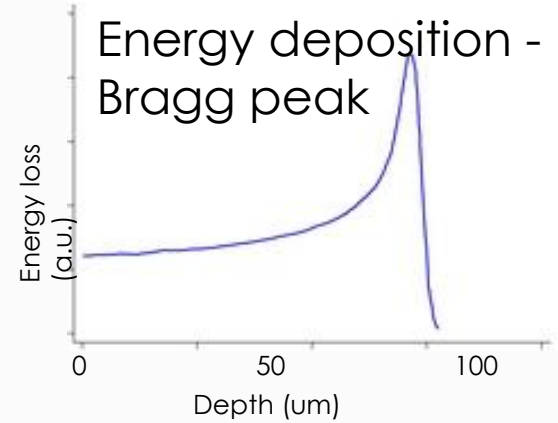
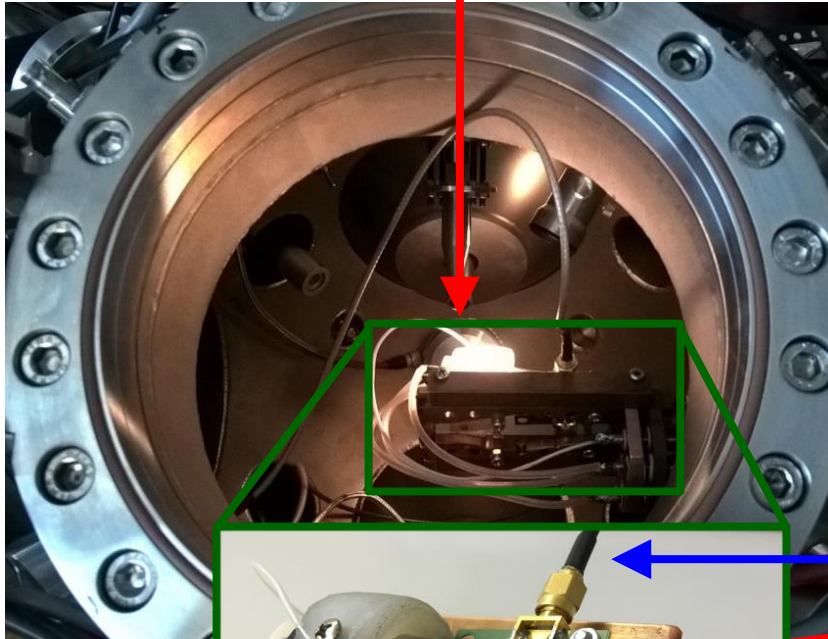
# 3D Detector Characterization

- Proton Micro-beam: 4.5 MeV p

# Proton micro-beam measurements

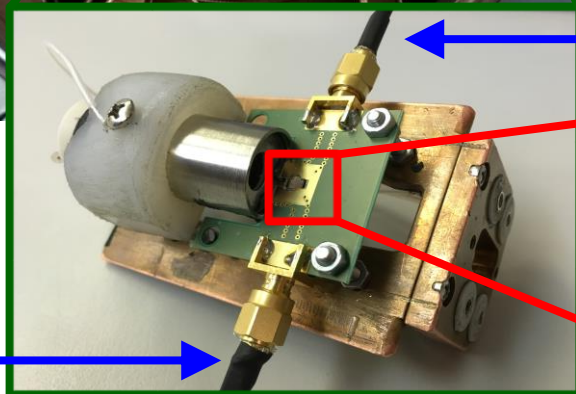


4.5 MeV  
protons

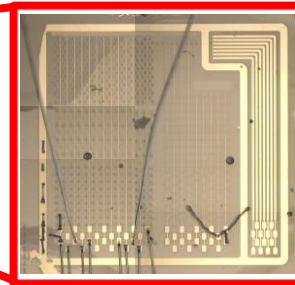


- Single particle beam.
- Rate ~ 1kHz.
- Beam position resolution < 2μm.

Read-out  
channel 1



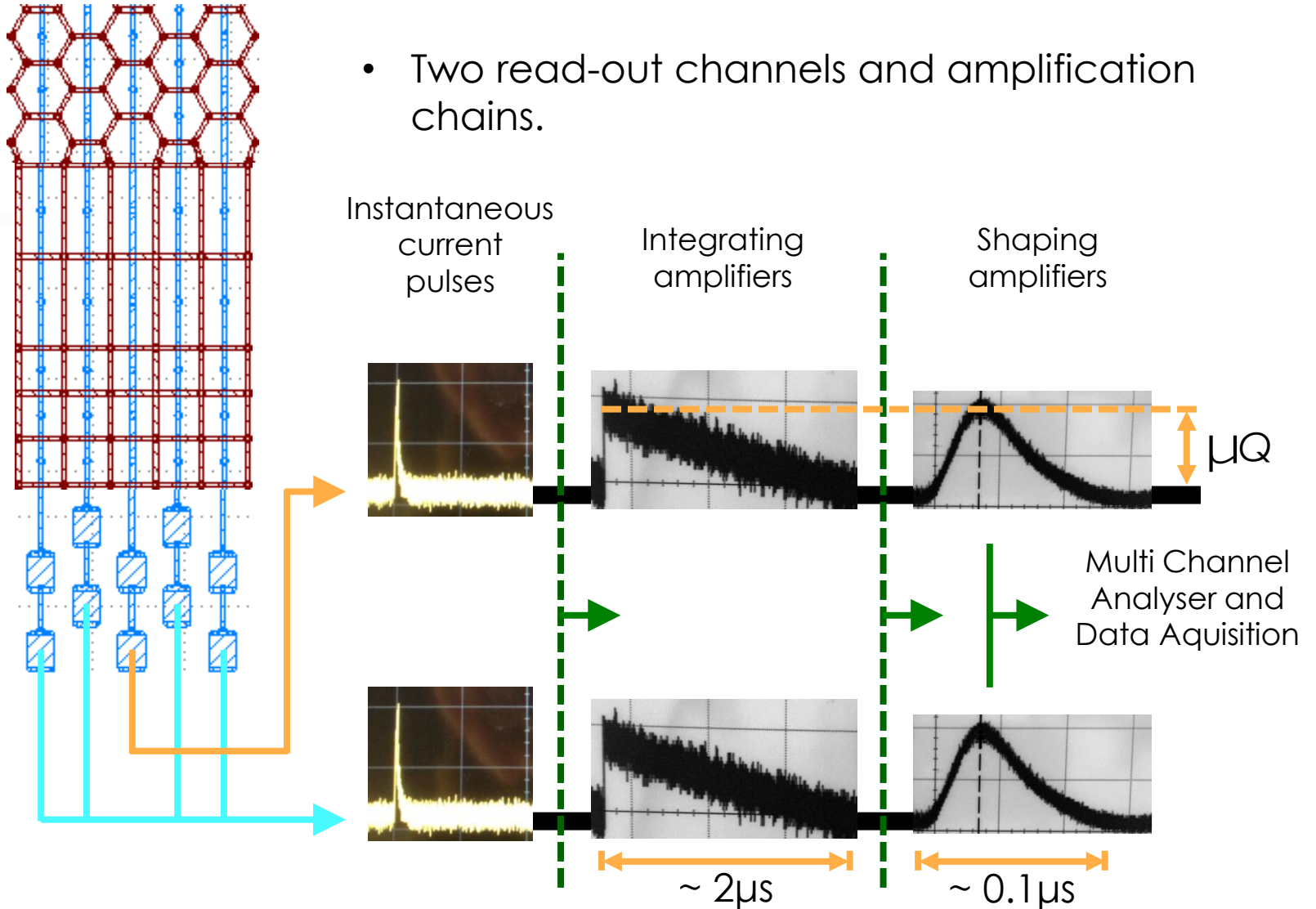
Read-out  
channel 2



3D diamond  
detector

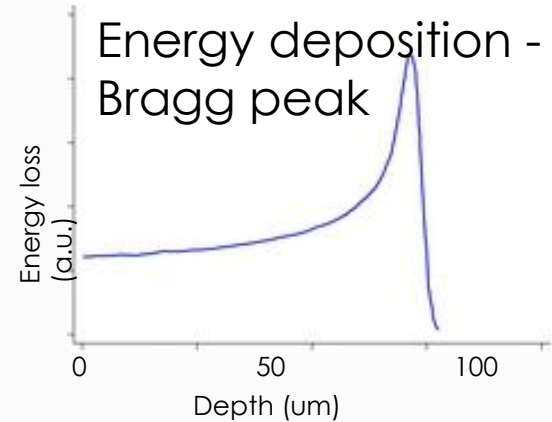
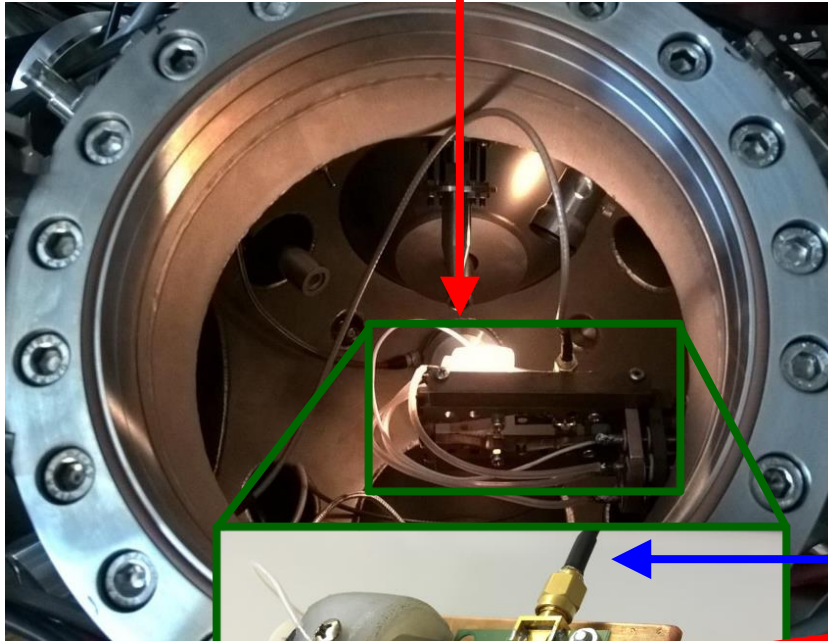
# IBIC - setup

- Two read-out channels and amplification chains.



# Proton micro-beam measurements

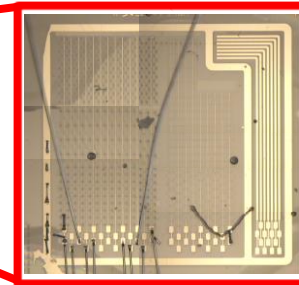
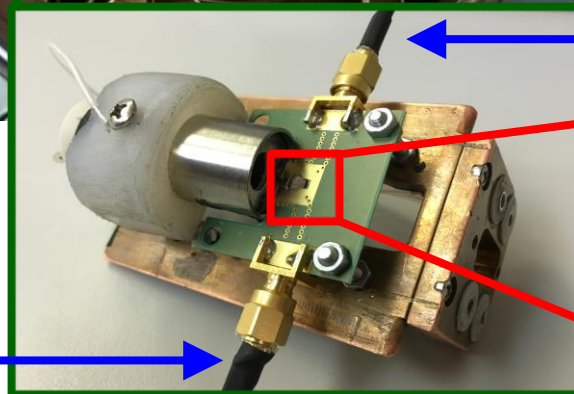
4.5 MeV  
protons



- Single particle beam.
- Rate ~ 1kHz.
- Beam position resolution < 2 $\mu$ m.

Read-out  
channel 1

Read-out  
channel 2

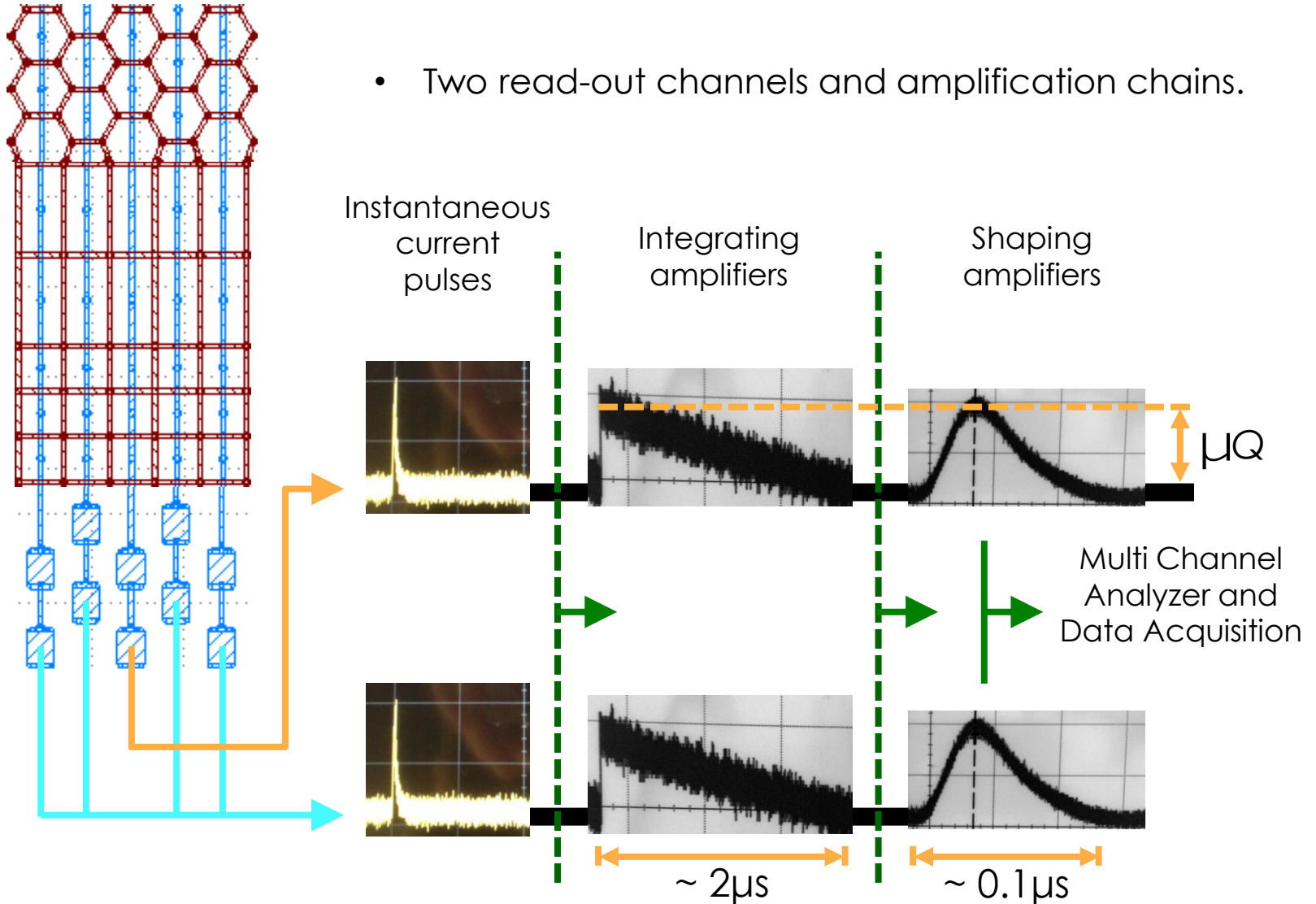


3D diamond  
detector

# (TR)IBIC

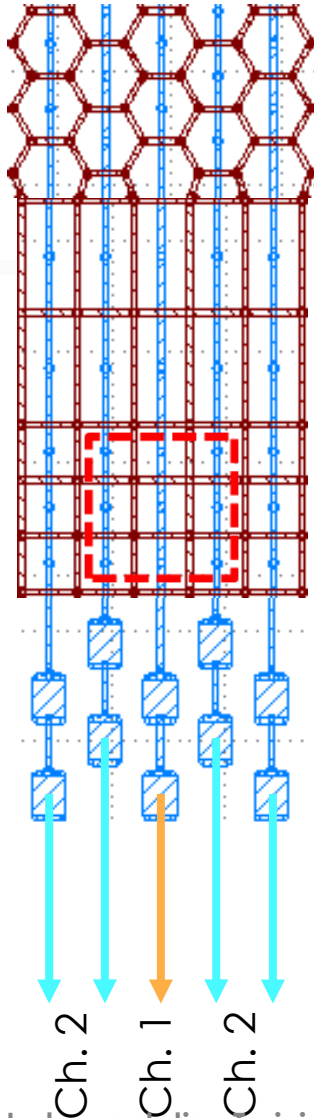
## (Time Resolved) Ion Beam Induced Current

- Two read-out channels and amplification chains.

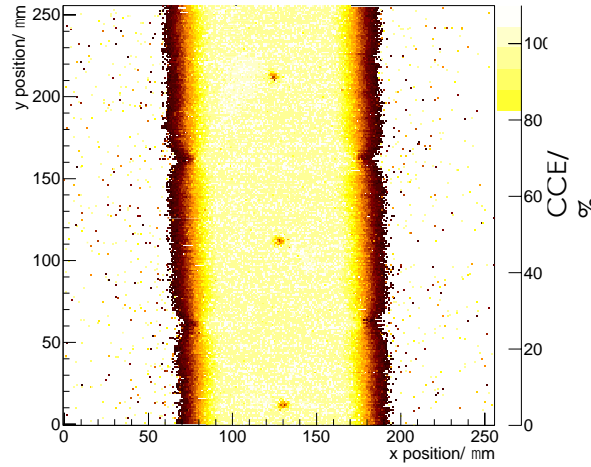


# Signal efficiency at +20V

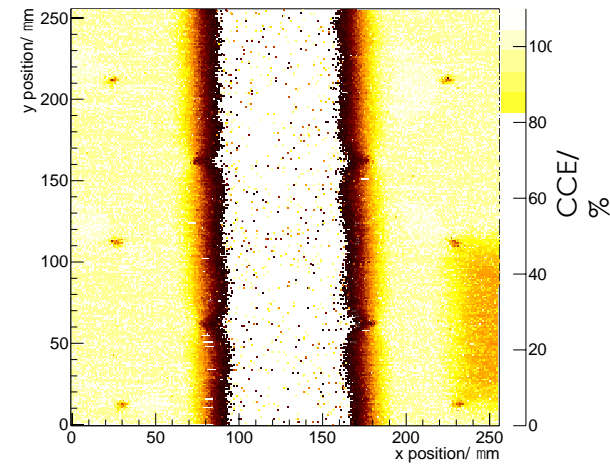
- Electronics chain calibrated with silicon detector.

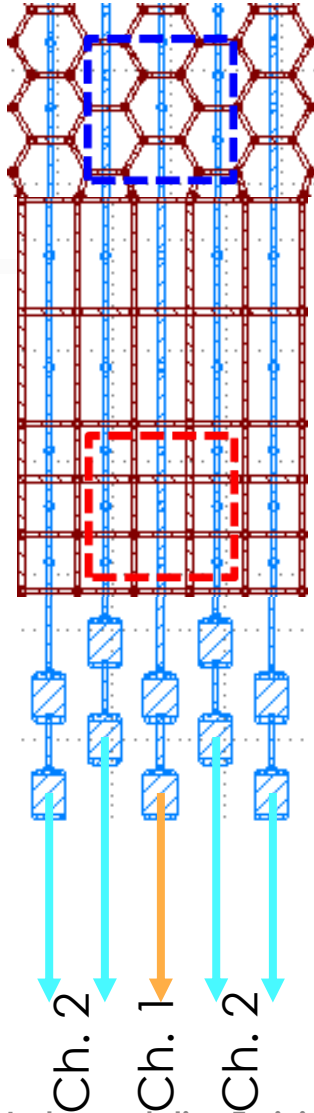


Channel 1



Channel 2





Charge Sharing

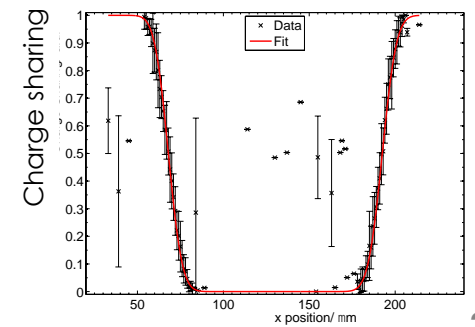
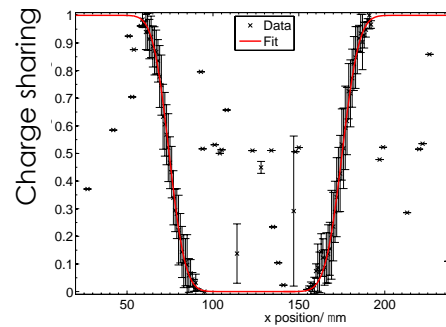
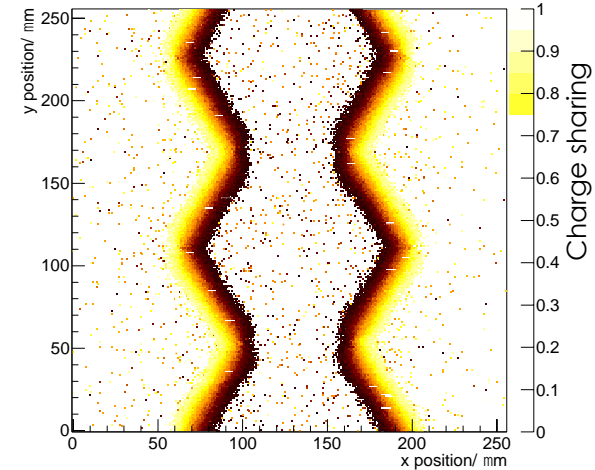
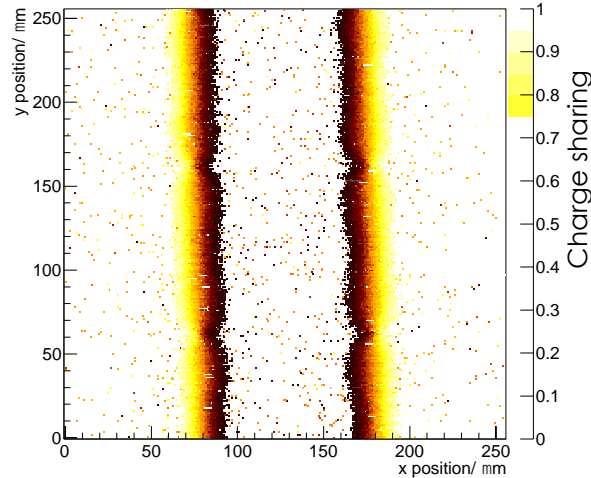
$$\rho = Q_2 / (Q_1 + Q_2)$$

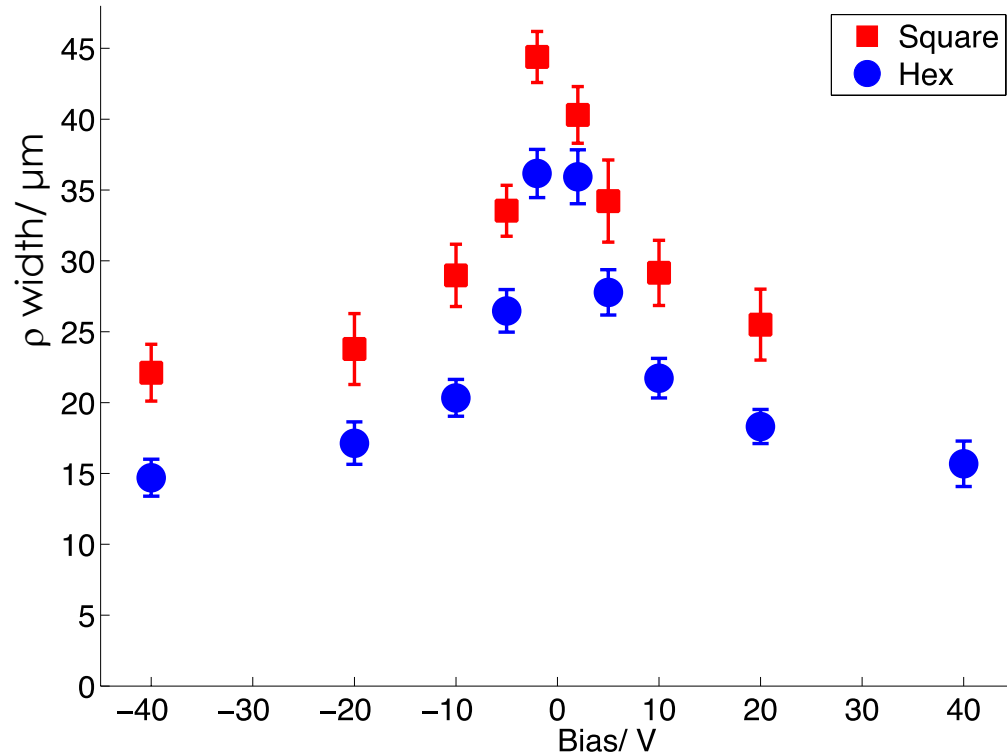
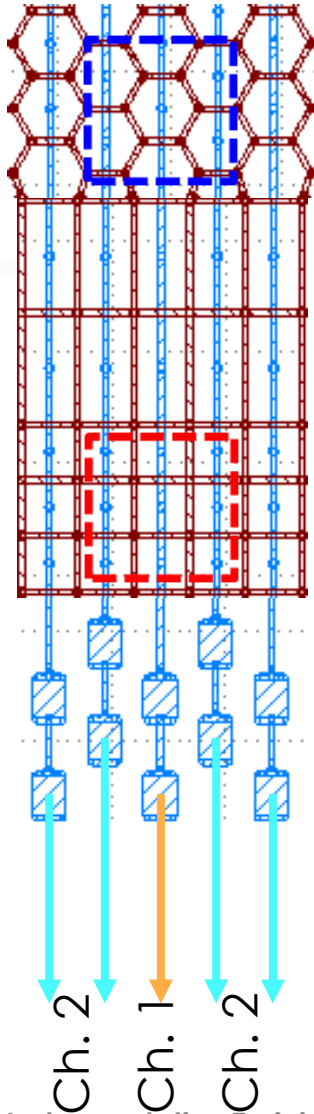
Induced charge on Ch. 2

Induced charge on Ch. 1

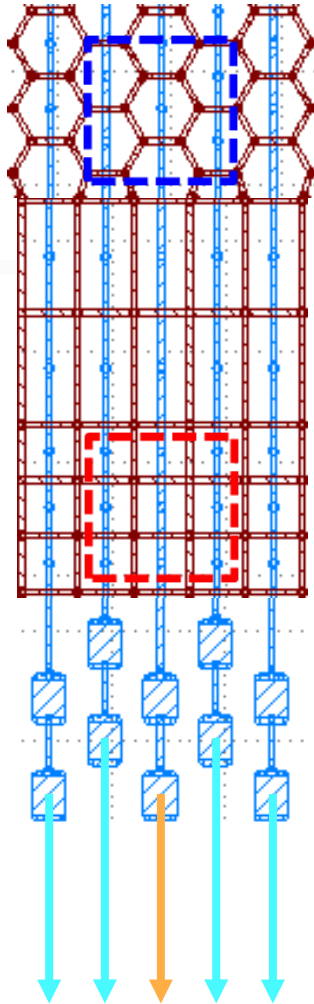
Square

Hexagonal



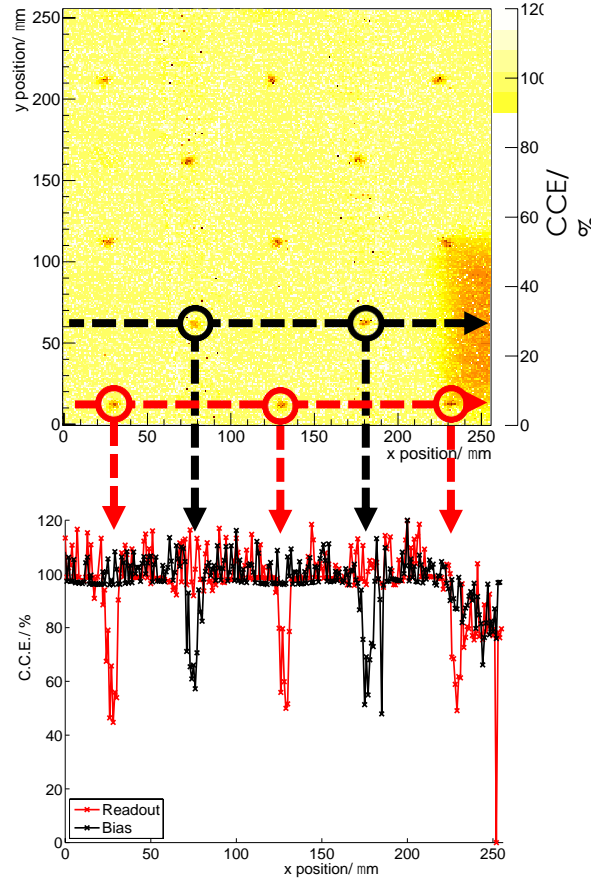


# Combined Ch. 1 and Ch. 2 at +20V

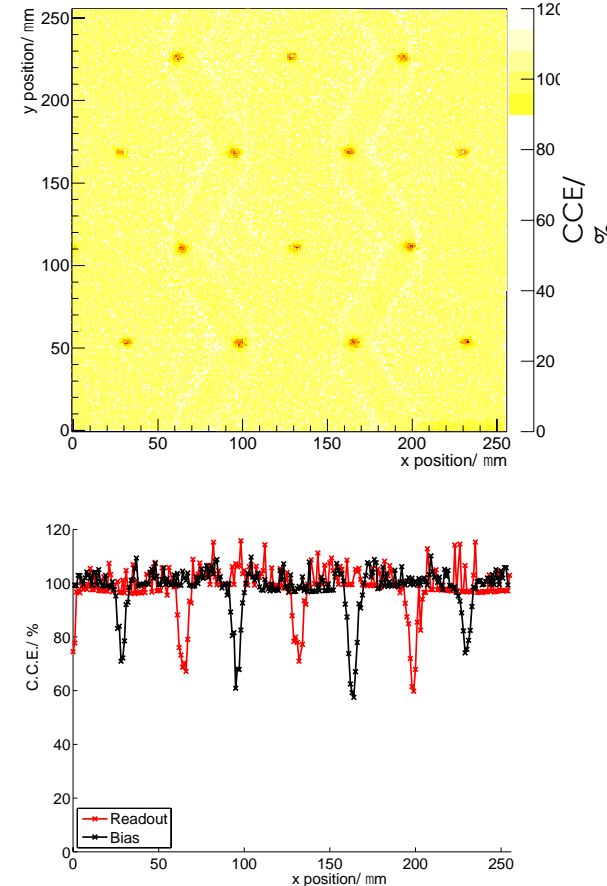


Combine

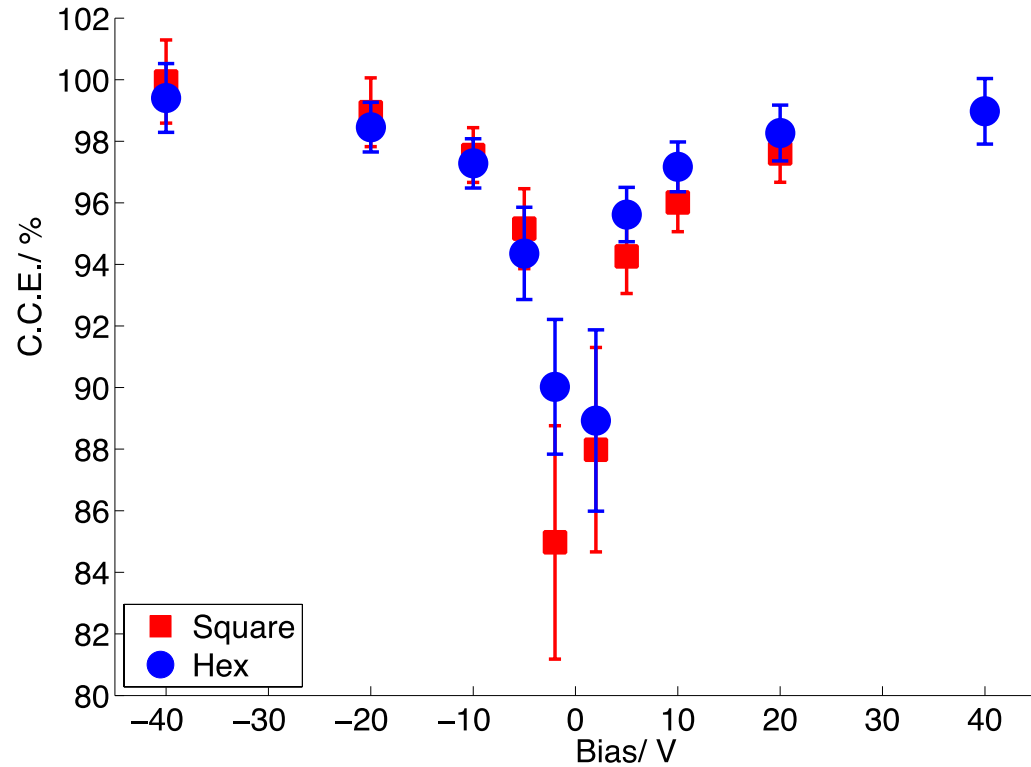
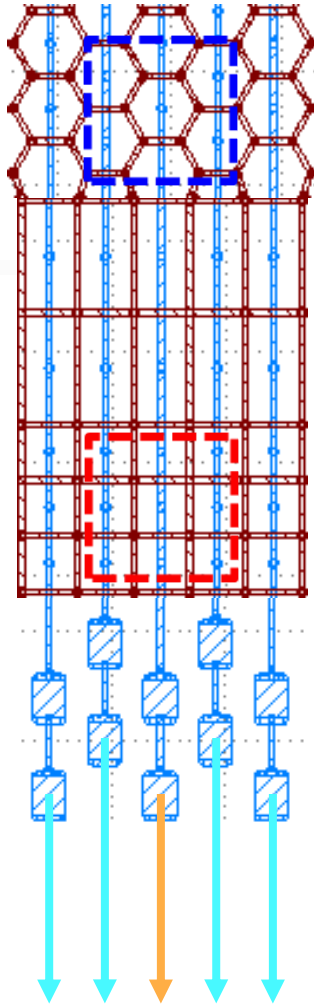
Square



Hexagonal



# Signal efficiency comparison



Combine

# Summary IBIC

- Measured the Signal Efficiency versus position.
- Both geometries show  $> 98\%$  CCE above 20V.
- There is a measured drop in signal due to columns of diameter  $\sim 6\mu\text{m}$ .
- A small region of charge sharing,  $\sim 20\mu\text{m}$ , is observed in both geometries.

# Time Resolved IBIC (TRIBIC)

The diagram shows the equation  $i = E_w q v$  centered within a white rectangular border. Four yellow labels with black arrows point to the variables: 'Instantaneous current' points to  $i$ , 'Carrier charge' points to  $q$ , 'Weighting field' points to  $E_w$ , and 'Carrier velocity' points to  $v$ .

$$i = E_w q v$$

Instantaneous current

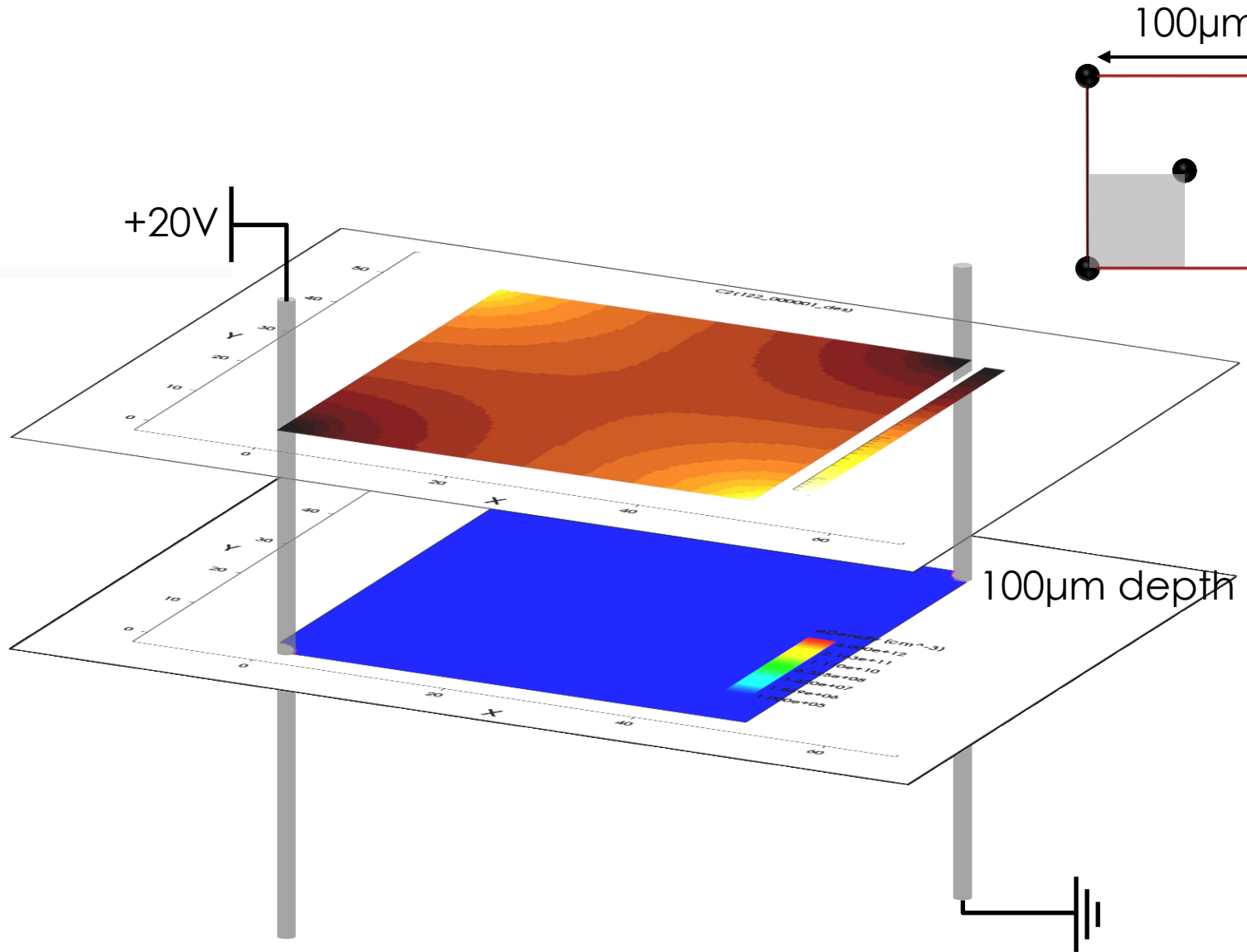
Carrier charge

Weighting field

Carrier velocity

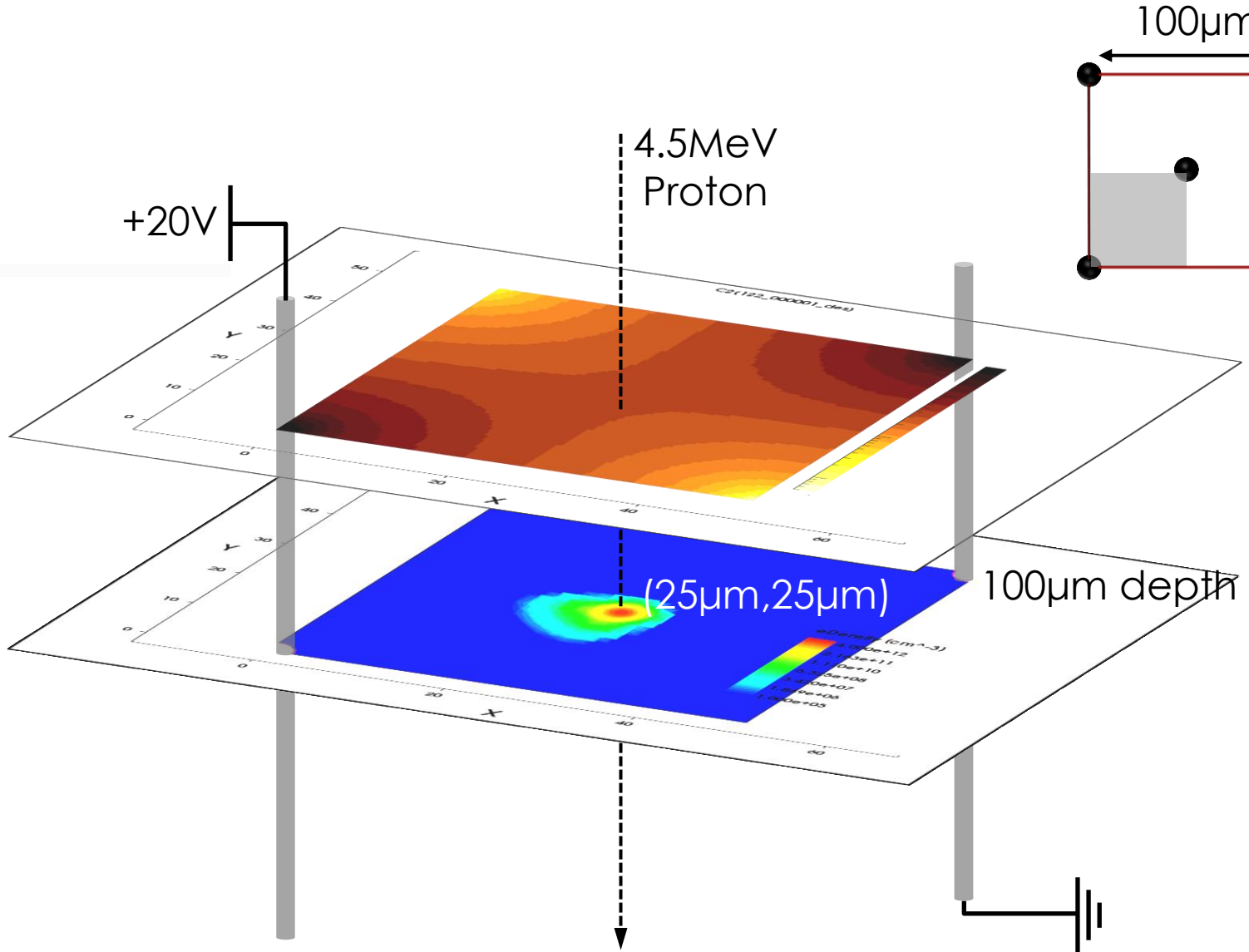
# Simulation

12  
9



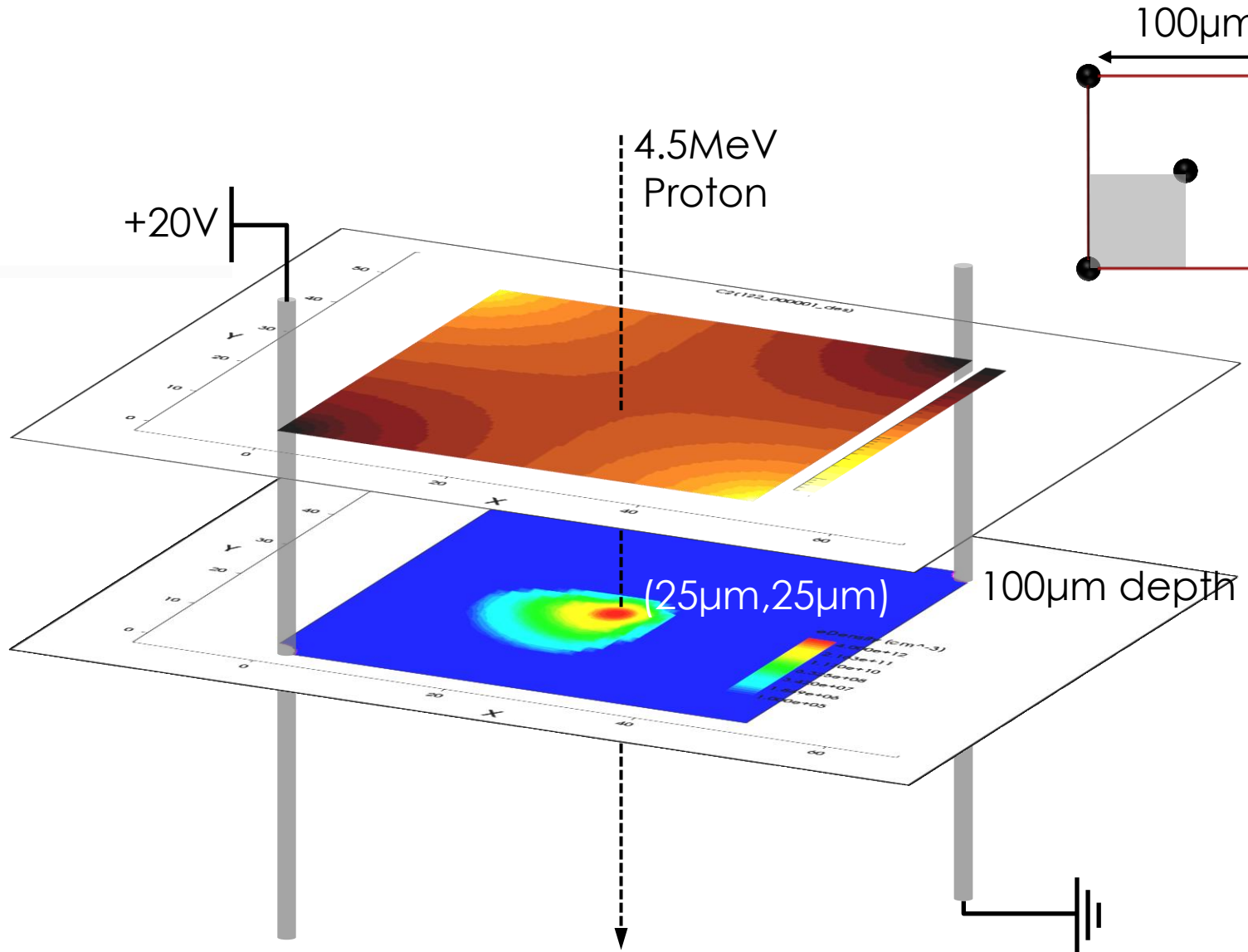
# Simulation

13  
0

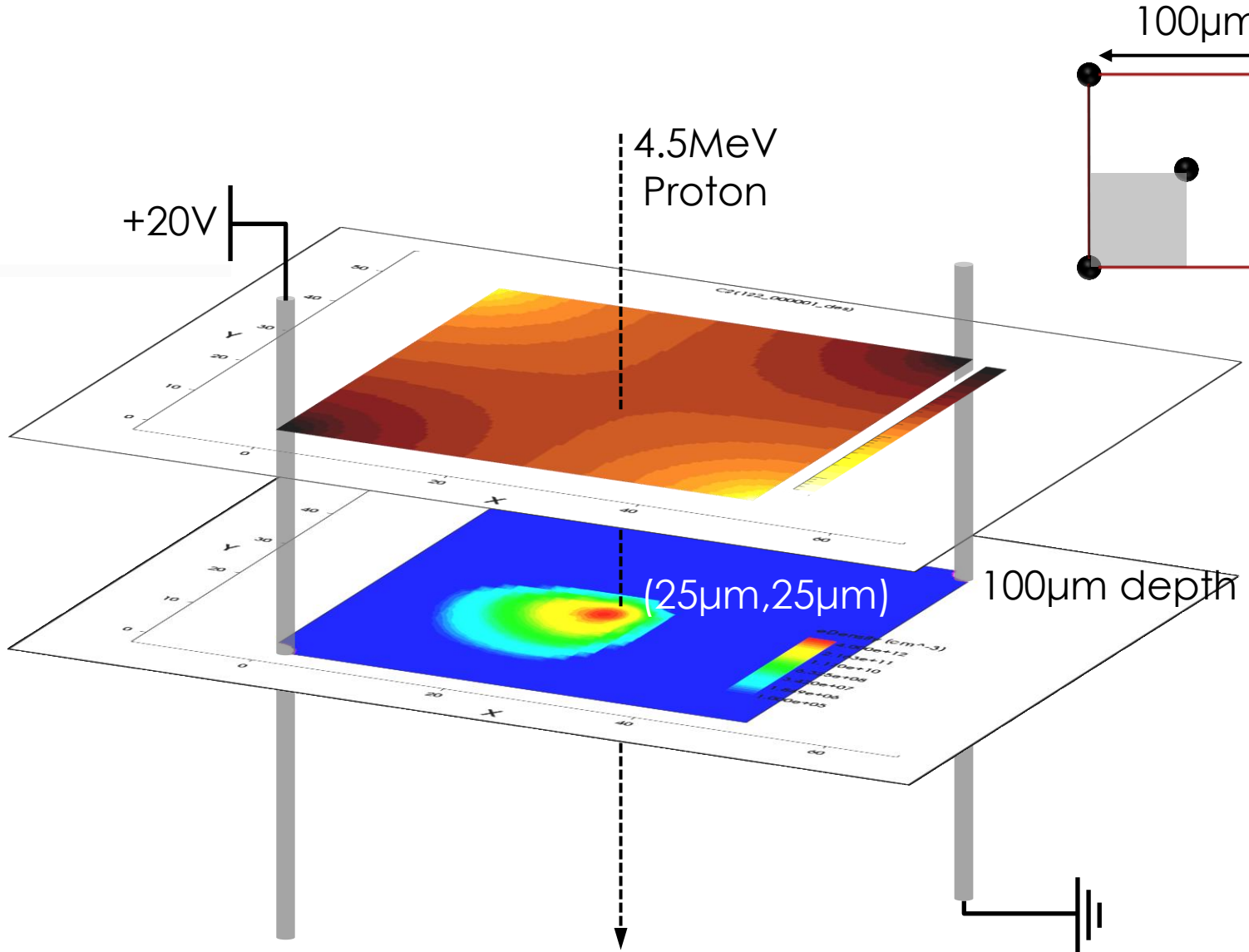


# Simulation

13  
1

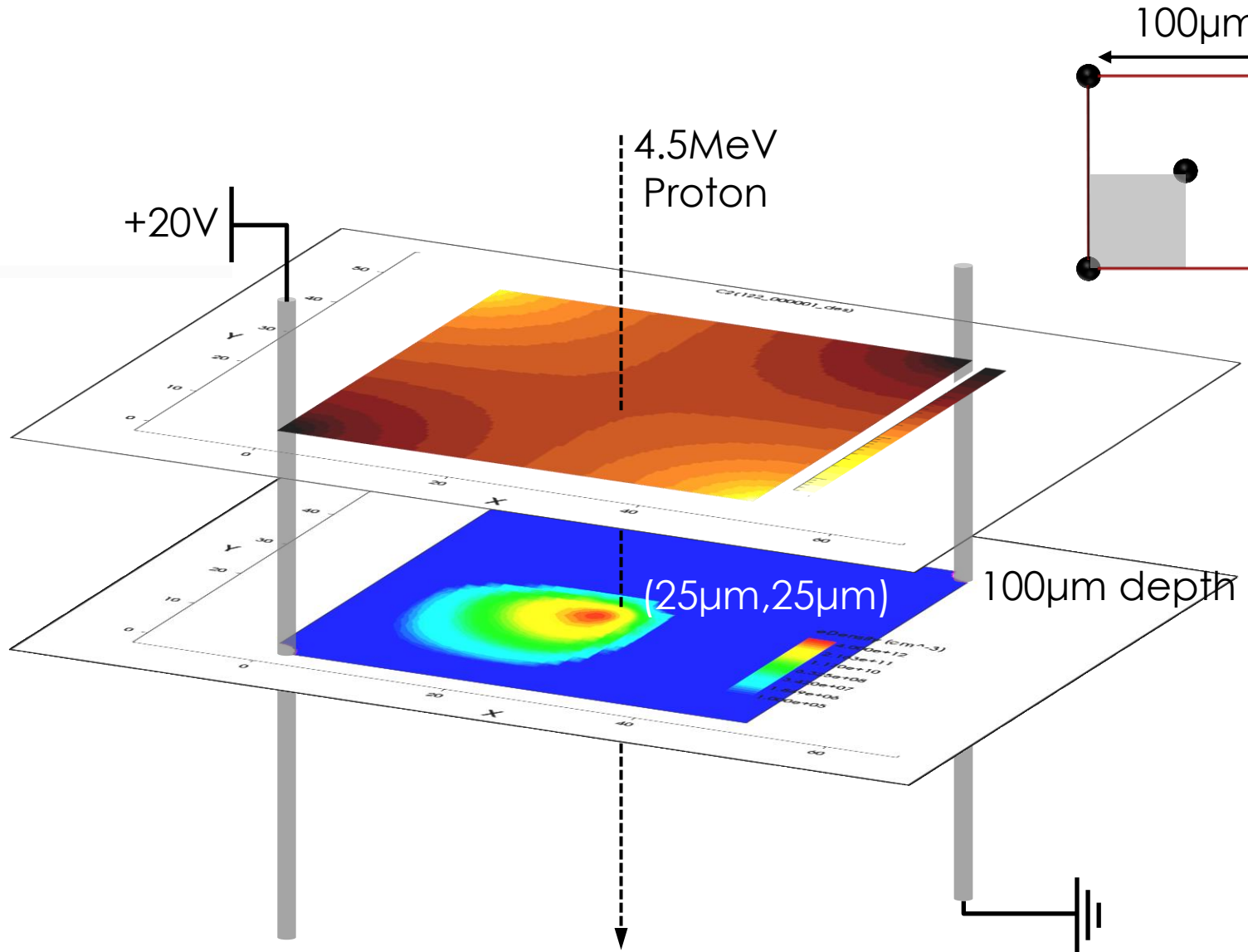


# Simulation



# Simulation

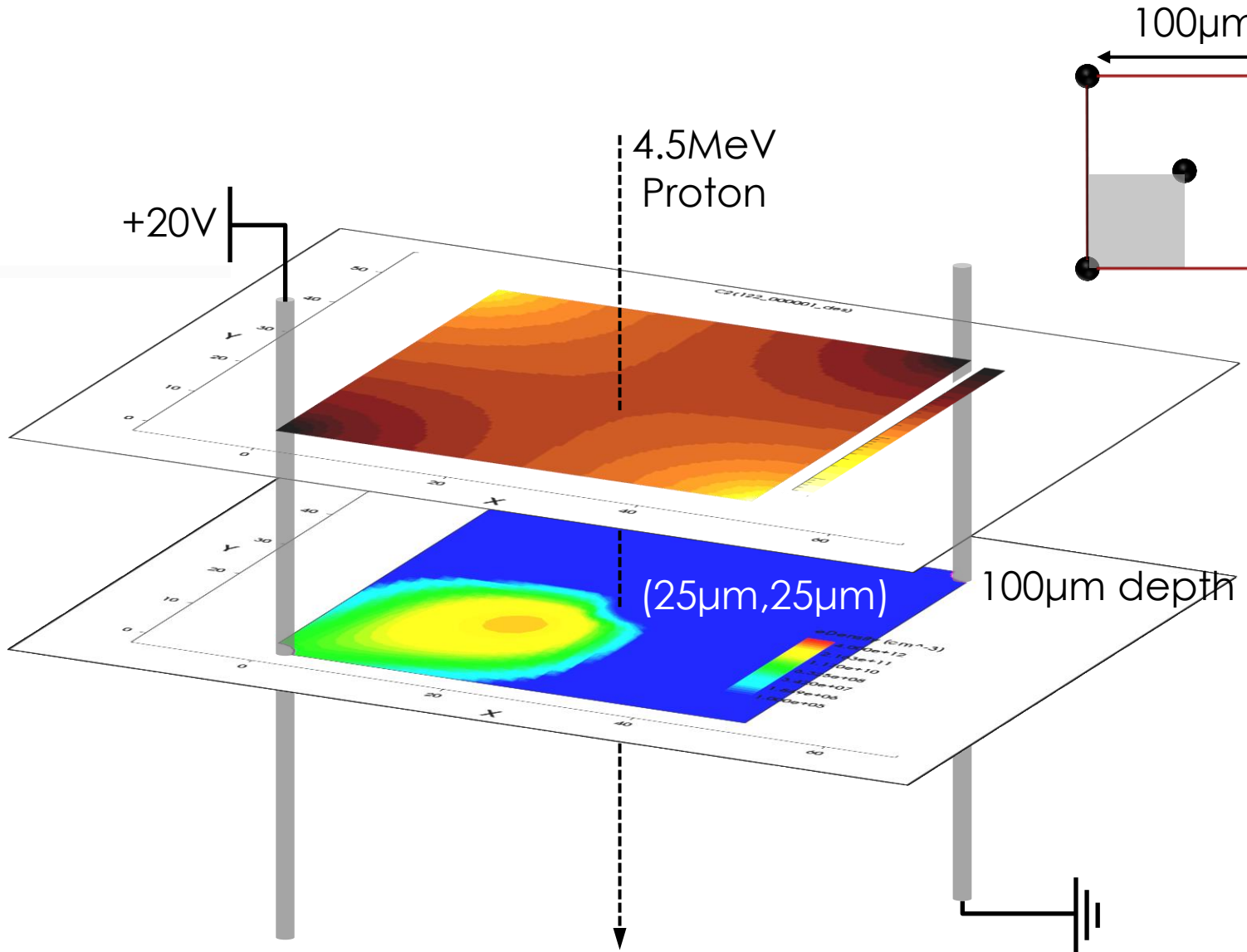
13  
3



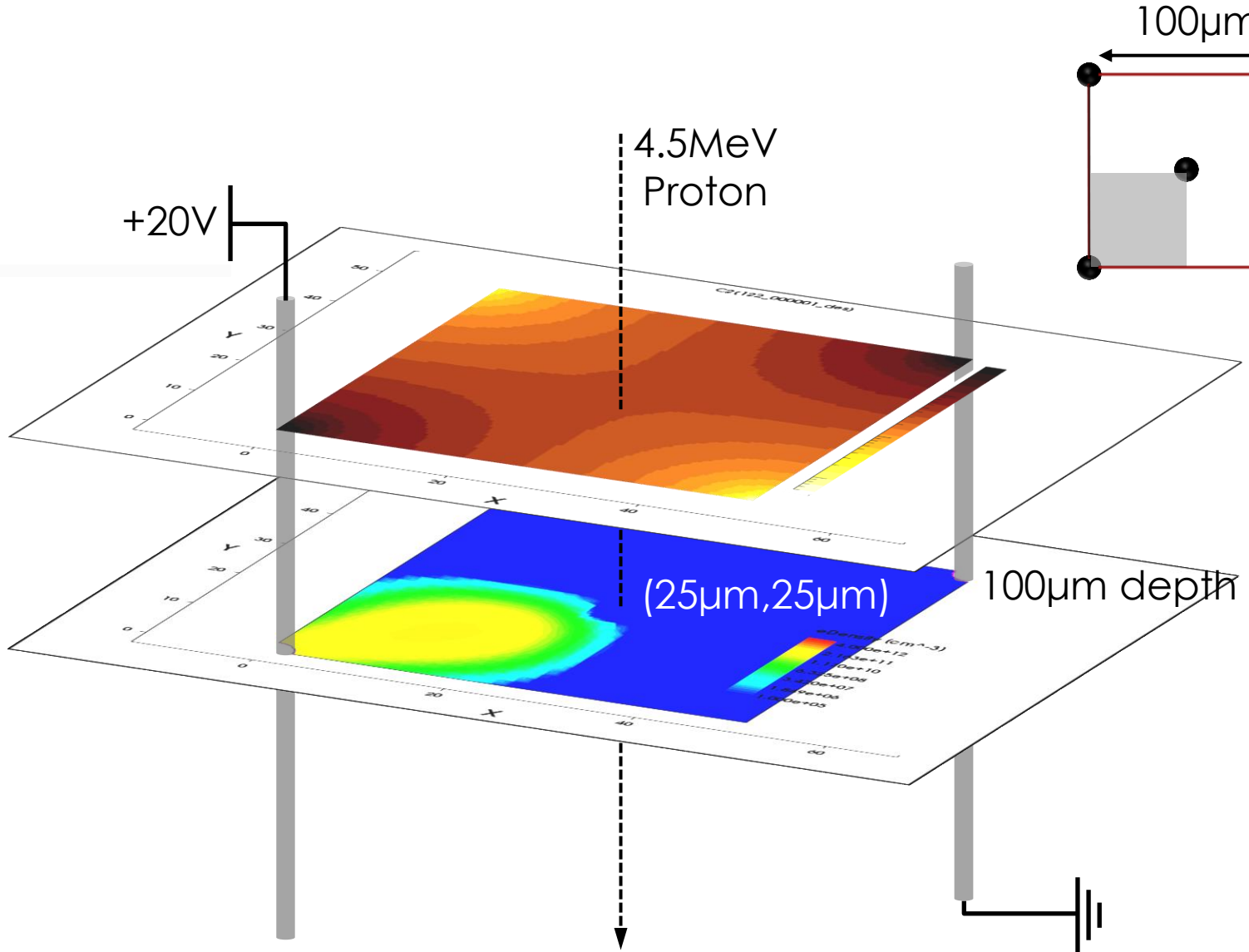


# Simulation

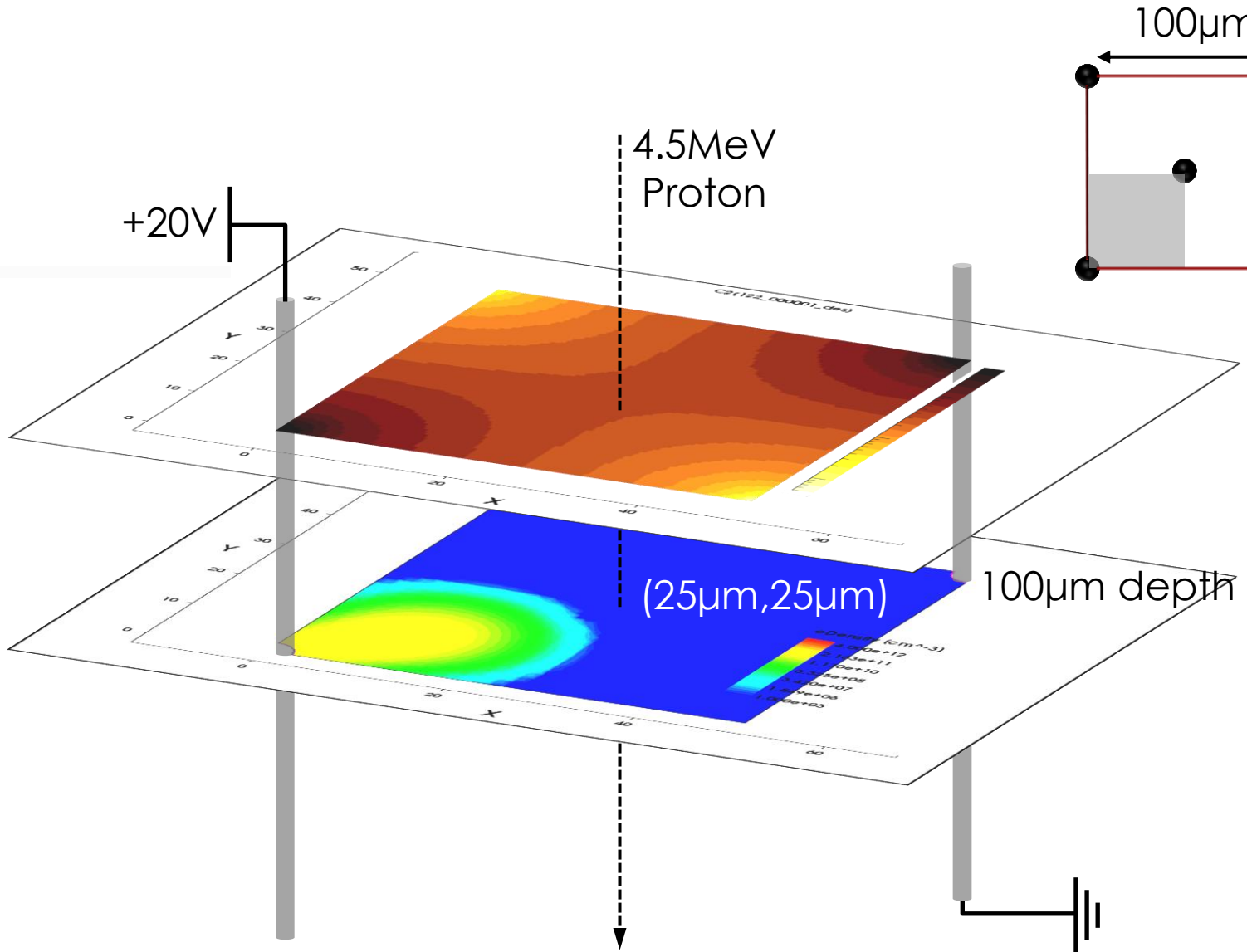
13  
5



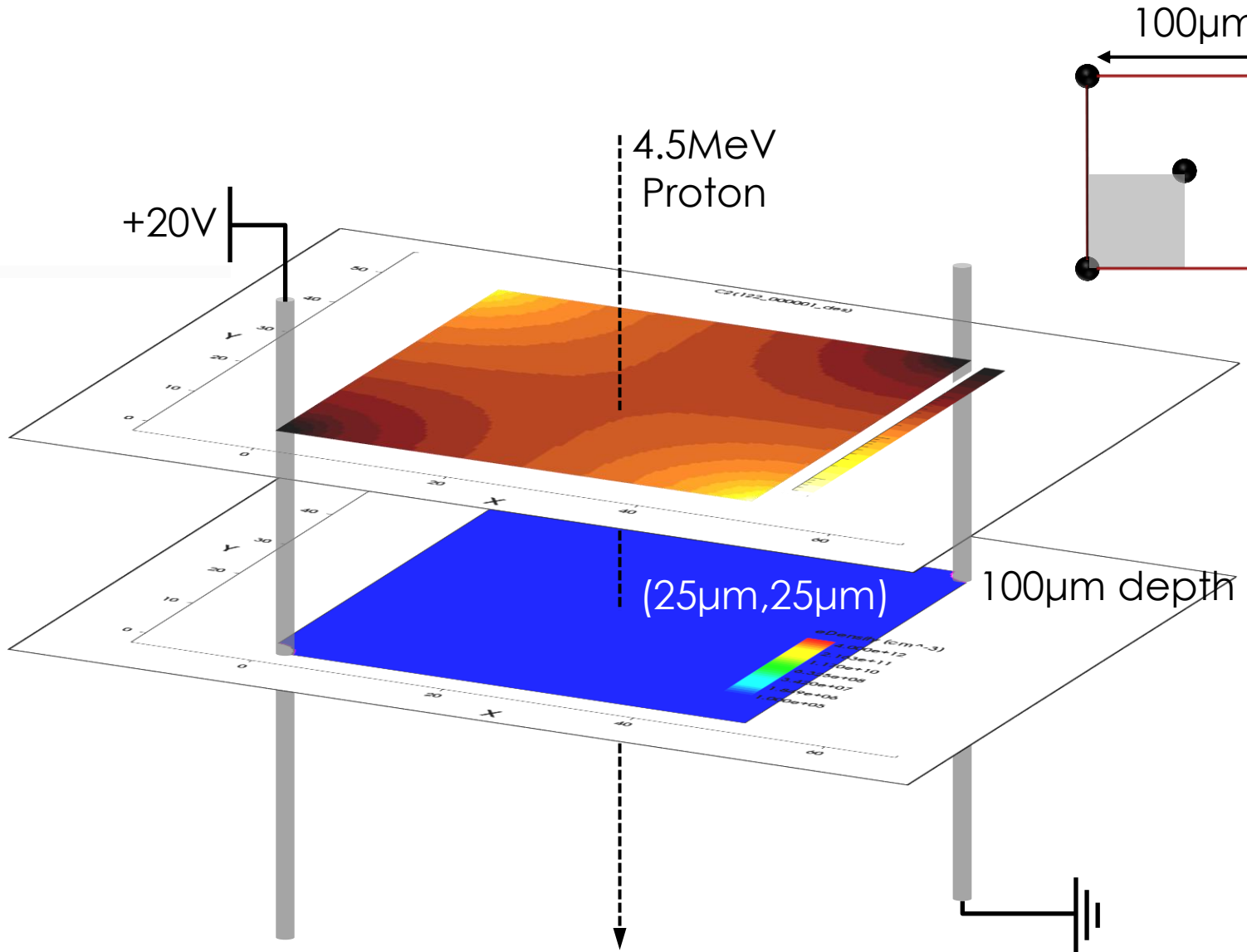
# Simulation

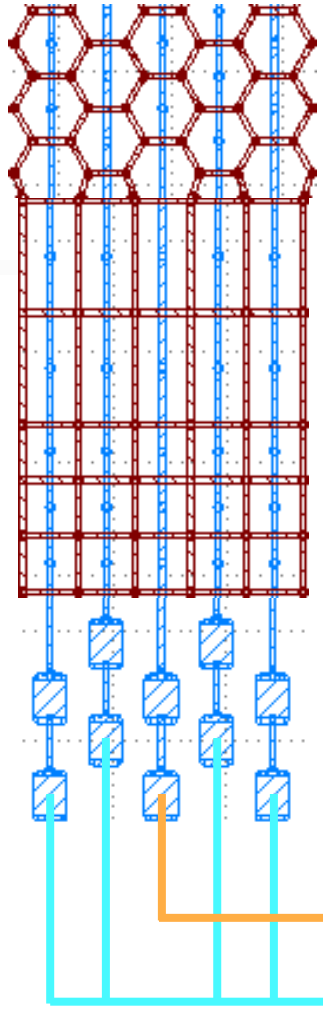


# Simulation



# Simulation

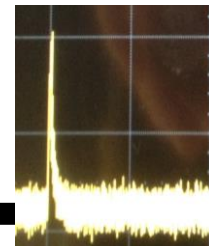
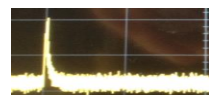
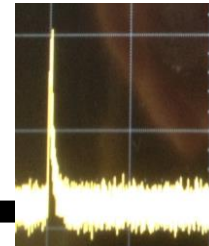
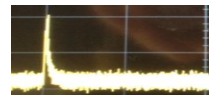


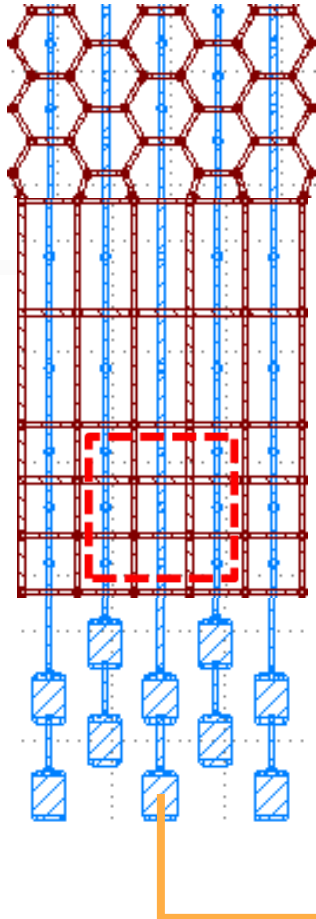


- Two read-out channels and amplification chains.

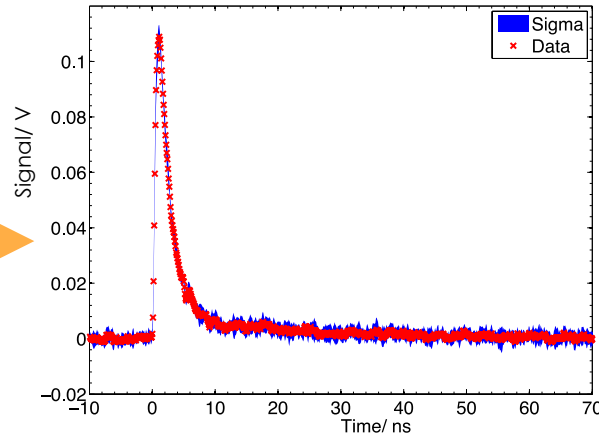
Instantaneous  
current  
pulses

Current  
amplifiers

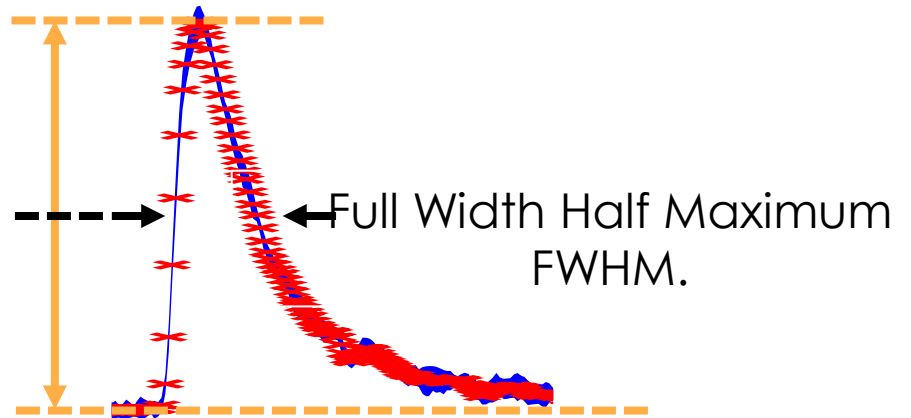
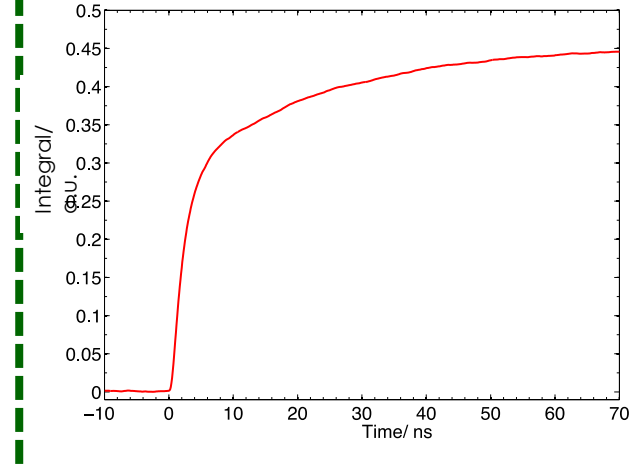




Instantaneous current pulse



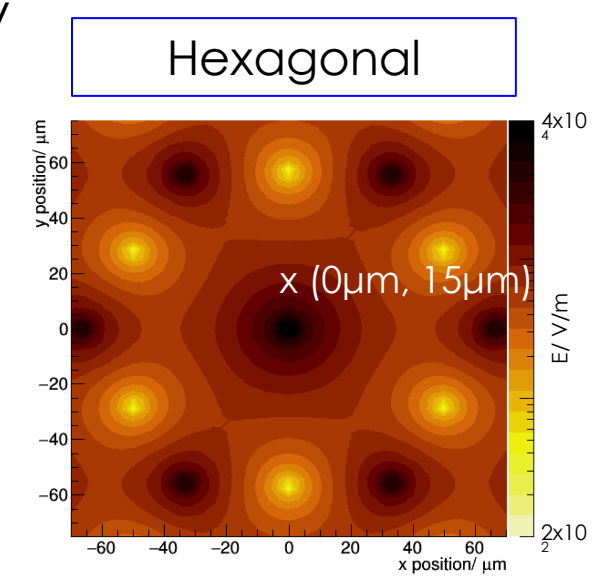
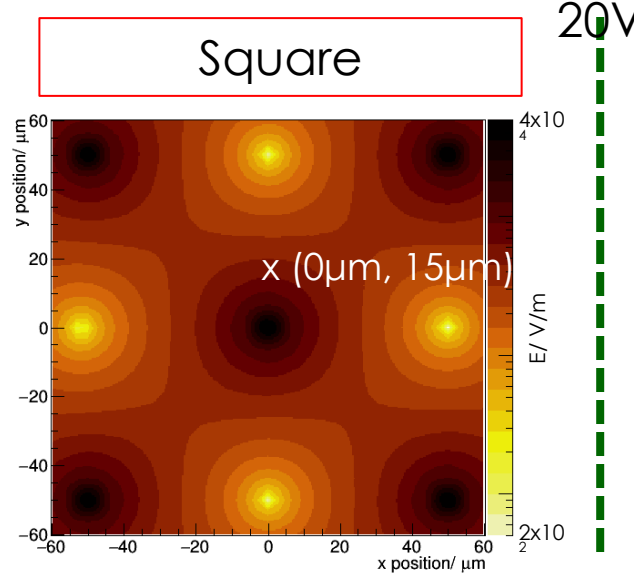
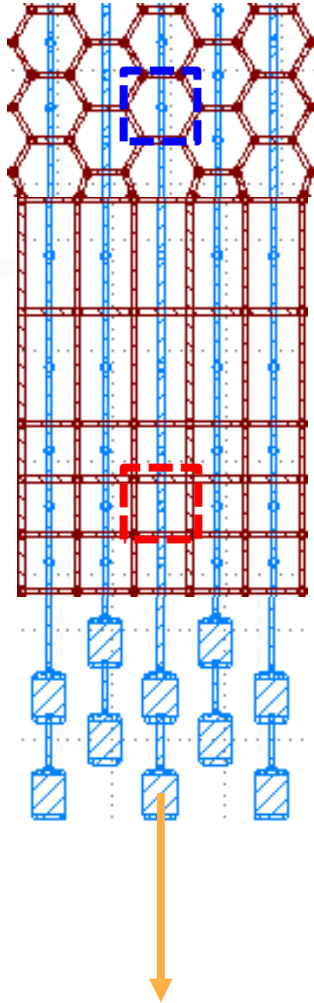
Integral



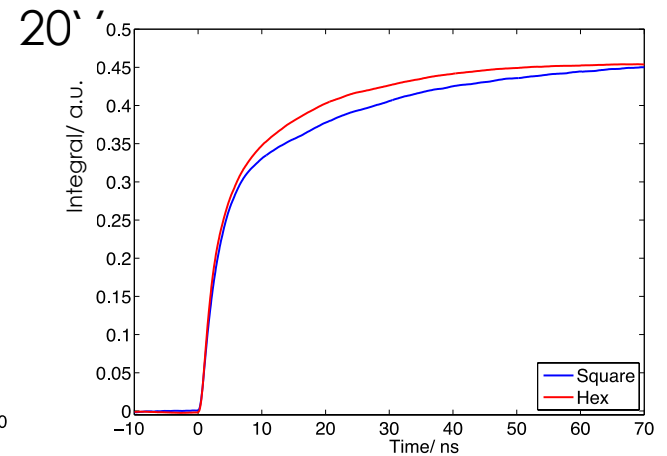
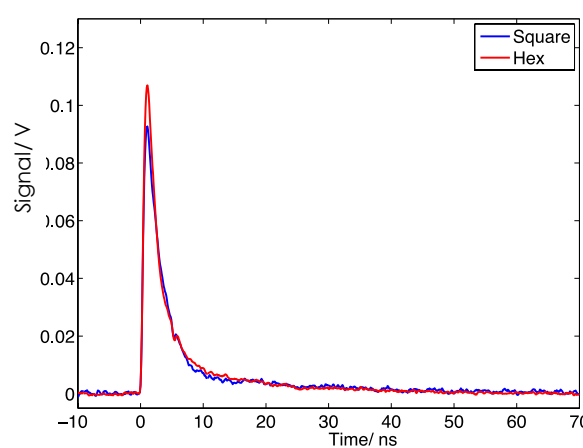
# Position dependence – near electrode

14  
1

Simulated electric field at



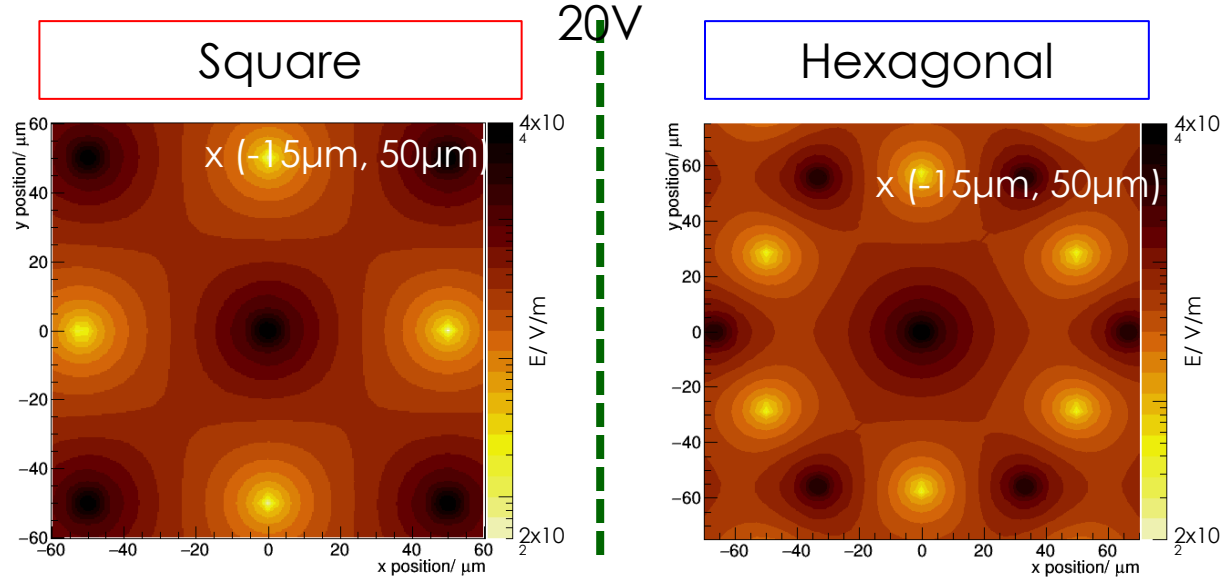
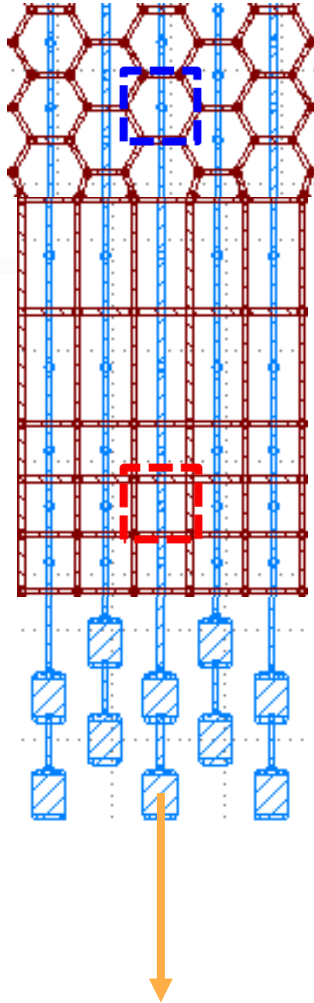
Measured current pulse at



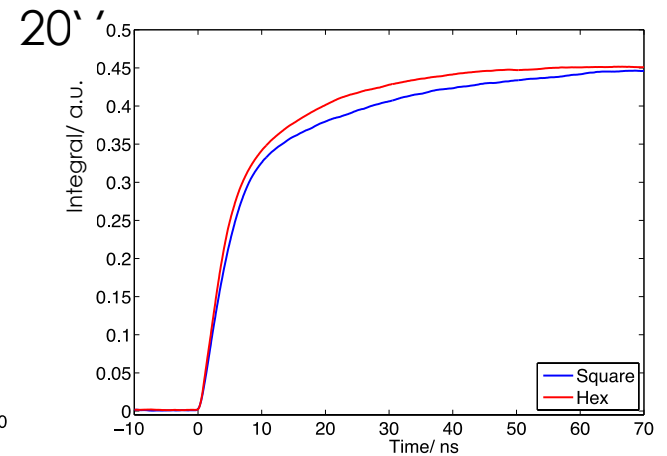
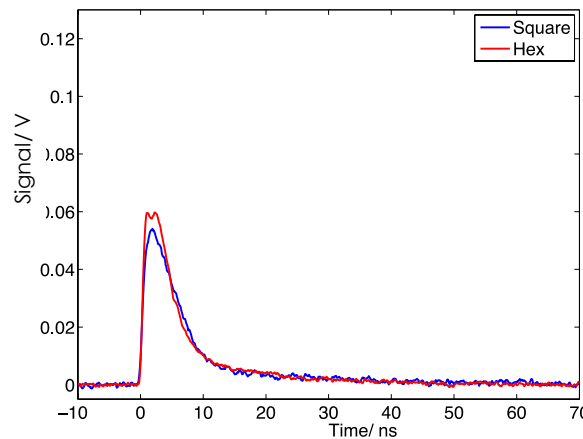
# Position dependence – far from electrode

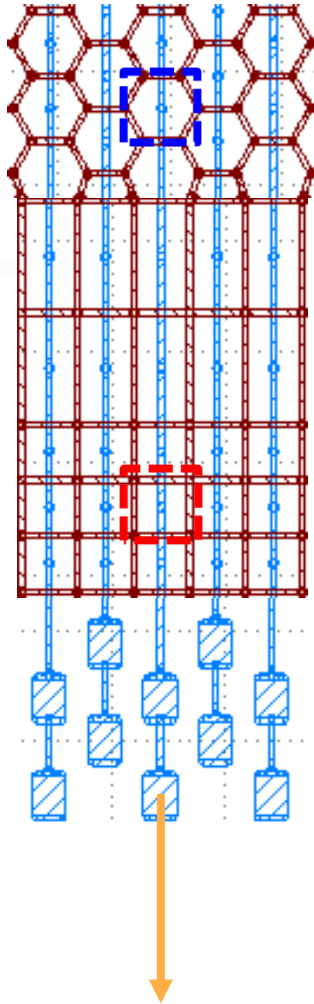
14  
2

Simulated electric field at

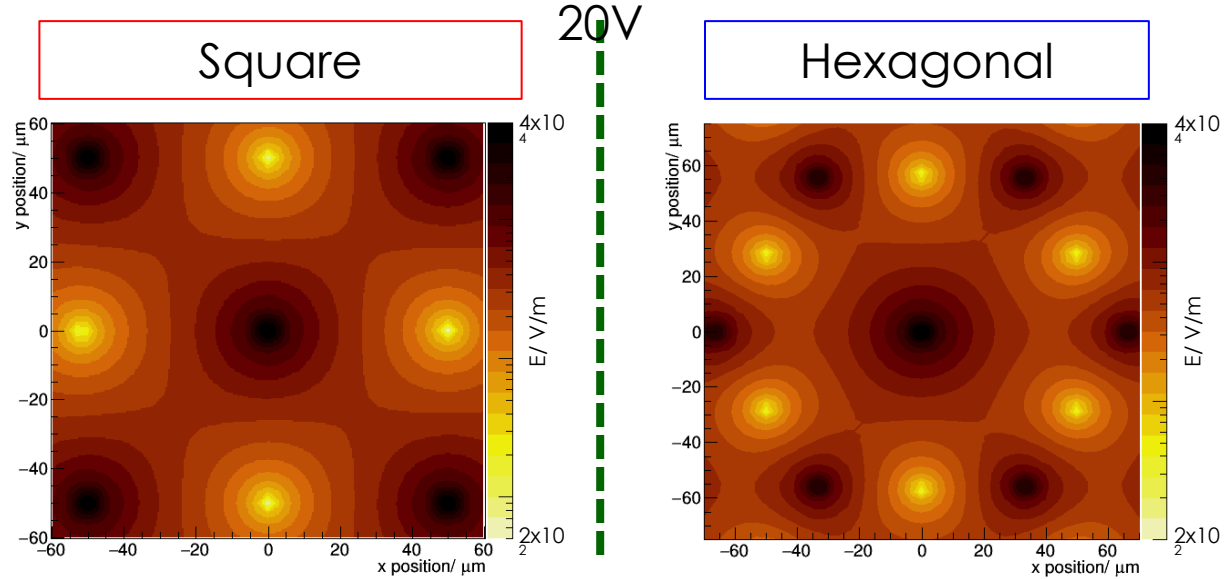


Measured current pulse at

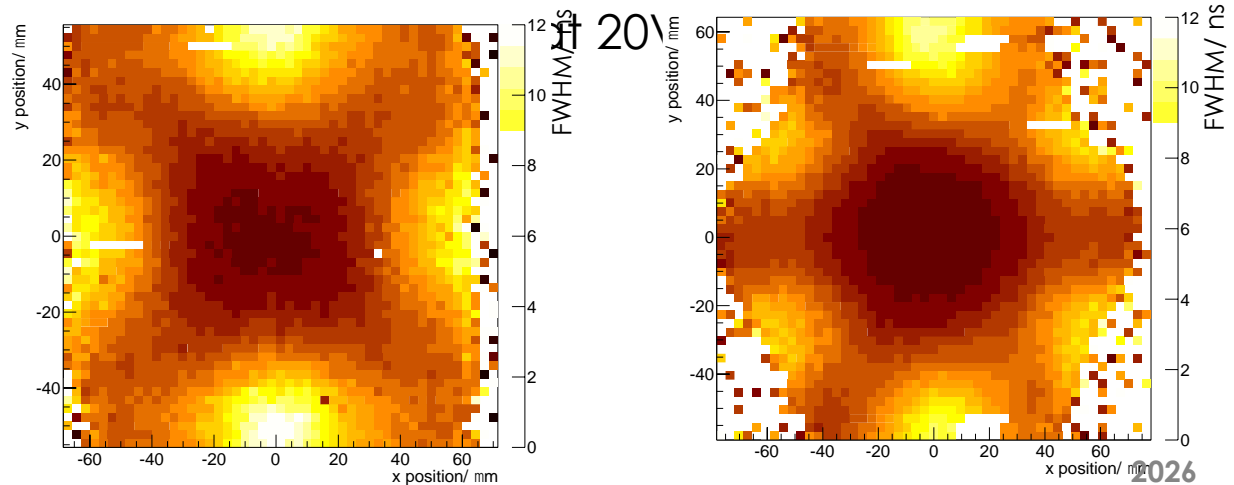




Simulated electric field at

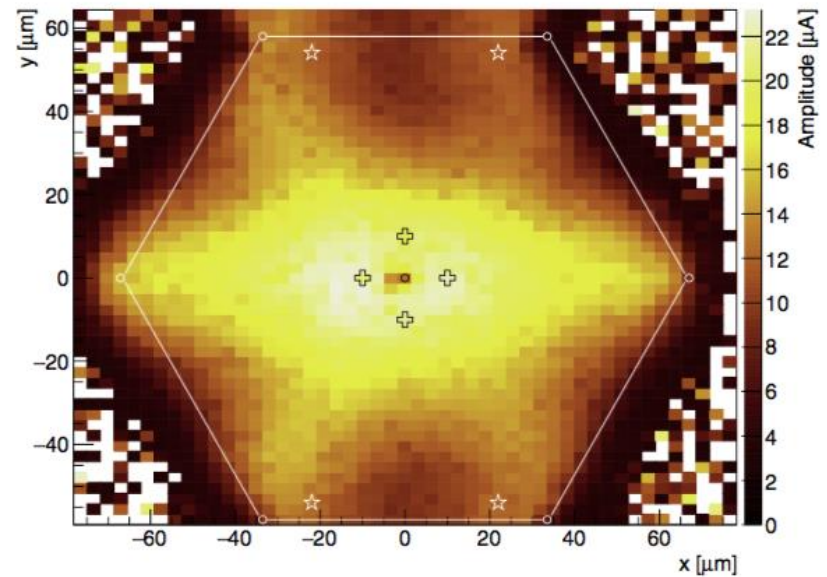
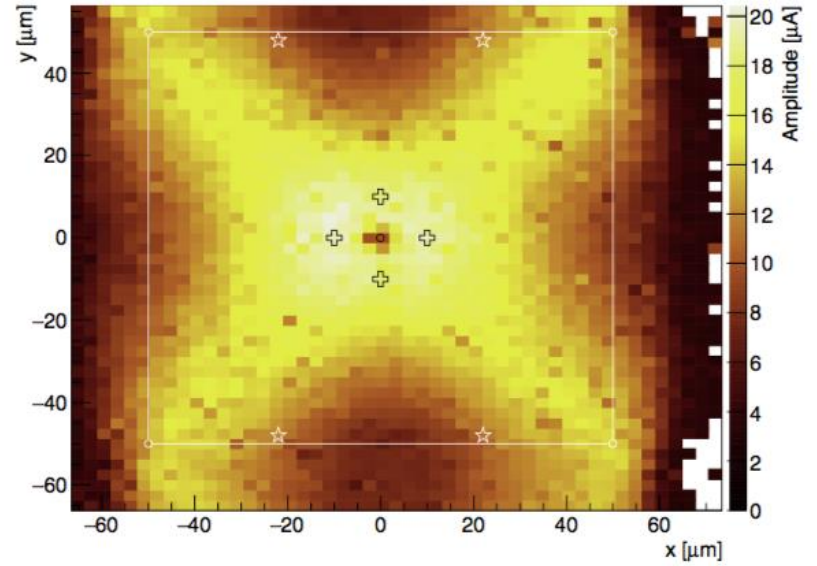
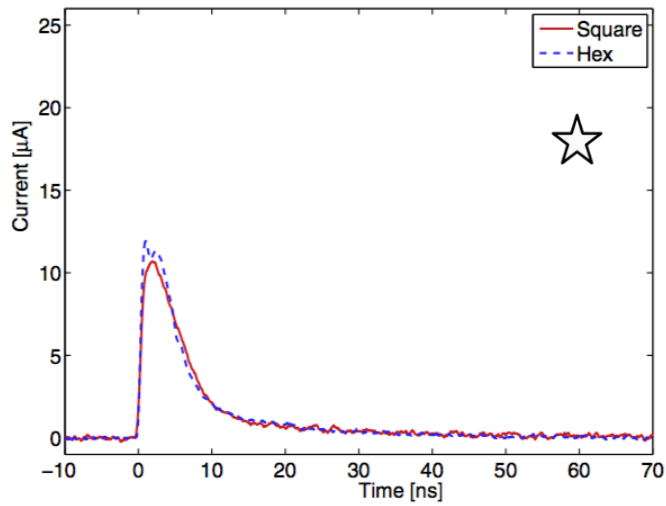
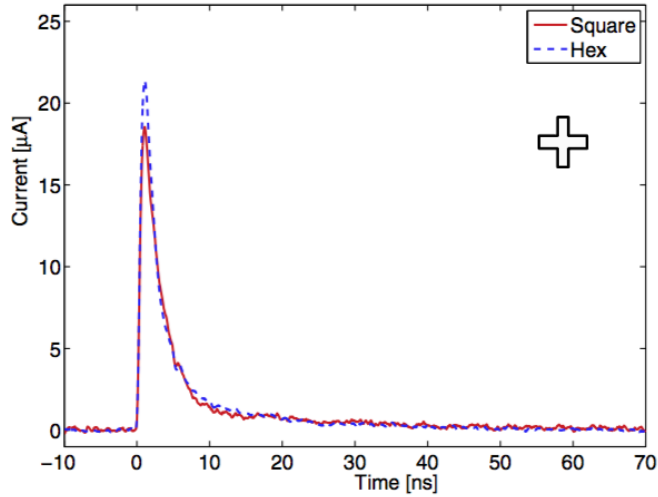


Measured FWHM of pulse

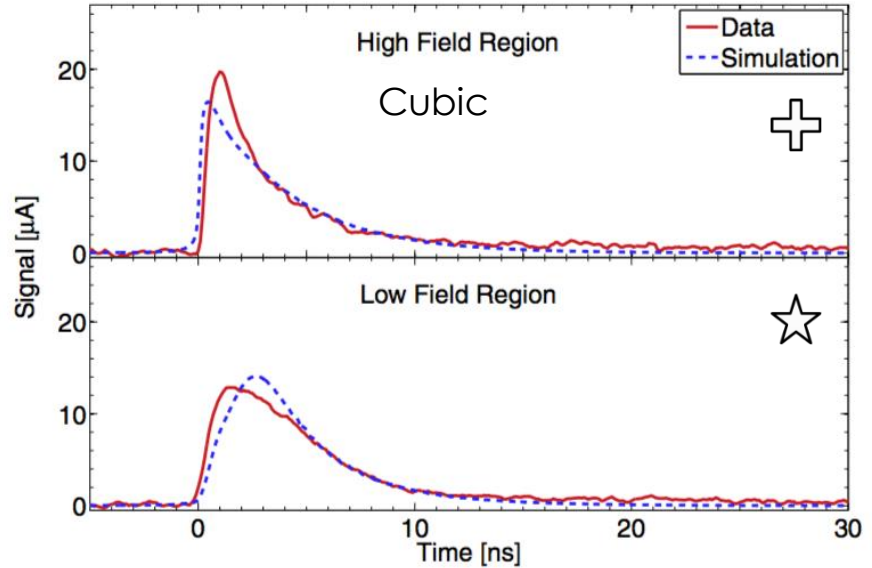
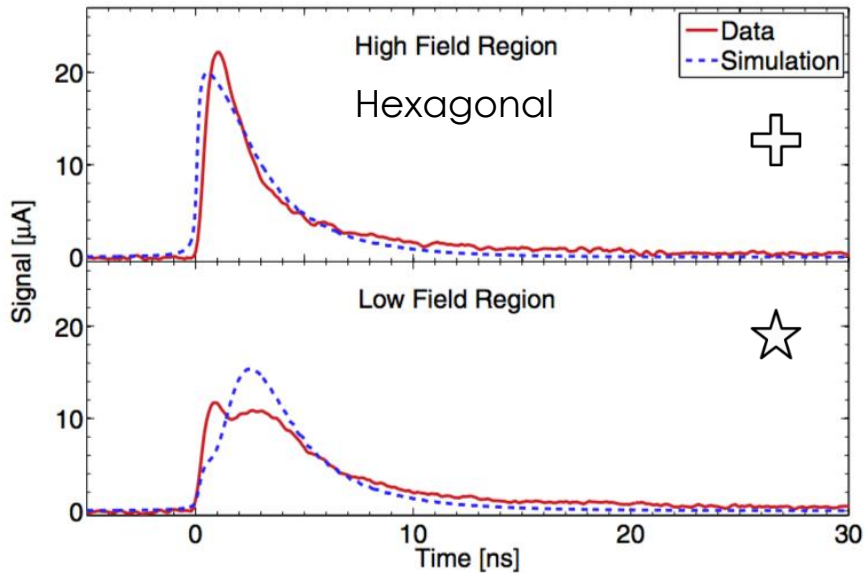


# TRIBIC

$U_b = -20V$



# TRIBIC: Results



Comparison with TCAD Simulation model:

- basic features qualitatively reproduced.
- Reasonable agreement, but simplified model.

# Summary TRIBIC

- First study of hexagonal and cubic 3D diamond cells with TRIBIC.
  - Hexagonal and cubic cells show expected characteristics.
  - Qualitative agreement with simulations.
- Results shown are preliminary, analysis ongoing.
- Next steps:
  - Quantitatively verify electrical field distribution.
  - Disentangle hole and electron contributions.
  - Radiation hardness studies.

# BACKUP

# 3D Diamond detector for medical dosimetry

# Dosimetry application

- Planning of dose distribution delivered dose distribution challenging with narrow field beams.
- Need high spatial resolution of tissue equivalent dose deposited.
- Target numbers:
  - Dose uncertainty  $<1\%$
  - Spatial resolution  $\sim 0.1\text{mm}$



# Dosimetry application

## ■ Diamond key properties for dosimetry

- Tissue equivalence
- Radiation hardness
- Room temperature operation
- bio-compatibility

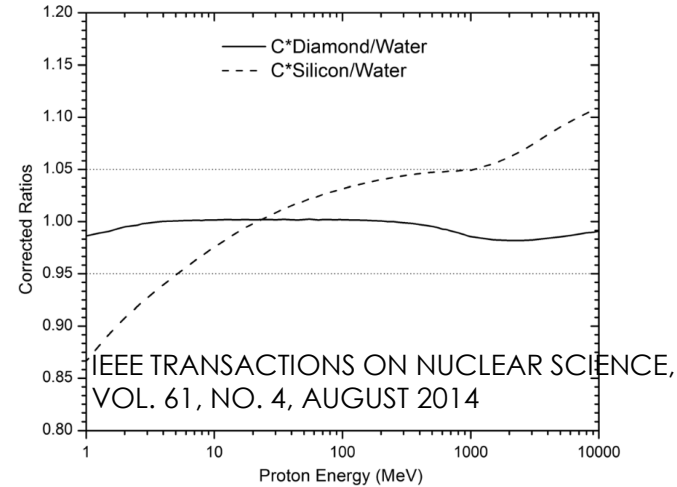
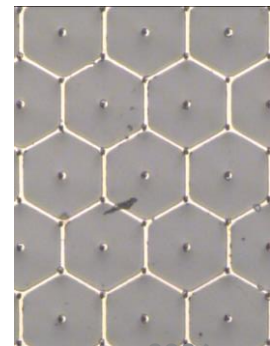
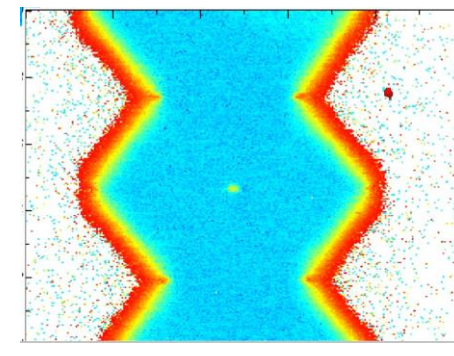
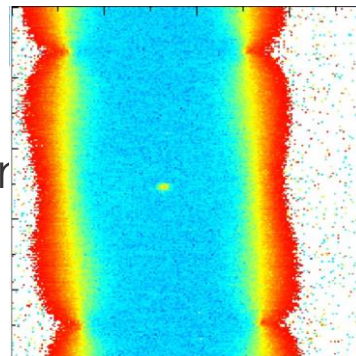


Fig. 14. Comparison of the corrected ratio of stopping powers for protons of diamond and silicon with water.

## ■ 3D Advantage

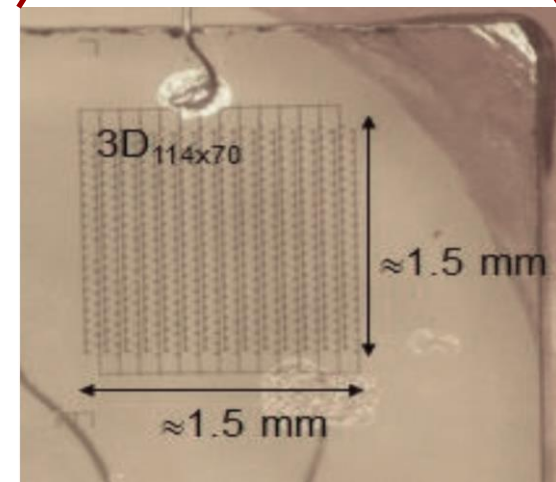
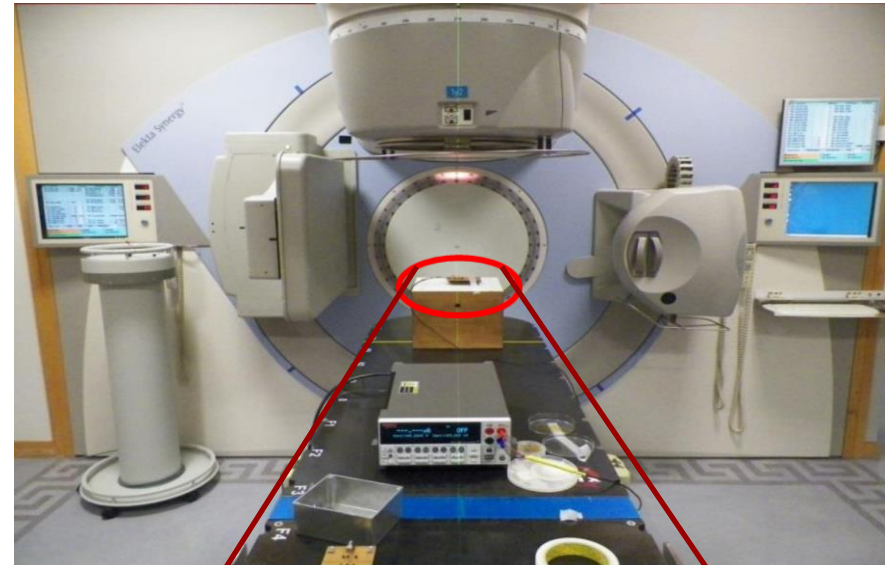
- Flexible active volume
- Radiation hardness
- Potential for 3D position information



# Dosimetry application

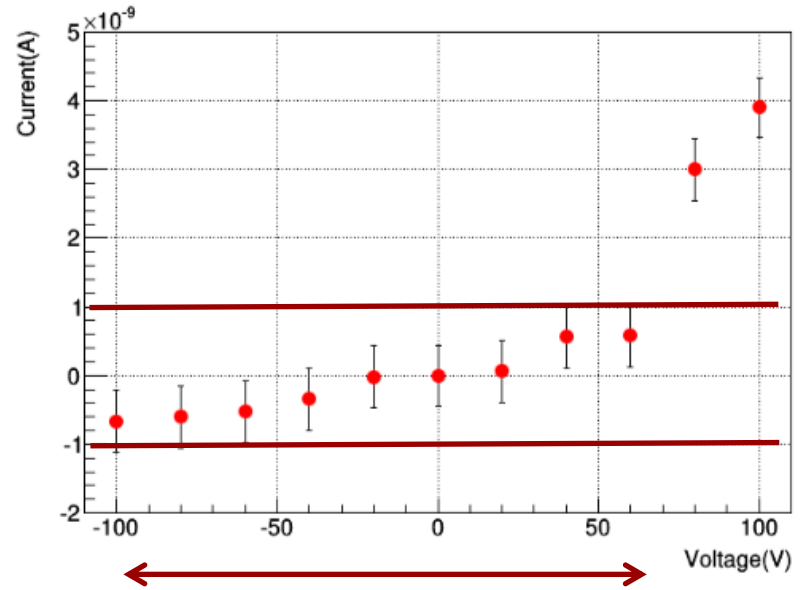
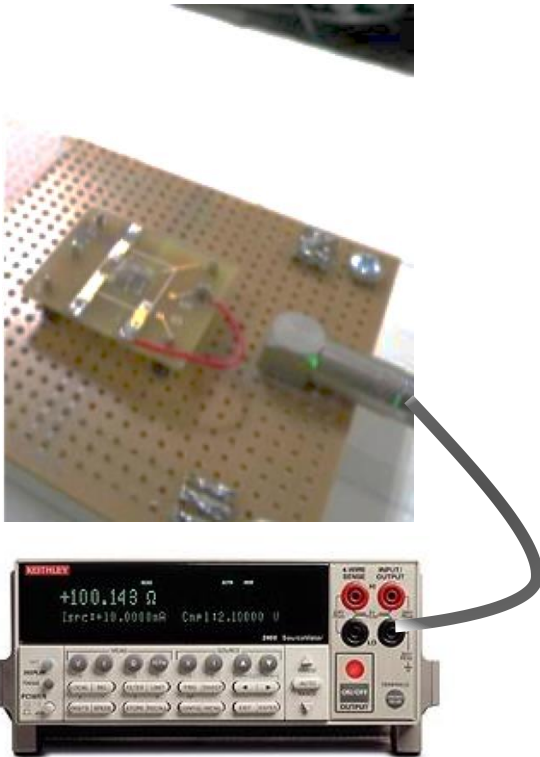


- **The Christie Hospital, Manchester**
  - medical linear accelerator (Elekta Synergy Sband)
  - 6MV and 10MV acceleration.
  - 10x10cm radiation field.
  - Dose rate dependence.
  - Photon beam profile.



# Dosimetry application

- Test set-up:

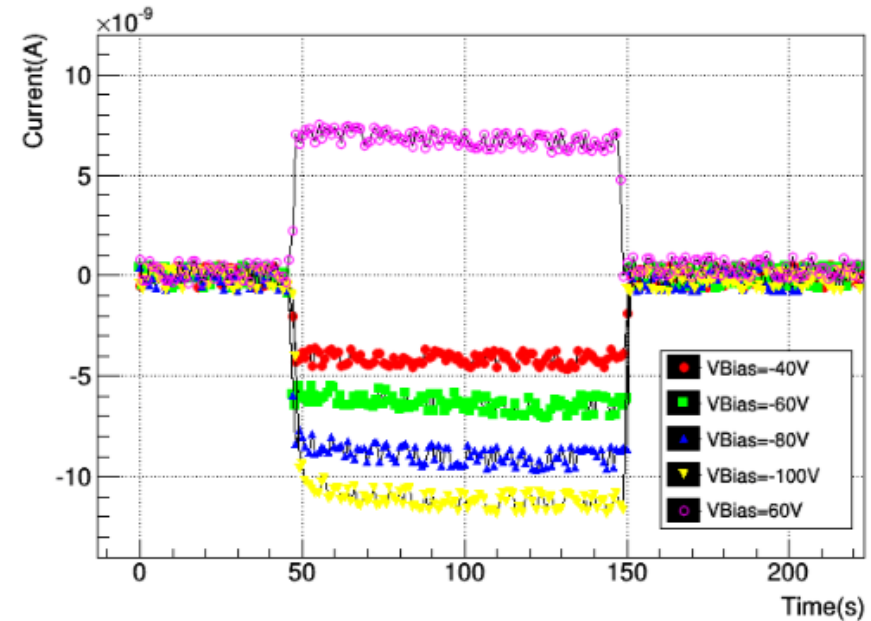


Asymmetric leakage current.  
 $I_{leak} < 1 \text{ nA}$  for  $-100\text{V}$  to  $+60\text{V}$

# Dosimetry application

First 3D diamond results:

- Pre-irradiated with 5 Gy.
- Clear response to presence to 6MV photons.
- Return to baseline <1s, no significant baseline shift.
- Plateau stability needs further studies.

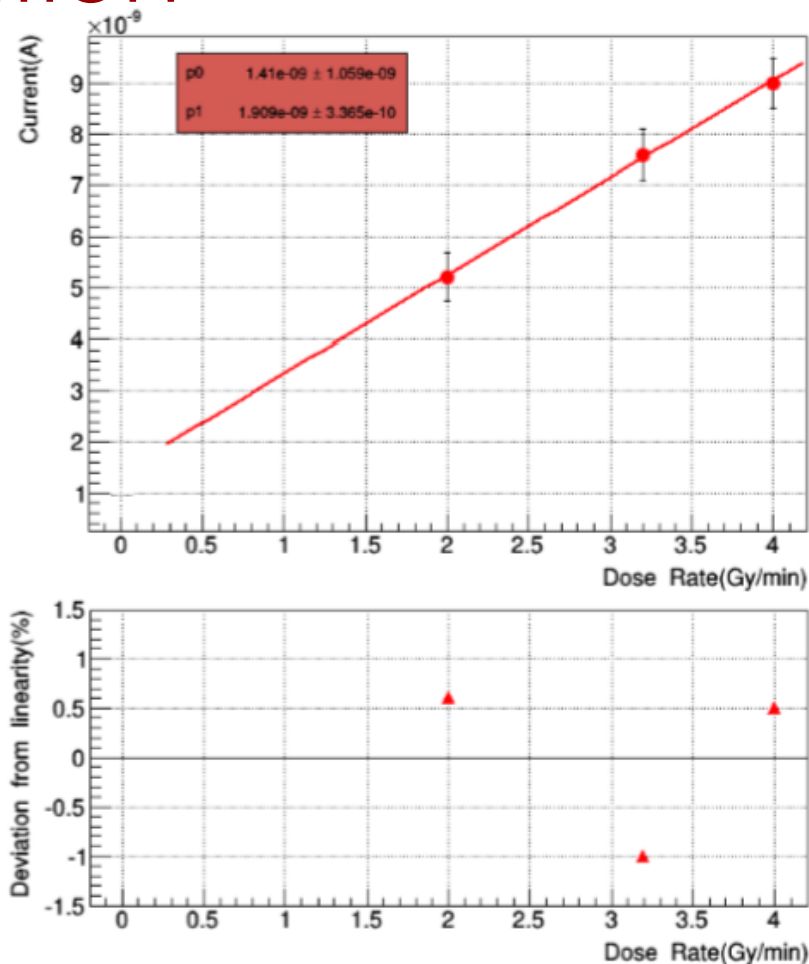


On-off response to 6MV photon beam with 4Gy/min.  
Variation of bias voltage.

# Dosimetry application

First 3D diamond results:

- Good linearity of  $\sim 1\%$  over **dose rate** range of 2-4 Gy/min.

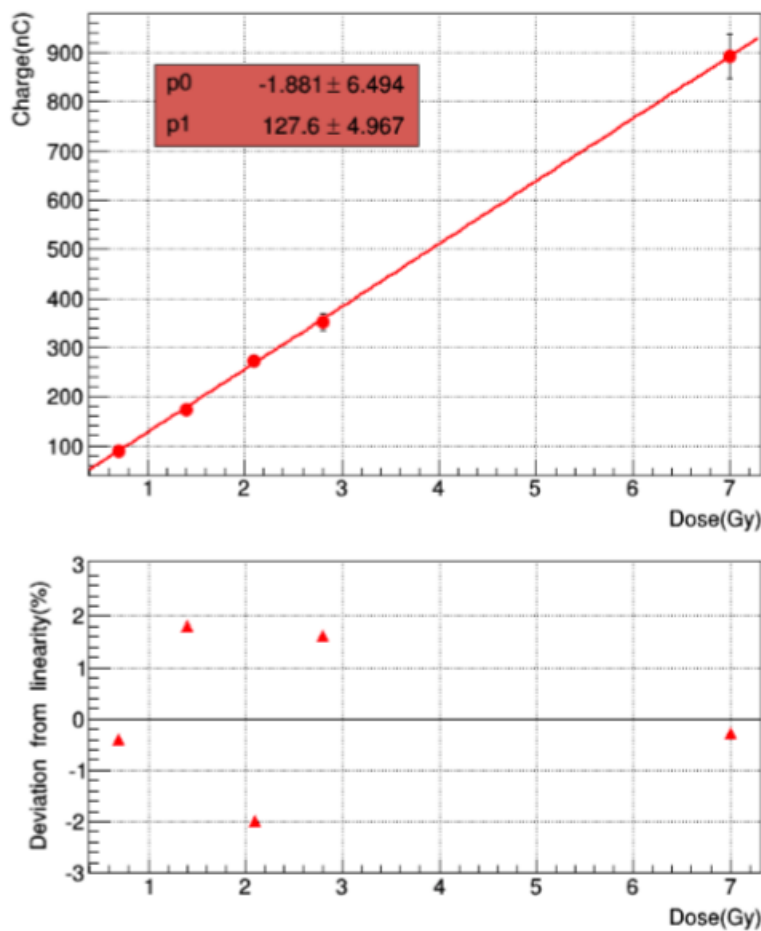


Dose rate linearity for 6MV photons at -80V

# Dosimetry application

## First 3D diamond results:

- Good linearity of  $\sim 1\%$  over dose rate range of 2-4 Gy/min.
- Good linearity of  $\sim 2\%$  over **dose range** of 0.5 to 7 Gy.

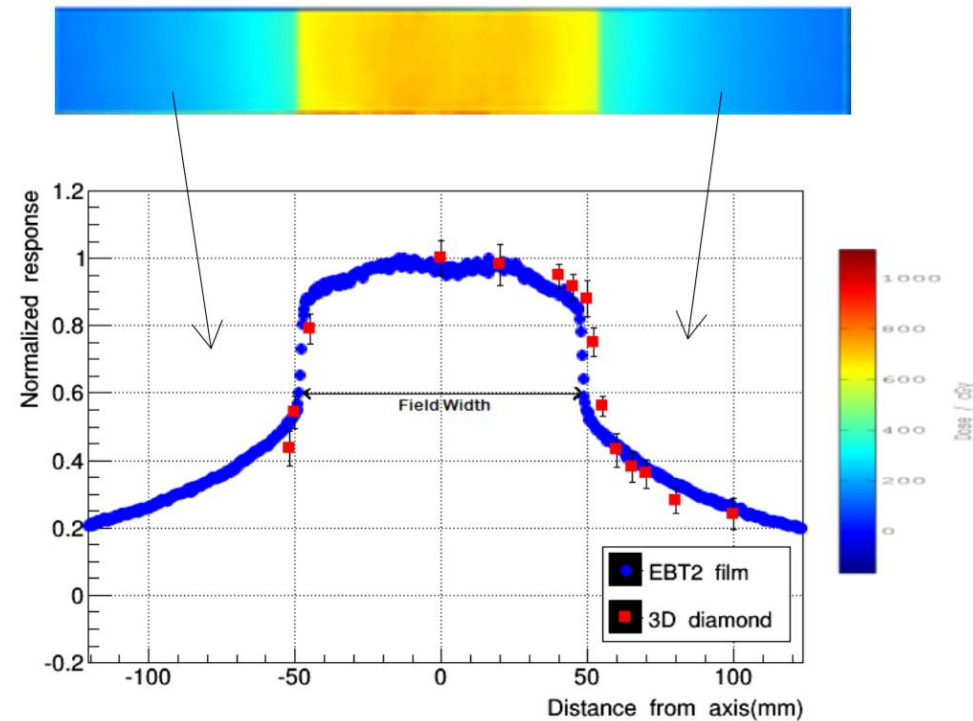


Dose linearity for 6MV photons at -80V

# Dosimetry application

## First 3D diamond results:

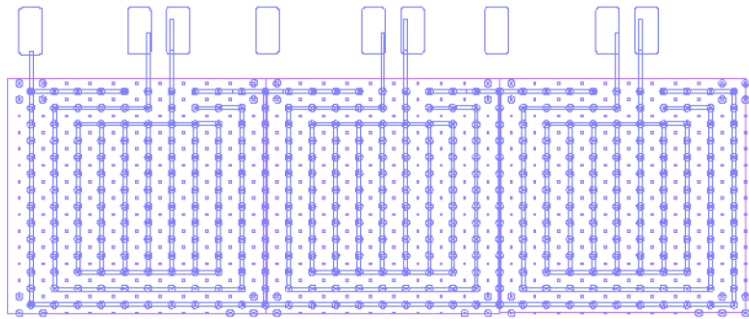
- Good linearity of  $\sim 1\%$  over dose rate range of 2-4 Gy/min.
- Good linearity of  $\sim 2\%$  over dose range of 0.5 to 7 Gy.
- **Beam width** well reproduced to 1% when compared to GafChromic film measurement.



10cm beam profile measured with 3D diamond at -80V, 4Gy/min and film.

# Next generation:

- Next generation tests with variable array sizes.



3166.0205

